

AD \_\_\_\_\_

Award Number: DAMD17-99-1-9094

TITLE: BAG Family Proteins: Regulators of Cancer Cell Growth  
Through Molecular Chaperones

PRINCIPAL INVESTIGATOR: Shinichi Takayama, M.D., Ph.D.

CONTRACTING ORGANIZATION: The Burnham Institute  
La Jolla, California 92037

REPORT DATE: June 2002

TYPE OF REPORT: Final

PREPARED FOR: U.S. Army Medical Research and Materiel Command  
Fort Detrick, Maryland 21702-5012

DISTRIBUTION STATEMENT: Approved for Public Release;  
Distribution Unlimited

The views, opinions and/or findings contained in this report are those of the author(s) and should not be construed as an official Department of the Army position, policy or decision unless so designated by other documentation.

6  
26

REPORT DOCUMENTATION PAGE			Form Approved OMB No. 074-0188	
Public reporting burden for this collection of information is estimated to average 1 hour per response, including the time for reviewing instructions, searching existing data sources, gathering and maintaining the data needed, and completing and reviewing this collection of information. Send comments regarding this burden estimate or any other aspect of this collection of information, including suggestions for reducing this burden to Washington Headquarters Services, Directorate for Information Operations and Reports, 1215 Jefferson Davis Highway, Suite 1204, Arlington, VA 22202-4302, and to the Office of Management and Budget, Paperwork Reduction Project (0704-0188), Washington, DC 20503				
1. AGENCY USE ONLY (Leave blank)	2. REPORT DATE June 2002	3. REPORT TYPE AND DATES COVERED Final (1 Jun 99 - 31 May 02)		
4. TITLE AND SUBTITLE BAG Family Proteins: Regulators of Cancer Cell Growth Through Molecular Chaperones		5. FUNDING NUMBERS DAMD17-99-1-9094		
6. AUTHOR(S) Shinichi Takayama, M.D., Ph.D.				
7. PERFORMING ORGANIZATION NAME(S) AND ADDRESS(ES)  The Burnham Institute La Jolla, California 92037  E-Mail:stakayama@burnham.org		8. PERFORMING ORGANIZATION REPORT NUMBER		
9. SPONSORING / MONITORING AGENCY NAME(S) AND ADDRESS(ES)  U.S. Army Medical Research and Materiel Command Fort Detrick, Maryland 21702-5012		10. SPONSORING / MONITORING AGENCY REPORT NUMBER		
11. SUPPLEMENTARY NOTES report contains color				
12a. DISTRIBUTION / AVAILABILITY STATEMENT Approved for Public Release; Distribution Unlimited			12b. DISTRIBUTION CODE	
13. Abstract (Maximum 200 Words) (abstract should contain no proprietary or confidential information) BAG-family proteins regulate diverse cellular functions, including cell survival, cell proliferation, and cell motility. BAG-family proteins contain a conserved domain that allows them to bind 70-kD heat shock (Hsp70) family molecular chaperones and regulate their activity. Structural analysis of the Hsc70-binding BAG domain of BAG family protein has revealed an anti-parallel two helix bundle, preceded by an additional long $\alpha$ -helix. Site-directed mutagenesis has confirmed that the polar surfaces of the $\alpha$ -helices in the BAG domain are directly involved in chaperone binding, which has been confirmed by NMR experiments (BAG1 and BAG4). Similarly, an ~80 amino acid region (229-308) of Hsc70 has been determined to represent a minimal domain sufficient for binding the BAG domain. In addition to the Hsp70-binding domain, BAG-family proteins also contain a diversity of additional domains, which allow them to interact with specific target proteins or which target them to specific locations within cells. The BAG-family proteins operate as bridging molecules that recruit molecular chaperones to target proteins and ultimately affecting diverse cellular behaviors including cell division, migration, differentiation, and death in cancer cells. Recently we found BAG3 as a regulator of cell growth and motility.				
14. SUBJECT TERMS breast cancer			15. NUMBER OF PAGES 72	
			16. PRICE CODE	
17. SECURITY CLASSIFICATION OF REPORT Unclassified	18. SECURITY CLASSIFICATION OF THIS PAGE Unclassified	19. SECURITY CLASSIFICATION OF ABSTRACT Unclassified	20. LIMITATION OF ABSTRACT Unlimited	

## Table of Contents

Introduction .....	4
Body .....	5
Key Research Accomplishments.....	15
Reportable Outcome.....	15
Conclusion.....	15
References .....	17

20021114 269

## INTRODUCTION

Heat Shock Protein 70-kDa (Hsp70) and related proteins function as molecular chaperones, which modulate a wide variety of biochemical events in cells. Hsp70/Hsc70-family molecular chaperones regulate the activity of a several signal transducing protein kinases and transcription factors of importance for cell growth, survival, and differentiation. Over-expression of Hsp70/Hsc70 family proteins has been reported in some tumors and has been associated with stress-resistance, resistant to apoptosis, and malignant transformation.

We have discovered a family of Hsp70/Hsc70 regulators known as the BAG-family. BAG-family proteins contain a conserved ~80 amino acid domain near their carboxyl-termini that binds the ATPase domain of Hsp70 and Hsc70 with high affinity. The N-terminal domains in these proteins target Hsp70/Hsc70 to different proteins and to different locations within cells.

In contrast to the conserved C-terminal BAG-domain found in all BAG-family members, the N-terminal regions of these proteins are highly divergent and contain some interesting domains. For instance, BAG1 (both the short and long isoforms) and BAG6 (also known as BAT3 and Scythe) contain an ubiquitin-like (UBL) domain. Though the function of this domain is presently unknown, its conservation in the *C. elegans* and *S. pombe* homologs of BAG1 implies that the UBL domain plays an important role in some aspect of either the function of this protein or its regulation. The longer isoform, BAG1L, contains a nucleoplasmin-like and an SV40 large-T-like nuclear targeting sequence not found in the shorter BAG1 protein. We and others have determined that the BAG1L protein resides predominantly in the nucleus, whereas BAG1 is found preferentially in the cytosol, though it can also enter the nucleus probably as a result of interactions with other proteins (1, 2). The N-terminal domain of the human BAG2 protein contains potential kinase phosphorylation sites, but otherwise shares no apparent similarity with other proteins or other functional domains. However, the strong conservation of this N-terminal region of BAG2 in humans and *C. elegans* suggests the possibility of functional importance.

Recently, BAG3 was reported to be a Bcl-2 binding protein called Bis, for "Bcl-2 interacting death suppresser" (3). In gene transfer experiments where BAG3 was over-expressed, BAG3/Bis displayed little or no anti apoptotic activity, but can synergize with over-expressed Bcl-2 in preventing Bax-induced and Fas-mediated apoptosis (3). Thus, it is possible that BAG3 can modulate the function of Bcl-2, at least when over-expressed. BAG3 was also reported independently to be the same as a protein called CAIR-1, CAI stressed-1 (4). BAG3/CAIR-1 expression was reported to become induced in A2058 human melanoma cells by exposure to CAI, an inhibitor of non-voltage-gated calcium channels. BAG3/CAIR-1 reportedly also forms complexes with Hsc70/Hsp70 and latent phospholipase C- $\gamma$ , following stimulation of cells with EGF. Since CAI causes tumor and endothelial cell cytoostasis and inhibits cell attachment,

migration and angiogenesis, the authors speculated that BAG3 functions as a modulator of a cell growth or adhesion pathway involving PLC $\gamma$ .

BAG4 contains a unique N-terminal domain that reportedly allows it to associate with the Death Domains of TNFR1 and DR3 (5). BAG4 (also known as Sodd, Silencer of Death Domain) is speculated to recruit Hsp70/Hsc70 to unliganded TNF-family death receptors, preventing them from clustering and signaling in the absence of ligand (5). BAG5 is interesting because it contains four BAG-domains. BAG6 (Scythe; BAT3) is a nuclear protein, which regulates apoptosis, and which is conserved throughout metazoan evolution, with homologues in flies, frogs, and humans. BAG6 binds apoptosis-inducer Reaper, and sequesters an unidentified pro-apoptotic molecule that causes cytochrome *c* release from mitochondria, an event linked to apoptosis induction (Figure 1).

The central hypothesis of this grant proposal was that BAG family protein might represents a novel proto-oncogene that can promote aggressive behaviors of tumor cells through its ability to interact with molecular chaperones and other proteins involved in control of cell growth or adhesion. At least four out of 6 family proteins were involved in apoptosis from literatures. BAG1, 3 and 4 were reported as over-expressing protein in some type of cancer. Thus we investigated the BAG family proteins in tumor growth to find clues to explore breast cancer biology.

## BODY

**Task1.** Deduce the Complete Primary Aminoacid Sequences of BAG-3, BAG-4 and BAG-5. (Months 1-6)

We have discovered a family of Hsp70/Hsc70 regulators known as the BAG-family. BAG-family proteins contain a conserved ~80 amino acid domain near their carboxyl-termini that binds the ATPase domain of Hsp70 and Hsc70 with high affinity. The N-terminal domains in these proteins target Hsp70/Hsc70 to different proteins and to different locations within cells. BAG-family genes are evolutionarily conserved, with homologues identified in *C. elegans*, *Drosophila*, *Arabidopsis thaliana* and yeast. To date, 6 members of the BAG-family have been identified in humans, including BAG1(RAP46), BAG2, BAG3 (Bis, CAIR-1), BAG4 (Sodd), BAG5 and BAG6 (BAT3, Scythe). Five of these six BAG-family proteins were discovered and all nucleotide sequences were determined by myself (see attached genbank data in the appendices).

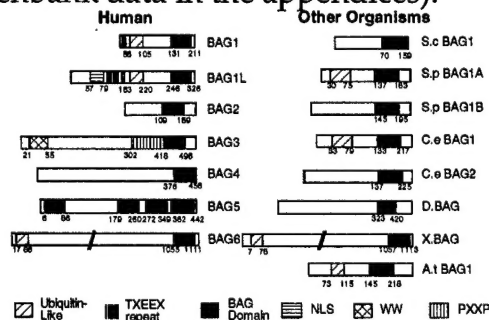


**Figure 1. The BAG Family.** The structures of the BAG-family proteins are depicted, showing the conserved BAG domains, as well as other domains found in selected members of the family such as an ubiquitin-like (UBL) domain, nuclear targeting sequences, WW domain, and PXXP motifs. Human BAG-family proteins are presented on the left and homologs in other organisms are shown on the right, including BAG-family proteins from *S. cerevisiae* (S.c), *S. pombe* (S.p.), *C. elegans* (C.e.), *Drosophila melanogaster* (D), *Xenopus laevis* (X), and *Arabidopsis thaliana* (A.t.). Additional plant homologs are not shown.

**Task 2.** Determine the biochemical effects of BAG-family proteins on Hsc70 chaperone function (Months 6-12).

- 1) Subclone cDNAs into pGEX4T-1 for production of GST fusion proteins. Each region of BAG domains was determined by ClustalW alignment program. All fragments were amplified by PCR based method and were subcloned into pCR2.1 TOPO vector following nucleotide sequence determination.
- 2) Produce and purify BAG-family proteins from bacteria. BAG family cDNAs were subcloned into pGEX vector. GST fusion protein was purified from *E. coli* as described previously.

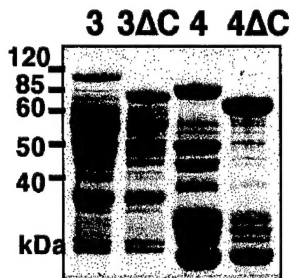


**Figure2. BAG3 and BAG4 GST fusion protein has additional bands.** BAG3 and BAG4 GST fusion protein has been purified and run on SDS-PAGE gel following Coomassie Blue staining. Each lane shows additional bands indicating degraded or contaminated proteins were purified with GST BAG proteins. 3 and 3ΔC represent GST-BAG3 and GST-BAG3 deletion BAG domain. 4 and 4ΔC is GST-BAG4 and GST BAG4 deletion BAG domain.

- 3) Perform biochemical assays of BAG-family protein effects on Hsc70 chaperone activity (refolding assays), ATPase activity, and ADP-ATP exchange. Full length GST fusion proteins show degradation problem as shown in figure2. Thus, we decided to accomplish Task3 prior to Task2.

**Task 3.** Map the domains within BAG-family proteins which are needed for interactions with Hsc70 (Months 13-16).

- 1) Create deletion mutant of BAG-1 family proteins by PCR mutagenesis of cDNAs. We have determined that the BAG-domains of BAG1, BAG2, and BAG3 are necessary and sufficient to bind the ATPase domains of Hsp70 and Hsc70 in vitro. The BAG domains of these proteins bind tightly to the ATPase domain of Hsc70 with  $K_D$ 's of 1-10 nM, as deduced from kinetic measurements performed using surface plasmon resonance (SPR) with purified recombinant proteins (6). Similar to BAG1, the in vitro chaperone activity of Hsc70 and/or

Hsp70 is inhibited by recombinant proteins containing the BAG domains of BAG2 and BAG3. Thus, it appears that the mammalian BAG1, BAG2, and BAG3 proteins have similar properties in terms of binding to the ATPase domain of Hsc70/Hsp70 and inhibiting its chaperone activity. Other BAG-family proteins have not yet been tested.

An amino acid sequence alignment of the BAG domains of the BAG-family proteins is presented in Figure x. Note that BAG2 and BAG6 are the least conserved among the known BAG-family proteins. Also, note that some BAG domains contain a segment of variable length (3 to 7 amino acids).

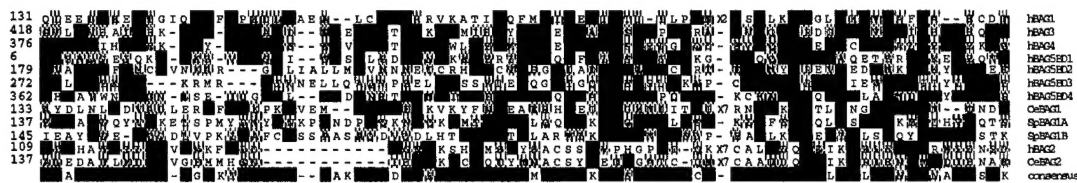


**Figure3.** The BAG-domains of the human BAG1, BAG3, BAG4, BAG5, and mouse BAG1, *C. elegans* BAG1, and *S. pombe* BAG1A and BAG1B proteins are aligned (single letter amino acid code). Black boxes indicate identical residues. Grey indicates conservative replacements. Dashes indicate gaps. Some members of the family contain an additional region of variable length (up to 7 amino acids) which is indicated in the figure by Xn.

- 2) Subclone into pGEX and yeast two hybrid plasmids. All of the BAG domain cDNA fragments were subcloned into pGEX vector and yeast two hybrid vector.
- 3) Perform Hsc70 interaction assays.

**Structure and mutational analysis of BAG domain.** Recently, in collaboration with Dr. Ely at our institution, we completed a NMR solution structure of a fragment of the mouse BAG1 protein (residues 90-219), representing the last 130 amino-acids which encompasses the BAG-domain and upstream region proximal to the UBL domain. The structure reveals three long  $\alpha$ -helices ( $\alpha$ 1,  $\alpha$ 2,  $\alpha$ 3), with the last two  $\alpha$ -helices ( $\alpha$ 2,  $\alpha$ 3) corresponding to the BAG domain. Alignment of the sequences corresponding to the BAG domains of the other BAG-family members, and secondary structure prediction algorithms, suggest that most of the BAG domains share this two  $\alpha$ -helix structure. Thus, the structural information derived for BAG1 should be relevant to our efforts to understand BAG family proteins through mutational analysis. Paper is attached with this report (7).

Mutant	$\alpha$ -helix	Residues	Hsp70 binding	AR Co-activation
Wild Type	NA	NA	++	++
H1A	$\alpha$ 1	E115A, K116A, N119A	++	NA
H1B	$\alpha$ 1	E123A, K126A	++	NA
H2A	$\alpha$ 2	D149A, R150A	++	NA
H2B	$\alpha$ 2	E157A, K161A	-	-
H3A	$\alpha$ 3	Q190A	$\pm$	NA
H3B	$\alpha$ 3	D197A, Q201A	-	-

**Table 1. Characterization of BAG domain mutants.** The mouse BAG1 protein (residues 90-219) or various mutants as indicated in the Table were expressed as GST fusion protein in bacterial and affinity purified. GST-BAG1 fusion proteins were assayed for ability to bind Hsc70/ATPase *in vitro*. To correlate *in vitro* binding with *in vivo* activity, some of the same mutants were produced in the BAG domain of the human BAG1L protein and their function was assessed by transient transfection reporter gene assays, using co-activation of the androgen receptor (AR) as a convenient read-out. Results are compared relative to wild-type BAG1. NA = not applicable/not tested.

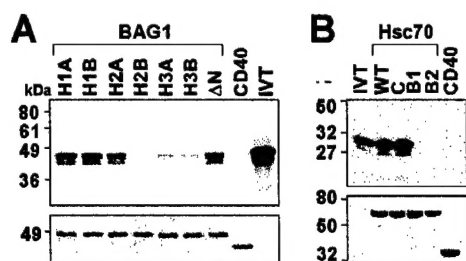


**Figure 4. Analysis of BAG-domain mutants and Hsc70 mutants.** A. GST fusion proteins were

immobilized on glutathione-Sepharose beads as indicated (5  $\mu$ g) and mixed in a volume of 0.1 ml with 1  $\mu$ l of *in vitro* translated  $^{35}$ S-L-methionine labeled ATPase domain of Hsc70. After 1hr incubation at 4°C, beads were washed 3 times with 1 ml of ice-cold 0.5% NP40, 20 mM HEPES (pH 7.7), 142 mM KCl, 5 mM  $MgCl_2$ , 2 mM EGTA. Following SDS-PAGE separation,

autoradiography was used to visualize the proteins. The GST fusion proteins represent mouse BAG1 (residues 90-219) expressed as either the wild-type ("ΔN") or mutant (H1A, H1B, H2A, H2B, H3A, H3B) proteins (see Table 1 for details). The coomassie stained gel is shown below, demonstrating loading of equivalent amounts of GST fusion portions. B. Mutations were generated in Hsc70 (residues 1-377) by PCR-based mutagenesis. GST fusion proteins were generated including, wild-type WT Hsc70 (residues 1-377), and mutants with alanine substitutions in either predicted BAG1-binding residues [mutant B1 (R258A, R262A); mutant B2 (E283A, D285A) or in control residue mutant C (E318A, E322A)] GST-CD40 intra-cytoplasmic domain was also employed as a control. Purified GST fusion proteins were used for binding assay as described above with 1  $\mu$ l of *in vitro* translated  $^{35}$ S-L-methionine labeled mouse BAG-1 (8). 0.2  $\mu$ l of *in vitro* translated product was run in gels as a control (INV). Lower panel represents coomassie blue staining of the same gel.

Next, we determined the minimum region of Hsc70, which is responsible for binding to BAG1 BAG domain. In earlier studies, we showed that residues in the N-terminal lobe of the ATPase domain (residues 1-186) were not required for binding BAG1 (9). In the course of defining the contact interface between BAG1 and the ATPase domain, careful inspection of the crystal structure of the Hsc70 domain revealed a sub-domain that contains the contacts required for binding to BAG proteins. The ATPase domain is bi-lobed with an N-terminal lobe and C-terminal lobe each consisting of separately folded units. In fact, the C-terminal lobe is encoded by a single exon. A deep nucleotide binding crevice exists between the two lobes and ATP/ADP exchange occurs through this crevice. All of the residues shown by mutagenesis to be necessary for BAG1 binding (7) were contained in an 80-residue sub-domain of the C-terminal lobe. Binding of Hsc70min to BAG1 was examined by *in vitro* protein interaction assays. GST-fusion-proteins representing the Hsc70min domain (residues 229-309) or full-

length Hsc70 ATPase domain (residues 1-377) were immobilized on glutathione-Sepharose beads and tested for binding to *in vitro*-translated  $^{35}\text{S}$ -BAG1.  $^{35}\text{S}$ -BAG1 bound to both the Hsc70min and Hsc70 ATPase proteins but not to control proteins (see Figure 4), indicating that Hsc70min retained the capacity to bind to BAG1, apparently including the necessary contact residues. This is consistent with our previous results from deletion analysis indicating that the minimal contact region in Hsc70 for BAG1 recognition is localized within residues 186-377 (9). The results indicate that an independently folded sub-domain encompassing residues 229-309 from the Hsc70 ATPase domain is sufficient for binding to BAG1. For detailed report, see attached paper (10).

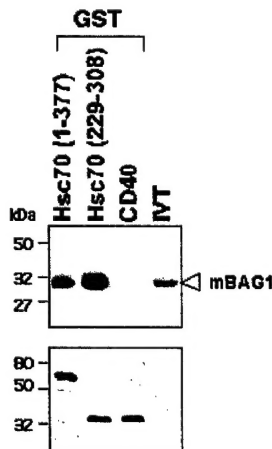


**Figure 5 Mini domain of ATPase domain is minimum region of BAG binding.** An independently folded sub-domain of the C-terminal lobe in the ATPase domain of Hsc70 is sufficient for binding to BAG1. The results of an *in vitro* protein interaction assay are shown. The GST-fusion proteins representing full length Hsc70 ATPase domain (1-377) or Hsc70min (229-309) proteins were tested for binding to *in vitro*-translated BAG1. Samples were analyzed by SDS-PAGE and autoradiography to detect bound BAG1 (upper panel). A GST-fusion of the cytoplasmic domain of CD40 was used as a control. IVT shows 0.2  $\mu\text{L}$  *in vitro* -translated mBAG1. The Coomassie blue stained gel is shown in the lower panel, demonstrating loading of equivalent amounts of GST-fusion proteins.

Even we have some problem in purification of each GST fusion protein of BAGs as shown in Figure 2. We performed *in vitro* binding assay using GST fusion protein of BAG3, BAG4, BAG5 and deletion mutants. Full-length BAG3 and the fragment containing only the BAG domain (BD) bound to GST-Hsc70, whereas BAG3 lacking the BAG domain ( $\Delta\text{BD}$ ) did not. Similar results were obtained with BAG4. The BAG5 protein contains four potential BAG domains. Expression of each of these individually demonstrated that only the first (most N-terminal) of the BAG domains binds Hsc70 *in vitro*.

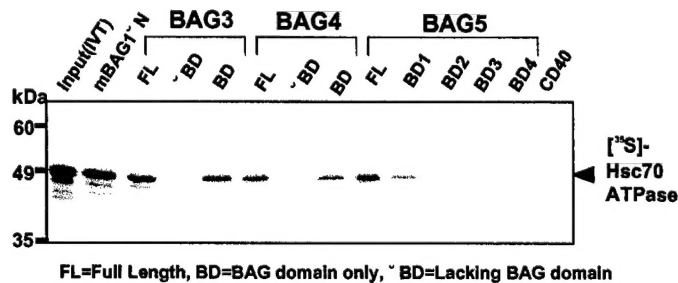


**Figure 6. BAG domain binds ATPase domain of Hsc70 *in vitro*.** GST fusion proteins were immobilized on glutathione-Sepharose beads as indicated (5  $\mu\text{g}$ ) and mixed in a volume of 0.1 ml with 1  $\mu\text{L}$  of *in vitro* translated  $^{35}\text{S}$ -L-methionine labeled ATPase domain of Hsc70. After 1 hr incubation at

4°C, beads were washed 3 times with 1 ml of ice-cold 0.5% NP40, 20 mM HEPES (pH 7.7), 142 mM KCl, 5 mM  $\text{MgCl}_2$ , 2 mM EGTA. Following SDS-PAGE separation, autoradiography was used to visualize the proteins. The GST fusion proteins represented full-length BAG3, 4, or 5, or fragments corresponding only to the BAG Domains (BD), or fragments lacking the BAG-domains ( $\Delta\text{BD}$ ). Note that BAG5 contains four potential BAG-domains, labeled BD1, BD2, BD3, and BD4. GST-CD40 served as a negative control.

We performed similar interaction assay using yeast two hybrid system. In this assay system, we have two reporter systems (leucine assay and the other is beta-gal). As shown in Figure6, beta-gal assay shows high background. On leucine assay, we can see BAG4 $\Delta$ C has some positive grow and BAG5 full length has no growth at all. Because of false positive problem with yeast two hybrid assay, we think this assay is not suitable for BAG domain and Hsc70 interaction assay. But at least, we conclude for BAG3 the result of in vitro binding assay (Figure5) and yeast two hybrid shows the same result, showing that BAG domain of BAG3 is sufficient for binding to Hsc70.

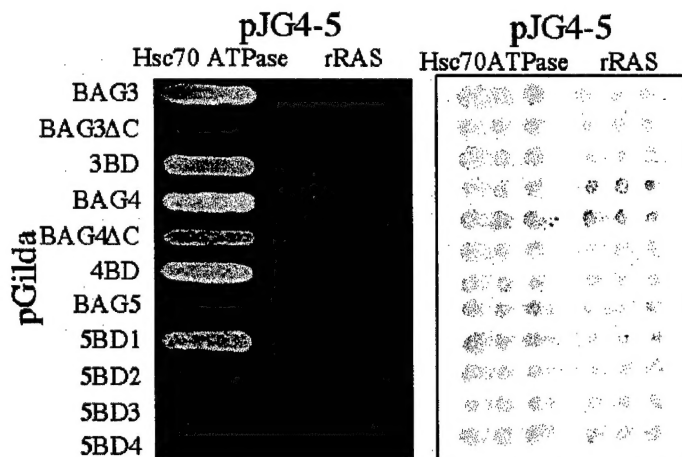


**Figure7 Yeast two hybrid assay of BAG family proteins, BAG domains and Hsc70.** Yeast strain EGY48 cells were transformed with pJG4-5 ATPase domain of Hsc70 or Ras (negative control) and pSH18-34  $\beta$ -galactosidase reporter plasmid in combination with different LexA plasmids. (1) BAG3 (2) BAG3 deletion BAG domain (3) BAG3 BAG domain (4) BAG4 (5) BAG4 deletion BAG domain (6) BAG4 BAG domain (7) BAG5 (8) BAG5 BAG domain1 (9) BAG5 BAG domain 2 (10) BAG5 BAG domain3 (11) BAG5 BAG domain4.

Transformants were streaked in triplicate on leucine-deficient medium (Left) or subjected to filter-based  $\beta$ -galactosidase assays (Right). Results were scored after 4 day (leucine selection) or 1 hr ( $\beta$ -gal), respectively. Expression of all proteins was confirmed by immunoblot analysis of lysates from transformed yeast (not shown). For the experiment shown, 3 replicate colonies were streaked for each transformant.

**Structure of the BAG domain from BAG4.** We have determined the solution structure of BAG4 BAG domain, using multidimensional NMR methods. Similar to its BAG1 counterpart, the BAG4 BAG domain is a three-helix bundle. The three helices in BAG4 BD, which correspond to residues 380-399 (alpha helix 1), 407-423 (alpha helix 2) and 432-456 (alpha helix 3), are substantially shorter than those in BAG1. BAG4, each helix in this bundle is three to four turns shorter than its counterpart in BAG1, which reduces the length of the domain by one-third. BAG4 BD thus represents a prototype of the minimal functional fragment that is capable of binding to Hsc70. The structural comparison defines three subfamilies of mammalian BAG domain-containing proteins. One subfamily includes the closely related BAG3, BAG4 and BAG5 proteins, and the other is represented by BAG1, which contains a structurally and evolutionarily distinct BAG domain. And the last subfamily contains BAG2 and BAG6, which represent less homology to other family of proteins.

The binding interface in BAG4 BD across the conserved helices  $\alpha$ 2 and  $\alpha$ 3, we used site-directed mutagenesis of the predicted contact residues within these helices. The results indicated that Glu414 and Asp424 from  $\alpha$ 2, as well as Arg438,

Lys439 and Gln446 from  $\alpha 3$  are important for interaction of BAG4 with Hsc70, since mutating these residues to alanine abolished or weakened the binding. See detail in the attached paper (7).

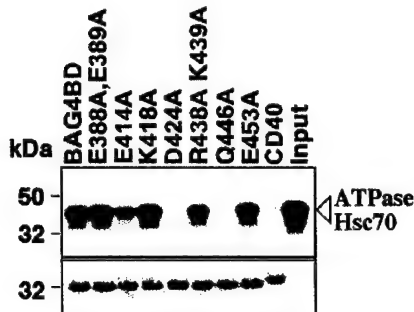
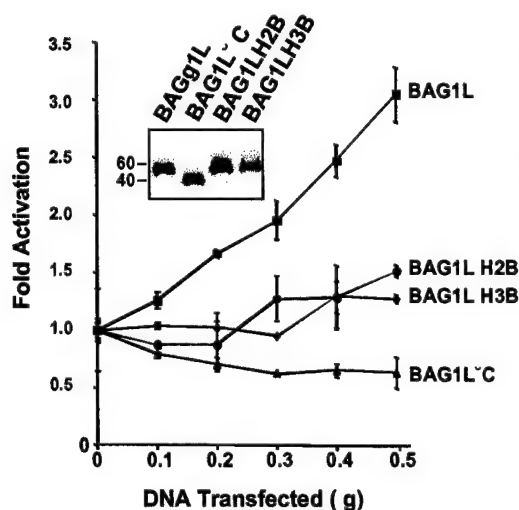


**Figure8 Mutational analysis of human BAG4 BAG domain to Hsc70.** GST fusion proteins representing wild type BAG4, mutants or CD40 negative control were tested. Mutans were made by substituting Alanin for surface residue in each  $\alpha$ -helix. Proteins were immobilized on glutathione sepharose beads and tested for in vitro binding to in vitro translated 35S-L-Methionine labeled Hsc70 (67-377). Samples were analyzed by SDS-PAGE and autoradiography to detect bound Hsc70 and with Coomassie blue staining to verify loading of equivalent amounts of GST fusion proteins. Numbers of each lanes

are represented as follows. Input lane shows 1/5 of total in vitro translated protein, which was mixed with GST fusion protein.

#### Task 4. Examine effects of BAG-family proteins on Estrogen Receptor Function. (Months 17-20)

For the model system of this analysis, we examined BAG1 on ER reporter gene assay as the similar method as AR reporter gene assay published by John Reed lab (11). Previous findings from Dr. Reed's laboratory show that the nuclear-targeted longer isoform of BAG1 (called BAG1L) binds nuclear steroid receptors such as the Androgen Receptor (AR) and enhances their trans-activity. Because this phenotype is dependent on the Hsc70-binding domain of BAG1L (12), it provides a convenient end-point for assessing the effects of the alanine-substitution mutations, since co-activation of AR by BAG1L can be studied by transient transfection reporter gene assays (12). We engineered some of the same



mutation studies in the mouse BAG1 protein into expression plasmids encoding human BAG1L and tested their effects on AR activity in reporter gene assays. As shown in Figure 6, wild-type BAG1L enhanced in a dose-dependent manner the AR-mediated trans-activation of a AR-response element driving a CAT reporter plasmid (pLCI). A mutant of BAG1L lacking the BAG-domain ( $\Delta$ C) failed to co-activate AR. Similarly, the H2B and H3B mutants, which failed to bind Hsc70 in vitro also failed to co-activate AR. Immunoblot assays confirmed production of wild-type and mutant BAG1L proteins.

Comparing to AR reporter gene assay system, ER reporter gene assay has some difficulty to interpret, for example fold activation is not really high (~2) in our system. We are still working on the determination of appropriate conditions.

**Figure9. BAG1L mutants which fail to bind Hsc70 also fail to co-activate AR.** COS-7 cells were transfected with 0.04 µg of pSG5-AR, 0.5 µg of pLCI, 0.06 µg of pCMV-β-gal and increasing amount of pcDNA3-BAG1L mutant or wild-type plasmids. Total DNA was maintained at 1.4 µg by the addition of empty plasmid. At 30 hrs after transfection, cells were stimulated with 1nM R1881. Cell extracts were prepared and assayed for CAT and β-galactosidase activity at 40 hrs after transfection. Data are expressed as fold activation compared to the amount of AR-mediated reporter gene activation in the absence of BAG1L (mean ± S.D.; n=3). The inset shows an immunoblot analysis of lysates (25 µg total protein) prepared from an aliquot of the same transfected cells, using anti-BAG1 monoclonal antibody KS6C8 (1, 13).

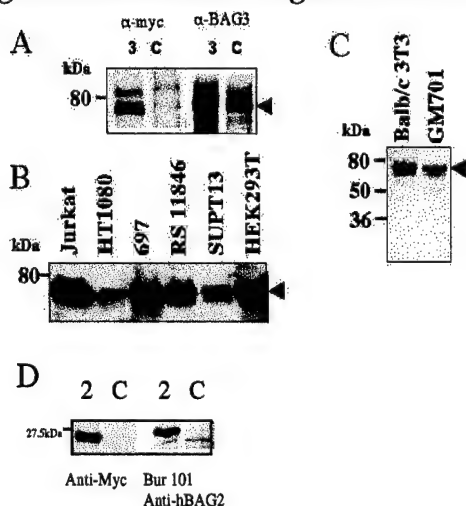
**Task 5.** Explore the effects of BAG-family proteins on in vitro behaviors of breast cancer cells (Months 21-36) Our initial investigation about BAG2, 3 represent overexpression of BAG3 protein in breast cancer cell lines.

**BAG3 displays transforming activity in 3T3 cell transfection assays.** The effects of BAG3 and various other proteins on morphological transformation of Balb/c 3T3 cells were tested by transfection assay. pcDNA3 parent (Control) plasmid and a plasmid encoding the BAG1L protein failed to induce significant numbers of transformed foci, whereas oncogenic Ras (Val12) served as a positive control for the assay. Both full-length BAG3 and a mutant lacking the C-terminal Hsc70-binding domain induced a significant increase in transformed foci in this assay. These data imply that BAG3 has at least modest transforming activity and that Hsc70-binding is not required for this activity.

Overexpression of BAG3 protein are observed in several cancer cell lines, including breast cancer cell lines (see result in the task6). The human BAG3 protein is a cytosolic protein of 575 amino-acids length, which contains a WW domain, followed by a proline rich region, and then the Hsc70/Hsp70-binding BAG domain. WW domains are found in several proteins of relevance to signal transduction, and are known to bind XPPXY motifs. The proline-rich region of BAG3 contains several PXXP motifs, which are known to interact with SH3 domains, and indeed BAG3 has been reported to bind the SH3 protein, Phospholipase Cγ (PLCγ). These structural features of the BAG3 protein suggest that BAG3 is involved in some aspect of signal transduction. In this regard, using two-hybrid methods, we have identified candidate BAG3 binding proteins, including a Guanine Nucleotide Exchange Factor, which is believed to regulate small GTPases, and we have confirmed its association with BAG3 in vitro and in vivo. Our hypothesis therefore is that BAG3 coordinates signals related to cell adhesion, cytoskeleton regulation, or related processes. Therefore we expect BAG3 may be an important regulator of malignant transformation, tumor invasion or metastasis. Based on these preliminary results, we would like to examine BAG3 first (BAG2, BAG4, BAG5 will be analyzed later) in breast cancer biology.

**Task 6.** Determine the incidence of BAG-family protein expression in breast cancers (months 12-36).

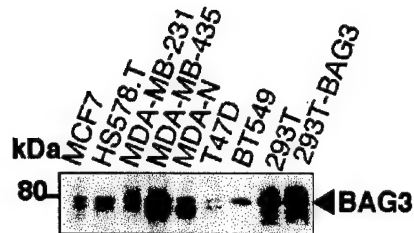
We have generated polyclonal antisera in rabbits for immunodetection of BAG3, using a recombinant GST fusion protein containing residues 380-575 of the human BAG protein and BAG3 protein specific peptides (276-294: REGSPARSSTPLHSPSPIR) conjugated to KLH and OVA (Pierce, Inc.) as immunogens. For production of GST-BAG3 protein, a partial BAG3 cDNA was subcloned into pGEX 4T-1 and transformed into *E. coli*. Cells in late-stage log-growth were induced using 0.1 mM IPTG and harvested after overnight culture at 25°C. *E. coli* cells were collected and lysed by sonication. Recombinant GST-fusion protein was then purified by affinity chromatography using glutathione-Sepharose. New Zealand White female rabbits were injected s.c with either 0.25ml of GST fusion protein (0.5mg/ml) or combination of 0.25 ml each of KLH-peptide (1mg/ml) and OVA-peptide (1 mg/ml) immunogens in Freund's incomplete adjuvant (dose divided over 10 injection sites) and then boosted three times at weekly intervals. The polyclonal anti-BAG3 peptide antibody was used for immunoblot assays, using lysates from several cell lines, including Jurkat T cell, HT1080, 697 B cell, RS11846 B cell, SupT13 T cell and HEK293T. In Figure 7C, lysates from mouse cell lines were used for immunoblot assays to explore whether our antibody can cross-react with the murine BAG3 protein. Anti-recombinant BAG3 antibody detected a single ~80kDa band, which fits with expectations for the size of mouse BAG3. Since human and mouse BAG3 amino acid sequences share 84% identity and 88% similarity, it is not surprising that this antibody can detect mouse BAG3 as well as human BAG3. Recently, we generated antisera against all BAG family proteins. Characterization of BAG4 and 5 antibody is underway.



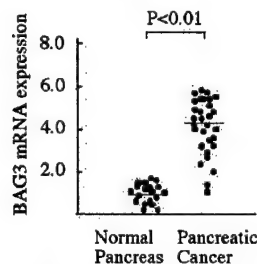
**Figure 10. Specificity of polyclonal anti-BAG3 and BAG2.** (A) pcDNA3 myc BAG3 and pcDNA3 control plasmids were transfected into HEK293T cells. At 24 hrs after transfection, cells were harvested and lysed in 0.5% NP40, 20 mM HEPES (pH 7.7), 142 mM KCl, 5 mM MgCl<sub>2</sub>, 2 mM EGTA. Samples were normalized for protein content (25 µg) and subjected to SDS-PAGE, then transferred on nitrocellulose membrane by electro-transfer. Protein from cells transfected with pcDNA3myc-BAG3 ("3") and pcDNA3 control vector ("C") were run side by side in duplicate blots, which were incubated with either anti myc monoclonal antibody (9E10: Santa Cruz biotech) (left) or anti-BAG3 polyclonal antibody (Bur102) (right), followed by detection using an ECL kit (Amersham). (B) Protein lysates were made as described above from various cell lines as indicated. Immunoblot analysis was performed using anti BAG3 peptide antibody, in combination with ECL-based detection. (C) Anti-recombinant BAG3 antibody was used for western blot analysis. Protein lysates were made from Balb/c 3T3 and GM701 fibroblast cell lines. (D) Same experiment as A using MycBAG2 expression vector and Bur101 anti-BAG2 antibody.

**Figure 11. Immunoblot analysis of BAG3 protein expression in human breast cancer cell lines.**

Detergent lysates (RIPA buffer) were prepared from human breast tumor cell lines, normalized for protein content (25 µg), and subjected to SDS-PAGE (12% gels)/immunoblot analysis using anti-BAG3 polyclonal antibody with ECL-based detection. Each blot contains lysates from untransfected 293T cells and 293T cells transfected with pcDNA3myc-BAG3, serving as a control and for normalization of results.

**BAG3 is over-expressed in pancreatic cancer.**

Pancreatic cancer accounts for 6% of all cancer deaths in the United States and has one of the worst prognoses of all human malignancies, with an overall 5 year survival rates of less than 1% when all stages are combined (14, 15). These highly fatal cancers have a deceptively silent growth habit, so that by the time they are diagnosed they are rarely curable. One of the reasons for the dismal prognosis is the general resistance of pancreatic cancer to chemotherapy and radiation. In collaboration with Dr. Markus Buchler of the U. Bern, we analysed BAG3 expression in human pancreatic cancer tissues and cell lines. BAG3 mRNA was expressed at moderate to high levels in all pancreatic samples, but at low levels in normal pancreas. Quantitative comparisons of relative mRNA levels revealed a significant increase in BAG3 mRNA in pancreatic cancers compared to normal pancreas (Figure 10). In situ hybridization assay and immunohistochemistry analysis revealed that BAG3 was over-expressed in the pancreatic cancer cells (see manuscript provided in appendix). Interestingly, BAG3 expression levels in pancreatic cancer cell were also highly upregulated after heat stress. These findings strongly suggest that BAG3 expression become pathologically elevated in most pancreatic cancers, providing additional evidence that BAG3 is a cancer-relevant gene.

**Figure 12. Over-expression of BAG3 mRNA in pancreatic**

**cancers.** Relative levels of BAG3 mRNA compared for pancreatic cancers (n = 30) and normal pancreas (n = 19) specimens. Total RNA (20 µg) isolated from normal and cancerous pancreatic tissues was subjected to Northern blot analysis and hybridized with the <sup>32</sup>P-labeled BAG3 cDNA probe. Blots were subsequently rehybridized with a 7S cDNA probe to verify equivalent RNA loading. Densitometry was used to

quantify Northern blot data. Relative BAG3 mRNA expression was calculated as OD<sub>BAG3</sub>/OD<sub>7S</sub> for each sample, and the fold increase over the mean in the normal pancreatic tissues was calculated. Horizontal lines represent the mean values of each group.

We recently found that Cytosolic immunostaining for BAG-1 was upregulated in 79 (65%) of 122 invasive breast cancers (P < .001) compared with normal breast. Elevated BAG-1 was significantly associated with longer DMFS and OS, overall (stages 1 and II) and in node-negative (stage I only) patients, on the basis of univariate and multivariate analyses (DMFS, P = .005; OS, P = .01, in multivariate analysis of all patients; DMFS, P = .005; OS, P = .001, in multivariate analysis of

node-negative patients). All other biomarkers failed to reach statistical significance in multivariate analysis. Clinical stage was an independent predictor of OS ( $P = .04$ ) and DMFS ( $P = .02$ ). These findings provide preliminary evidence that BAG-1 represents a potential marker of improved survival in early-stage breast cancer patients, independent of the status of axillary lymph nodes. See attached paper, Turner et al J Clin Oncol, 2001.

### **KEY RESEARCH ACCOMPLISHMENTS**

- 1 We determined structure of BAG domains in BAG1, BAG4 by NMR analysis.
- 2 GST fusion protein of BAG domain from BAG3-5 was purified. We found that not all of these BAG domain can bind to ATPase domain of Hsp70.
- 3 Cytosolic immunostaining for BAG-1 was upregulated in invasive breast cancer comparing with normal breast.
- 4 Rabbit antisera have been generated and characterized against all protein of BAG family.
- 5 BAG3 represent over expression in breast cancer cell lines and shows tumorigenic activity in Balb/c 3T3 cell line. BAG3 also overexpressed in pancreatic adenocarcinoma.
- 6 We cloned guanine nucleotide exchange factor as a BAG3 binding protein.

### **REPORTABLE OUTCOME**

- 1 Brikanova et al Nature Structure Biology, 2001
- 2 Turner et al, Journal of Clinical Oncology, 2001
- 3 Takayama et al, Nature Cell Biology, Review, 2001
- 4 Brikanova et al Journal of Biological Chemistry in press 2002
- 5 Lee et al FEBS letter 2001
- 6 Brive et al BBRC, 2001

### **CONCLUSIONS**

Structural analysis of the Hsc70-binding BAG domain of BAG1 has revealed an anti-parallel two helix bundle, proceeded by an additional long  $\alpha$ -helix. Site-directed mutagenesis has confirmed that the polar surfaces of the  $\alpha$ -helices in the BAG domain are directly involved in chaperone binding, which has been confirmed by NMR experiments. Similarly, an ~80 amino acid region (229-308) of Hsc70 has been determined to represent a minimal domain sufficient for binding the BAG domain. The conserved BAG domains of BAG1 family protein from plant and yeast also bind the Hsc70 ATPase domain. Recently, the solution structure of BAG domain from BAG4 has been determined by multidimensional nuclear magnetic resonance methods and compared to the corresponding domain in BAG1. In BAG4, each helix in this bundle is three to four turns shorter than its counterpart in BAG1, which reduces the length of the

domain by one-third. We also determine the interaction surface and responsible amino acid, which interact to Hsc70. Using these knowledge, we will try to see the structure functional analysis of BAG family proteins in breast cancer growth.

In addition to the Hsp70-binding domain, BAG-family proteins also contain a diversity of additional domains, which allow them to interact with specific target proteins or which target them to specific locations within cells. The BAG-family proteins operate as bridging molecules that recruit molecular chaperones to target proteins, presumably modulating protein functions through alterations in their conformations, and ultimately affecting diverse cellular behaviors including cell division, migration, differentiation, and death. Emerging knowledge about BAG-family proteins suggests a mechanism for influencing signal transduction through non-covalent post-translational modifications. From the effort to explore N-terminal domain, we found several interacting partners for BAG3.

Cytosolic immunostaining for BAG-1 was upregulated in 79 (65%) of 122 invasive breast cancers ( $P < .001$ ) compared with normal breast. These findings provide preliminary evidence that BAG-1 represents a potential marker of improved survival in early-stage breast cancer patients, independent of the status of axillary lymph nodes. We therefore will examine BAG family proteins as potential biomarkers for breast cancers.

The human BAG3 protein is a cytosolic protein of 575 amino-acids length which contains a WW domain, followed by a proline rich region, and then the Hsc70/Hsp70-binding BAG domain. WW domains are found in several proteins of relevance to signal transduction, and are known to bind XPPXY motifs. The proline-rich region of BAG3 contains several PXXP motifs, which are known to interact with SH3 domains, and indeed BAG3 has been reported to bind the SH3 protein, Phospholipase C $\gamma$  (PLC $\gamma$ ). These structural features of the BAG3 proteins suggest that BAG3 is involved in some aspect of signal transduction. In this regard, using two-hybrid methods, we have identified candidate BAG3 binding proteins, including a Guanine Nucleotide Exchange Factor and we have confirmed its association with BAG3 in vitro and in vivo. Our hypothesis therefore is that BAG3 co-ordinates signals related to cell adhesion, cytoskeleton regulation, or related processes. Consistent with this hypothesis, over-expression of BAG3 is transforming in 3T3 fibroblasts. Interestingly, our preliminary data also suggest that BAG3 is over-expressing in cancer cells. As such, BAG3 may be an important regulator of malignant transformation, tumor invasion or metastasis.

During these three years, we investigated fundamental biology of BAG family proteins. We hope that we can extend this project for further findings to establish new treatment and diagnosis of breast cancer.

## **REFERENCES**

1. Takayama, S., Krajewski, S., Krajewska, M., Kitada, S., Zapata, J. M., Kochel, K., Knee, D., Scudiero, D., Tudor, G., Miller, G. J., Miyashita, T., Yamada, M., and Reed, J. C. Expression and location of Hsp70/Hsc-

- binding anti-apoptotic protein BAG-1 and its variants in normal tissues and tumor cell lines., *Cancer Res.* 58: 3116-3131, 1998.
2. Packham, G., Brimmell, M., and Cleveland, J. L. Mammalian cells express two differently localized Bag-1 isoforms generated by alternative translation initiation, *Biochem. J.* 328: 807-813, 1997.
3. Lee, J. H., Takahashi, T., Yasuhara, N., Inazawa, J., Kamada, S., and Tsujimoto, Y. Bis, a bcl-2 binding protein that synergizes with bcl-2 in preventing cell death., *Oncogene.* 18: 6183-6190, 1999.
4. Doong, H., Price, J., Kim, Y. S., Gasbarre, C., Probst, J., Liotta, L. A., Blanchette, J., Rizzo, K., and Kohn, E. CAIR-1/BAG-3 forms an EGF-regulated ternary complex with phospholipase C- $\gamma$  and hsp70/hsc70, *Oncogene.* 19: 4385-4395, 2000.
5. Jiang, Y., Woronicz, J. D., Liu, W., and Goeddel, D. V. Prevention of constitutive TNF receptor 1 signaling by silencer of death domains, *Science.* 283: 543-546, 1999.
6. Takayama, S., Xie, Z., and Reed, J. An evolutionarily conserved family of Hsp70/Hsc70 molecular chaperone regulators, *J. Biol. Chem.* 274: 781-786, 1999.
7. Briknarová, K., Takayama, S., Homma, S., Baker, K., Cabezas, E., Hoyt, D. W., Li, Z., Satterthwait, A. C., and Ely, K. R. BAG4/SODD protein contains a short BAG domain, *J Biol Chem.* *In press*, 2002.
8. Takayama, S., Sato, T., Krajewski, S., Kochel, K., Irie, S., Millan, J. A., and Reed, J. C. Cloning and functional analysis of BAG-1: a novel Bcl-2 binding protein with anti-cell death activity., *Cell.* 80: 279-284, 1995.
9. Takayama, S., Bimston, D. N., Matsuzawa, S., Freeman, B. C., Aime-Sempe, C., Xie, Z., Morimoto, R. J., and Reed, J. C. BAG-1 modulates the chaperone activity of Hsp70/Hsc70., *EMBO J.* 16: 4887-4896, 1997.
10. Brive, L., Takayama, S., Briknarová, K., Homma, S., Ishida, S. K., Reed, J. C., and Ely, K. R. The carboxyl-terminal lobe of Hsc70 ATPase domain is sufficient for binding to BAG1, *Biochem Biophys Res Comm.* 289: 1099-1105, 2001.
11. Knee, D. A., Froesch, B. A., Nuber, U., Takayama, S., and Reed, J. C. Structure-function analysis of Bag1 proteins: effects on androgen receptor transcriptional activity., *J Biol Chem.* 276: 12718-12724, 2001.
12. Froesch, B. A., Takayama, S., and Reed, J. C. BAG-1L protein enhances androgen receptor function., *J Biol Chem.* 273: 11660-11666, 1998.
13. Takayama, S., Kochel, K., Irie, S., Inazawa, J., Abe, T., Sato, T., Druck, T., Huebner, K., and Reed, J. C. Cloning of cDNAs encoding the human BAG1 protein and localization of the human BAG1 gene to chromosome 9p12, *Genomics.* 35: 494-498, 1996.
14. Alanen, K. A. and Joensuu, H. Long-term survival after pancreatic adenocarcinoma--often a misdiagnosis?, *Br J Cancer.* 68: 1004-5., 1993.
15. Tsiotos, G. G., Farnell, M. B., and Sarr, M. G. Are the results of pancreatectomy for pancreatic cancer improving?, *World J Surg.* 23: 913-9., 1999.

that BAG4 recruits Hsp70 to these receptors, thereby resulting in conformational changes in TNFR1 and DR3 that prevent them from clustering and initiating a signal-transducing complex in the absence of extracellular ligand<sup>34,35</sup>. Elevated levels of BAG4 mRNA have been described in pancreatic cancer, in association with resistance to TNF $\alpha$ <sup>36</sup>.

**BAG6.** BAG6 is a nuclear protein, which regulates apoptosis, and which is conserved throughout metazoan evolution, with homologues in flies, frogs and humans. The *Xenopus* homologue was first identified as a target of the *Drosophila* killer protein Reaper<sup>37</sup>. BAG6 binds apoptosis-inducer Reaper, and purportedly sequesters an unidentified pro-apoptotic molecule that causes cytochrome *c* release from mitochondria, an event linked to apoptosis induction. A model based on the available data has been presented in which it is speculated the existence of a ternary complex, containing BAG6, Hsp70 and the mystery apoptosis-inducer<sup>38</sup>. The model proposes that the substrate-binding domain of Hsp70 traps the pro-apoptotic factor, while the BAG domain of BAG6 binds the ATPase domain of Hsp70. Reaper binding to BAG6 induces release of the ATPase domain of Hsp70 and frees the pro-apoptotic factor<sup>38</sup>. Because many of these studies have thus far been executed using ectopic introduction of *Drosophila* Reaper in vertebrate cells or extracts, it will be interesting to explore whether the recently described mammalian Reaper-like protein SMAC(Diablo) similarly interacts with BAG6.

### Co-chaperone activity of BAG-family proteins

The C-terminal BAG domains of BAG1, BAG2, BAG3 and BAG6 have been shown to be sufficient for binding and modulating Hsp70 chaperone activity *in vitro*<sup>1-3,38-42</sup>. In this regard, the peptide substrate refolding cycle of Hsp70 is regulated by the ATPase domain, which effects interactions of the carboxyl substrate-binding domain with polypeptide substrates, controlling substrate binding and release. This coordination of the two domains within Hsp70 chaperones is thought to occur through conformational changes, which are translated from the ATPase domain to the substrate-binding domain in concert with cycles of ATP binding, hydrolysis and ADP release<sup>8</sup>. BAG-family proteins have been reported as both negative and positive regulators of Hsp70-mediated refolding of denatured substrates *in vitro*, depending on the co-chaperone (Hdj1 or Hdj2), concentration of each component and the concentration of inorganic phosphorus (Pi)<sup>1-3,38-42</sup>. Precisely how the BAG domain does this is controversial, but some analogies have been drawn to chaperone regulation in prokaryotes<sup>39</sup>.

The bacterial Hsp70 homologue DnaK is regulated by the co-chaperones DnaJ and GrpE<sup>8</sup>. DnaJ promotes ATP hydrolysis by DnaK, resulting in the ADP-bound conformation of DnaK, which binds peptide substrate complexes tightly. The GrpE protein functions as an ADP-ATP exchange protein, which replaces ADP with ATP, enhancing release of substrate peptides. Together, DnaJ and GrpE promote rapid cycles of ATP hydrolysis, substrate binding, nucleotide exchange and peptide release. Eukaryotes contain DnaJ homologues such as Hdj1 (Hsp40), Hdj2 and Hsj1 in humans, which have analogous functions to their prokaryotic counterparts (reviewed in ref. 8). However, GrpE homologues do not exist in higher eukaryotes, indicating that there is a missing factor.

Could the missing co-chaperone be BAG1 and its relatives? The answer seems to be yes, but not exactly. Although BAG1 does regulate Hsp70 in a manner analogous to GrpE<sup>39,43</sup>, differences in GrpE and BAG1 in terms of nucleotide exchange mechanisms have been observed. In particular, GrpE stimulates both ATP and ADP release from DnaK, whereas BAG1 only releases ADP from the ATPase domain of Hsp70<sup>44</sup>. Also, unlike the effects of GrpE on DnaK where marked increases in DnaK's ATPase activity are seen, BAG1 has only modest effects (1–2-fold increase) on the overall ATPase activity of Hsp70. Thus, the importance of BAG1 as a nucleotide exchange factor remains controversial<sup>40,42</sup>. Moreover, in eukaryotes, several additional co-chaperones have been identified, including

Hip, Hop and Chip proteins, indicating greater complexity in higher organisms (reviewed in refs 45,46). Hip and BAG1 compete for binding to the ATPase domain of Hsp70, indicating that a proper balance of these proteins may be required for optimal protein substrate folding reactions. Thus, BAG-family proteins probably can have either net positive or negative influences on substrate folding *in vivo*, depending on the ratios of other co-chaperones and the specific substrate protein in question.

### Structure of BAG domain, implications for function

The three-dimensional structures of chaperone-binding fragments of BAG1 have recently been solved, permitting comparisons with the previously published GrpE-DnaK structure<sup>47</sup> and providing additional evidence of similarities in some of the functions of BAG family proteins and GrpE. The BAG1 structures include the final 124 residues of the human BAG1 protein in a complex with the ATPase domain of Hsc70 solved by X-ray crystallography, and a nuclear magnetic resonance solution-structure of the final 120 residues of murine BAG1 by itself<sup>48,49</sup>. Both GrpE and BAG1 contain a long  $\alpha$ -helix preceding the chaperone-binding BAG domain, but here the similarity ends. In GrpE, the DnaK-binding domain consists mostly of  $\beta$ -strands<sup>47</sup>. In contrast, the Hsp70-binding BAG domain of BAG1 consists of two amphipathic  $\alpha$ -helices arranged in an anti-parallel fashion that makes contact with Hsp70 through residues lining the polar surface of the domain. The ATP-binding pocket in Hsp70 and DnaK resides at the convergence of two globular lobes. Deletion of either of these lobes prevents stable binding of GrpE<sup>44,50</sup>. The structure of the BAG1/Hsc70 complex also reveals contacts with both lobes of the ATPase domain<sup>48</sup>. Thus, it can be speculated that both GrpE and BAG1 stabilize opening of the nucleotide-binding cleft between the lobes of the ATPase domain of DnaK and Hsp70, respectively. How these GrpE- and BAG1-mediated conformational changes in the ATPase domain are translated into changes in peptide substrate binding of the chaperones is unclear and presumably must await determination of the structures of full-length molecules.

The two anti-parallel  $\alpha$ -helices that constitute the Hsp70-binding BAG domain make contacts on their back-side with a long upstream  $\alpha$ -helix seen in the BAG1 structures, indicating that this additional  $\alpha$ -helix plays a potentially important role in fixing the angle of the Hsp70-binding  $\alpha$ -helices for insertion between the lobes of the ATPase domain of Hsp70<sup>48,49</sup>. Secondary structure prediction methods indicate that most BAG domains are preceded by an  $\alpha$ -helix of variable length (Fig. 3). Taken together, these observations imply that the relevant fold may be longer than the region originally defined as the 'BAG' domain based on amino-acid sequence alignments<sup>1</sup>, and indicate that a three rather than two  $\alpha$ -helical fold may constitute the true Hsp70-binding fold found in BAG-family proteins. A similar three  $\alpha$ -helix protein fold has been recognized in the Syntaxin proteins<sup>49,51,52</sup>. In these proteins, one of the  $\alpha$ -helices involved in intra-molecular associations can dislodge and interact with other proteins. A similar phenomenon may occur for some BAG-family proteins. For example, mutagenesis studies are consistent with Raf1 and Hsp70 interacting with overlapping regions on BAG1, with Raf1 binding the  $\alpha$ 1 and  $\alpha$ 2-helices and Hsp70 binding the  $\alpha$ 2 and  $\alpha$ 3 helices<sup>13</sup>. Likewise, the minimal region of Bcl-2 that binds BAG1 corresponds to  $\alpha$ 1 and  $\alpha$ 2 (unpublished data), whereas Hsp70 directly contacts  $\alpha$ 2 and  $\alpha$ 3 (see Fig. 3). Because Bcl-2 and related proteins contain a protein-binding pocket known to accept amphipathic  $\alpha$ -helical domains (BH3 domains)<sup>53</sup>, it is tempting to speculate that one of the  $\alpha$ -helical segments seen in the recent BAG1 structures interacts with Bcl-2 in an analogous manner. Thus,  $\alpha$ -helix swapping mechanisms may allow BAG1 to choose between different partners, with stress-induced increases in Hsp70 shifting the balance towards BAG1/Hsp70 complex formation at the expense of other possible interactions.



**Figure 3 Comparison of BAG domains.** The amino-acid sequences of several BAG-family proteins are aligned, using single-letter code, and showing identical residues in black boxes and similar residues in grey boxes. Insertions of variable length are indicated by Xn. Gaps are represented by dashes. Secondary structure

prediction indicates the presence of three helices in most BAG family proteins, with the distal  $\alpha$ -helices ( $\alpha 2$  and  $\alpha 3$ ) corresponding to the originally defined BAG domain<sup>1</sup> and  $\alpha 1$  representing an upstream  $\alpha$ -helix of variable length. The number at left of each sequence indicates its position in the full-length protein.

Hsp70 production increases, BAG1/Raf1 complexes are replaced by BAG1/Hsp70 complexes, resulting in diminished Raf1 signalling and correlating with inhibition of DNA synthesis and cell growth<sup>13</sup>. In this way, competition between BAG1 and Hsp70 for binding to Raf1 could represent a molecular switch that encourages cells either to proliferate in times of plenty or become quiescent at times of stress.

In addition to Raf1, BAG1 may also influence cell proliferation through effects on several other proteins. For example, BAG1 binds to and somehow interferes with the function of Siah-1<sup>14</sup>, a protein that forms complexes with ubiquitin-conjugating enzymes and controls the turnover of a variety of proteins relevant to cell proliferation and oncogenesis, including  $\beta$ -Catenin, c-Myb and DCC<sup>15</sup>. A role for BAG1 in growth-factor receptor signal transduction has also been suggested, with BAG1 reportedly associating with certain receptors (PDGF-R; HGF-R) and with gene transfer-mediated overexpression of BAG1 promoting factor-independent cell growth or survival<sup>16,17</sup>.

In addition to effects on cytosolic proteins, nuclear isoforms of BAG1 have been identified that modulate gene transcription through poorly defined mechanisms. An interesting feature of the human BAG1 gene is that four isoforms of the BAG1 protein (BAG1S, BAG1, BAG1M and BAG1L) can be produced from a common mRNA by use of alternative translation initiation sites, including a non-canonical CTG codon in one instance<sup>5,18,19</sup>. These isoforms all contain the BAG domain near their C terminus as well as the upstream UBL domain, but they differ in the lengths of their N-terminal regions. The longest, BAG1L ( $M_r$  ~50K), contains a nuclear localization signal (NLS) and resides in the nucleus, whereas BAG1M ( $M_r$  ~46K) has an incomplete NLS and distributes mainly in cytosol, unless dragged into the nucleus through interactions with other proteins<sup>5,6,18,19</sup>. Both BAG1L and BAG1M contain eight copies of a TXSEEX repeat that reportedly allows for their association with DNA *in vitro*<sup>20</sup>. BAG1L and BAG1M can also stimulate transcription from various gene promoters in an apparently 'nonspecific' manner, at least in transient transfection reporter gene assays<sup>21</sup>. It could be speculated therefore that at sites of transcription where DNA becomes exposed upon remodelling of chromatin (for example by co-activator histone acetyl transferases (HATs)), association of the longer isoforms of BAG1 with DNA would position the Hsp70-binding BAG domain of these proteins ideally for affecting the conformations of proteins in transcription complexes, thereby modulating their assembly, disassembly and stability.

In this regard, some BAG1 isoforms have been reported to associate with and regulate the activity of steroid hormone receptors and retinoic acid receptors (RARs), either enhancing or inhibiting their transcriptional activities<sup>22–27</sup>. Moreover, pathological elevations in the levels of BAG1 or its longer isoforms have been described in cancers and may underlie alterations in tumour responses to hormonal or retinoid-based therapies. For example, although BAG1L and BAG1M are minor products in most types of

cells, compared to the originally described BAG1 protein, some cancerous cells have increased levels of one or both of these proteins<sup>5,28</sup>. The BAG1L protein collaborates with the androgen receptor, enhancing its transcriptional activity and rendering this nuclear hormone receptor resistant to anti-androgen drugs, a finding of potential relevance to prostate cancer<sup>23</sup>. Mutations in the BAG-domain that impair Hsp70 binding abolish functional collaboration with androgen receptor, indicating Hsp70-dependence<sup>24</sup>. Conversely, BAG1M inhibits glucocorticoid receptor activity and BAG1 suppresses RAR activity<sup>26,27</sup>. Furthermore, overexpression of BAG1M and BAG1 has been reported to suppress apoptosis induced by glucocorticoids in a lymphocytic leukaemia and by retinoids in a breast cancer cell line, respectively<sup>26,27</sup>. Also, BAG1 gene expression (as assessed by immunohistochemistry) has prognostic significance in some types of cancer. Pathological overexpression of cytosolic BAG1 has been reported in about two-thirds of breast cancers, correlating with longer survival in patients with early-stage disease<sup>29</sup>. Conversely, nuclear BAG1 gene expression has been correlated with adverse outcome in patients with breast cancer or squamous cell carcinomas of the head and neck<sup>30,31</sup>.

**BAG3.** The human BAG3 (also known as CAIR-1 and Bis) protein contains a WW domain, followed by a proline-rich region, and then the Hsp70-binding BAG domain (Fig. 1). The BAG3 gene is inducibly expressed after exposure of cells to CAI, an inhibitor of nonvoltage-gated calcium influx, hence the alternative name, CAI stressed-1 (CAIR-1)<sup>32</sup>. CAIR-1/BAG3 forms an epidermal growth factor (EGF)-regulated ternary complex with Hsp70 and inactive phospholipase C- $\gamma$  (PLC $\gamma$ ). The proline-rich region of BAG3 contains several PXXP motifs, which are candidate interaction sites for SH3 domains. Indeed, BAG3 binds the SH3 domain of PLC $\gamma$ , possibly in a regulated fashion, given that a protein kinase C inhibitor reportedly induces this association. EGF stimulation releases PLC $\gamma$  from BAG3, in association with tyrosine phosphorylation of PLC $\gamma$ . These observations imply a role for BAG3 in modulating growth factor-induced activation of this phospholipase involved in generating second messengers for Ca<sup>2+</sup> mobilization and protein kinase C activation. However, other functions for BAG3 are also possible<sup>33</sup>.

**BAG4.** The tumour necrosis factor (TNF) receptor superfamily regulates signal transduction events implicated in apoptosis induction (caspase activation), such as NF- $\kappa$ B induction. Several members of this receptor family contain death domains within their cytosolic segments. BAG4 (also known as silencer of death domains (SODD)) binds the death domains of TNFR1 and DR3, preventing cell death signalling and NF- $\kappa$ B induction by suppressing ligand-independent receptor oligomerization<sup>34</sup>. Upon ligand binding, BAG4 dissociates from these receptors. Thus, it has been suggested that BAG4 ensures that these TNF-family receptors remain silent until stimulated by their cognate ligands<sup>34</sup>. Further, because the region upstream of the BAG domain is responsible for interactions with the cytosolic domains of TNFR1 and DR3, it has been argued

# Molecular chaperone targeting and regulation by BAG family proteins

Shinichi Takayama and John C. Reed

The Burnham Institute, 10901 North Torrey Pines Road, La Jolla, California 92037, USA; e-mail: jreed@burnham.org

Regulated changes in protein conformation can have profound effects on protein function, although routine laboratory methods often fail to detect them. The recently discovered BAG-family proteins may operate as bridging molecules that recruit molecular chaperones to target proteins, presumably modulating protein functions through alterations in their conformations, and ultimately affecting diverse cellular behaviours including cell division, migration, differentiation and death. Emerging knowledge about BAG-family proteins indicates that there may be a mechanism for influencing signal transduction through non-covalent post-translational modifications.

The genes of the BAG family are found throughout evolution, with homologues identified in yeast (*Saccharomyces cerevisiae*, *Schizosaccharomyces pombe*), invertebrates (*Caenorhabditis elegans*, *Drosophila*), amphibians (*Xenopus laevis*), mammals (humans, mice) and plants (*Arabidopsis thaliana*, *Oryza sativa*; Fig. 1). BAG proteins all contain at least one copy of a roughly 50 amino-acid evolutionarily conserved domain, the 'BAG-domain', that allows them to interact with and regulate Hsp70 (heat shock proteins of relative molecular mass ( $M_r$ ) 70,000 (70K)) family molecular chaperones. Hsp70 molecular chaperones possess an amino-terminal ATPase domain and a carboxy-terminal substrate-binding domain. It is the ATPase domain to which BAG-family proteins bind with high affinity<sup>2,3</sup>.

Humans contain six BAG-family members, including BAG1 (and its various isoforms including RAP46/HAP46), BAG2, BAG3 (CAIR-1; Bis), BAG4 (SODD), BAG5 and BAG6 (Scythe, BAT3;

Table 1). All of these BAG-family proteins contain a BAG-domain near their C terminus, except BAG5 which has four putative BAG domains. In addition to the conserved BAG domain, BAG-family proteins also contain a diversity of additional domains, which allows them to interact with specific target proteins or which targets them to specific locations within cells (Fig. 1). BAG1 and BAG6, for example, contain a ubiquitin-like (UBL) domain. Although the function of this domain is unknown, its conservation in the *C. elegans*, *S. pombe* and *A. thaliana* homologues of BAG1 implies that the UBL domain plays an important role in some aspect of either the function of this protein or its regulation. In this regard, UBL domains can be used either for controlling protein turnover rates or as protein-interaction domains that mediate binding to other proteins, including subunits of the 26S proteasome. Indeed, a recent report suggested the possibility that BAG1 might target interacting proteins to a proteasome-degradation

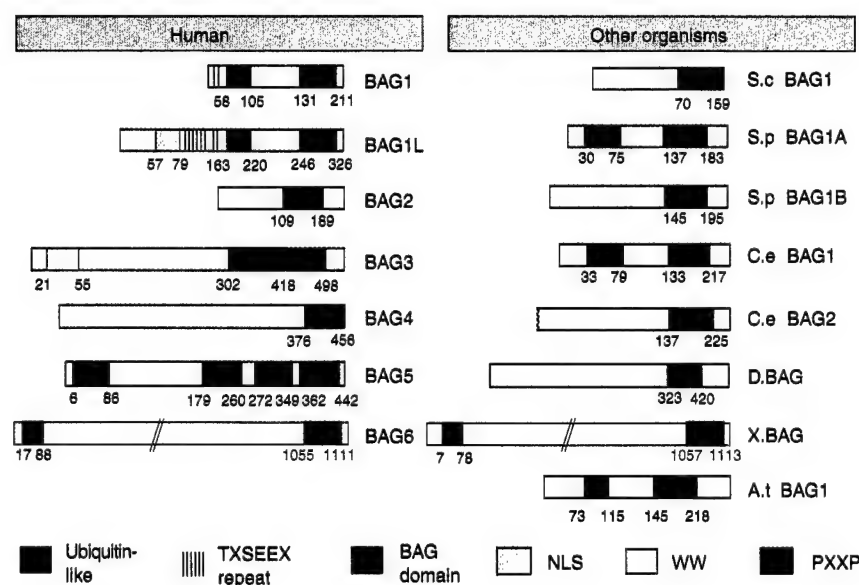


Figure 1 **The BAG family.** The structures of the BAG-family proteins are depicted, showing the conserved BAG domains, as well as other domains found in selected members of the family such as a ubiquitin-like (UBL) domain, nuclear localization signal (NLS), WW domain, TXSEEX repeat and PXXP motifs. Human BAG-family proteins are presented on the left and homologues in other organisms are shown on

the right, including BAG-family proteins from *S. cerevisiae* (S.c), *S. pombe* (S.p), *C. elegans* (C.e), *Drosophila melanogaster* (D), *Xenopus laevis* (X), and *Arabidopsis thaliana* (A.t). Additional plant homologues are not shown. Numbers refer to amino acid positions in the proteins.

pathway in cooperation with Hsp70 family molecular chaperones<sup>4</sup>. However, a lack of effects of BAG1 and BAG6 on the levels of proteins it associates with in cells indicates this is not a universal function of these proteins. BAG1L, a longer isoform of BAG1, contains a nuclear targeting sequence that accounts for its predominantly nuclear location, compared to the cytosolic distribution of BAG1<sup>5,6</sup>. BAG3 (CAIR-1; Bis) contains a WW domain<sup>1</sup>, which is found in several proteins of relevance to signal transduction, and binds peptidyl motifs, sometimes in a phosphorylation-dependent manner<sup>7</sup>.

Although speculative, the topology of BAG-family proteins, with diverse N-terminal domains and conserved Hsp70-binding C-terminal domains, indicates a function for these proteins in targeting molecular chaperones. The BAG-family proteins thus might be viewed as molecular bridges, with the N-terminal domains serving as devices for interactions with specific proteins and the C-terminal BAG domain recruiting Hsp70-family chaperones, thereby targeting the chaperones upon substrates.

# Cellular effects of BAG-family proteins.

In a similar way to Hsp70 molecular chaperones, which serve a wide variety of purposes in cells (reviewed in refs 8–10), BAG-family proteins reportedly can regulate diverse biochemical events, including protein kinase activity, receptor signalling and transcription-factor activity, thereby affecting several cell behaviours ranging from cell division and death to cell migration and differentiation. This functional diversity is paralleled by an abundance of protein targets

claimed to associate with BAG-family proteins, based on either *in vitro* protein interaction experiments or co-immunoprecipitation assays. In some cases, the association of BAG-family members with other proteins may occur as a result of a bridging effect of Hsp70, where the molecular chaperone's N-terminal ATPase domain associates with BAG-family proteins and its C-terminal substrate-binding domain interacts with various target proteins. Because the substrate-binding domain of Hsp70 can bind exposed hydrophobic patches on denatured proteins, this can result in low stoichiometry artifactual interactions with multiple proteins *in vitro*<sup>3</sup>. However, in other instances, BAG-family proteins may directly bind proteins, particularly through regions upstream of their BAG domains.

Of the mammalian BAG-family proteins, only BAG1, BAG3, BAG4 and BAG6 have been investigated for their potential cellular functions. Possibly because BAG1 is the most intensively studied of these proteins, more examples of target proteins are known for it compared to the other BAG-family members. Some of the attributes of the BAG-family proteins are summarized below and in Fig. 2. None of these genes has been ablated (knocked-out) in mice or other organisms to date, and thus the *in vivo* roles of these proteins remain undefined.

**BAG1.** The founding member of the family, BAG1, derives its name from its initial discovery in a screen for genes encoding Bcl-2-binding proteins (Bcl-2-associated athanogene-1)<sup>11</sup>. However, longer isoforms of BAG1 were also soon identified in interaction cloning experiments using other proteins as bait (termed receptor-associated protein of *M*<sub>r</sub> 46K (RAP46) or Hsp70-associated protein of *M*<sub>r</sub> 46K (HAP46)), making it clear that BAG1 can interact with more than one target<sup>3</sup>.

BAG1 overexpression by gene transfer renders cells more resistant to apoptosis, especially when combined with overexpression of the anti-apoptotic protein Bcl-2 (see for example reference 11). Binding of BAG1 to Bcl-2 *in vitro* is dependent on ATP hydrolysis, consistent with involvement of Hsp70-family proteins<sup>2</sup>. Bcl-2 and its homologues predominantly reside in the intracellular membranes of organelles, especially mitochondria, implying intracellular association of these proteins. Moreover, in some types of cells *in vivo*, BAG1 seems to be associated with mitochondria<sup>5</sup>. These observations indicate that BAG1 can modulate apoptosis pathways at least in part through its ability to form complexes with Bcl-2. Thus, it has been speculated<sup>2</sup> that BAG1/Hsp70 complexes modulate the function of Bcl-2 by inducing conformational changes in this anti-apoptosis protein, but direct proof of this is currently lacking.

Another protein target of BAG1 is the serine/threonine kinase Raf1 (ref. 12). BAG1 binds the catalytic domain of Raf1 and stimulates its activity. Recent data indicate that Hsp70 and Raf1 compete for binding to BAG1, with Hsp70 interacting with the BAG domain and Raf1 probably recognizing an overlapping region slightly upstream of the BAG domain<sup>13</sup>. Under stressful conditions, where

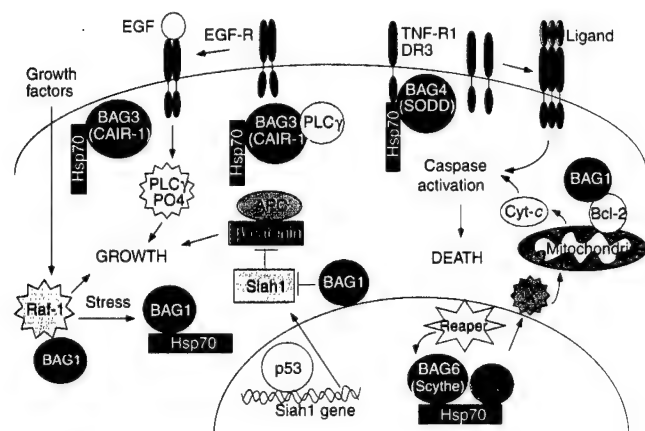


Figure 2 Cellular roles of BAG-family proteins. Some examples of participation of BAG-family proteins in cellular pathways linked to cell proliferation and cell death. See text for details.

Table 1 Human BAG family proteins

Member	Other names	Locus link*	Chromosome	Reported partners
BAG1	RAP46, HAP46, HAP50	#573	9p12	Bcl2; Raf1, Siah1, HGFR; PDGFR; steroid receptors; RAR
BAG2	–	#9532	6p11.2–12.3	–
BAG3	CAIR-1, Bis	#29810	10q25.2–q26.2	PLC $\gamma$ ; Bcl2
BAG4	Sodd	#9530	8p22	TNFR1; DR3
BAG5	–	#9529	14	–
BAG6	Scythe, BAT3	#7917	6p21.3	Reaper

\*Gene locus as indicated at <http://www.ncbi.nlm.nih.gov/locuslink>

## The Carboxyl-Terminal Lobe of Hsc70 ATPase Domain Is Sufficient for Binding to BAG1

Lars Brive, Shinichi Takayama, Klára Briknarová, Sachiko Homma, Stacie K. Ishida, John C. Reed, and Kathryn R. Ely<sup>1</sup>

The Burnham Institute, 10901 N. Torrey Pines Road, La Jolla, California 92037

Received November 7, 2001

**The molecular co-chaperone BAG1 and other members of the BAG family bind to Hsp70/Hsc70 heat shock proteins through a conserved BAG domain that interacts with the ATPase domain of the chaperone. BAG1 and other accessory proteins stimulate ATP hydrolysis and regulate the ATP-driven activity of the chaperone complexes. Contacts are made through residues in helices  $\alpha 2$  and  $\alpha 3$  of the BAG domain and predominantly residues in the C-terminal lobe of the bi-lobed Hsc70 ATPase domain. Within the C-terminal lobe, a subdomain exists that contains all the contacts shown by mutagenesis to be required for BAG1 recognition. In this study, the subdomain, representing Hsc70 residues 229–309, was cloned and expressed as a separately folded unit. The results of *in vitro* binding assays demonstrate that this subdomain is sufficient for binding to BAG1. Binding analyses with surface plasmon resonance indicated that the subdomain binds to BAG1 with a 10-fold decrease in equilibrium dissociation constant ( $K_D = 22$  nM) relative to the intact ATPase domain. This result suggests that the stabilizing contacts for docking of BAG1 to Hsc70 are located in the C-terminal lobe of the ATPase domain. These findings provide new insights into the role of co-chaperones as nucleotide exchange factors.** © 2001 Elsevier Science

**Key Words:** BAG family; heat shock protein; apoptosis; molecular chaperones; nucleotide exchange factor.

The 70-kDa heat shock protein (Hsp70) family constitutes an evolutionarily conserved group of molecular chaperones that are involved in diverse roles in eukaryotic cells, including folding and intracellular targeting of newly synthesized proteins, as well as regulation of signal transduction proteins and transcription factors (reviewed in 1 and 2). Members of the Hsp70

family bind to hydrophobic stretches in polypeptide chains that are exposed during folding or that occur in non-native protein conformations during cell stress. Binding is mediated by cycles of ATP hydrolysis, followed by ADP/ATP exchange and peptide release (3). Binding affinity for unfolded peptide or protein substrates is influenced by binding of nucleotide, such that the ATP-bound form of Hsp70/Hsc70 binds and releases peptide quickly whereas the ADP-bound form maintains tight interaction with substrate. This ATP-driven activity is also regulated by co-chaperones including Hdj-1 (Hsp40;) (4), BAG1 (5), also known as Rap46 and Hap46 (6, 7), Hip/p48 (8), dj2, dj3 (9) and HspBP1 (10). Co-chaperones or accessory proteins influence chaperone activity and protein refolding, stimulate ATP hydrolysis or affect assembly of the chaperone complexes by mechanisms that are not yet fully understood.

One of the major roles for BAG1 appears to be modulating the Hsp70/Hsc70 heat shock protein (5, 8). BAG1 and other members of the BAG family bind Hsc70 through a conserved BAG domain (5, 11) located toward the C-terminus of the various BAG family proteins BAG1 (BAG1M, BAG1L), BAG3, BAG4, BAG5, BAG6 (11). BAG domains are evolutionarily conserved with homologues or orthologues found in humans, mice, *Drosophila*, *C. elegans*, *S. pombe*, *S. cerevisiae* and plants (11, 12). The human homologues BAG1 (HAP46/RAP46), BAG3 (CAIR-1/Bis) (13, 14), BAG4 (SODD) (12, 15), and BAG6 (BAT3/Scythe) (16) function in cell death regulation. BAG1 consists of an antiparallel three-helix bundle (17, 18), with  $\alpha 2$ – $\alpha 3$  corresponding to the highly conserved BAG domain as defined by sequence alignments (11). Secondary structure prediction and sequence homology suggest that most BAG family proteins contain a similar three-helix structure. BAG1 binds tightly to the ATPase domain of Hsc70 ( $K_D = 500$  nM) (19) through one face of the conserved BAG domain with interactions mediated by residues in the second ( $\alpha 2$ ) and third ( $\alpha 3$ ) helices (17, 18). Binding to Hsp70/Hsc70 may be central to several

<sup>1</sup> To whom correspondence should be addressed. Fax: (858) 646-3196. E-mail: [ely@burnham.org](mailto:ely@burnham.org).

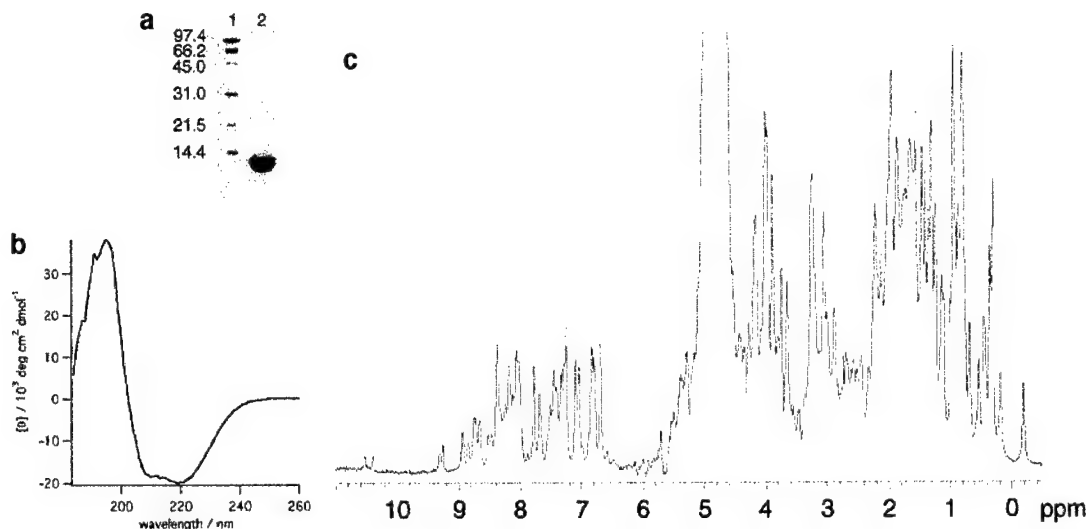


**FIG. 1.** Recombinant Hsc70min is homogeneous, soluble, and well-folded. (a) SDS-PAGE analysis of purified recombinant Hsc70min (residues 229–309) expressed in BL21(DE3) cells. Molecular weight standards are shown in the left lane for comparison. The calculated molecular weight of Hsc70min is 9500 daltons. (b) The circular dichroism spectrum of Hsc70min is typical for a highly helical protein. Calculation of the secondary structure content from the data yields 58% helix, 31% beta structure, and 11% loop, which agrees quite well with the corresponding region in the template (59% helix, 22% beta, 19% loop). (c) 1D  $^1\text{H}$  NMR spectrum of Hsc70min in 90%  $\text{H}_2\text{O}/10\%$   $\text{D}_2\text{O}$ , 150 mM KCl, 20 mM potassium phosphate, pH 6.8, 1 mM DTT, 0.1 mM EDTA. The spectrum was recorded at 37°C. Presaturation was used for solvent suppression.

roles that BAG proteins play in cell regulation. For example, it has been suggested that interaction of BAG1 with Hsc70 provides a bridge between nuclear receptors such as androgen receptor (20, 21) or that BAG1 may form a link between the heat shock chaperone system and the proteasome (22).

Hsp70 chaperones consist of distinct independently folded domains that bind either ADP/ATP or peptide substrate. The N-terminal ATPase domain (~45 kDa) is connected by a linker region to a C-terminal domain that is composed of a 15 kDa substrate-binding region and a 10 kDa module of unknown function. Structural analyses have demonstrated that the ATPase domain is bi-lobed with a central deep crevice where nucleotide is bound (23, 24, 25). In a previous study, we used site-directed mutations to identify surface residues on the ATPase domain of Hsc70 that are required for interaction with BAG1 (17). Loss of binding was observed for those mutations that occurred in the C-terminal lobe of the structure (17). The contacts reported in a crystal structure of BAG1 in complex with Hsc70 ATPase domain correlate well with these results, but also included interactions between BAG1 and the N-terminal lobe of the ATPase domain (18). Another study suggested that eight surface regions across both lobes of the ATPase domain contributed to the interactions with BAG1 (26). Thus it remains controversial whether binding of BAG1 to both the N- and C-terminal lobes of the ATPase domain is important under physiological conditions.

Previously, we localized the BAG1-binding region of Hsc70 to residues 186–377 of the ATPase domain (5).

Within this region, corresponding to the C-terminal lobe of the domain, a sub-domain exists that contains contacts for BAG1. This sub-domain has been expressed separately to probe its role in binding to BAG1. Here, we report that the minimal sub-domain is sufficient for strong binding to BAG1. The results from this study provide evidence that the C-terminal lobe of the ATPase domain of Hsc70 represents a dominant interaction region.

## MATERIALS AND METHODS

**Constructs and plasmids.** DNA encoding the BAG-binding sub-domain of Hsc70 (Hsc70min) corresponding to residues 229–309 in the C-terminal lobe of the ATPase domain was amplified from Hsc70 cDNA by PCR primers: Forward (BamHI-containing primer) GGG-GATCCGGTGGAGAAGATTTTGACAACCG and Reverse (XhoI-containing primer) CCTCGAGTCACCCGTCAGCATTCAGTTCTT-CCCATCGG. The amplified fragment was purified and subcloned into pCR2.1 TOPO T-vector (Invitrogen, San Diego). After sequencing to confirm the correct nucleotide sequence, the BamHI and XhoI digested insert was subcloned into the pGEX4T-1 vector (Pharmacia, Sweden) and transformed into BL21(DE3) strain of *E. coli*.

**Protein expression and purification.** The minimal BAG-binding domain of Hsc70 (Hsc70min) was expressed as a glutathione S-transferase (GST) fusion protein and purified by affinity chromatography on glutathione-agarose resin. For protein expression, a 300 ml overnight culture was diluted to 3.0 l LB medium containing 0.1 mg/ml ampicillin and shaken at 37°C for 85 min. The temperature was decreased to 30°C and IPTG was added to a final concentration of 0.1 mg/ml. After 170 min, cells were harvested by centrifugation and suspended in lysis buffer containing 50 mM Tris, pH 8.0, 0.04 mg/ml lysozyme, 5 mM EDTA, 5 mM  $\beta$ ME and 1 mM PMSF and lysed by douncing. The lysate was clarified by centrifugation. Fusion protein was purified from the lysate on a glutathione-agarose column equilibrated with 50 mM Tris pH 8, 100 mM NaCl. The GST-fusion



**FIG. 2.** An independently folded subdomain of the C-terminal lobe of the Hsc70 ATPase domain is sufficient for binding to BAG1. The results of an *in vitro* protein interaction assay are shown. The GST-fusion proteins representing full-length Hsc70 ATPase domain (1–377) or Hsc70min (229–309) proteins were tested for binding to *in-vitro*-translated BAG1. Samples were analyzed by SDS-PAGE and autoradiography to detect bound BAG1 (top). A GST-fusion of the cytoplasmic domain of CD40 was used as a control. IVT shows 0.2  $\mu$ l *in-vitro*-translated mBAG1. The Coomassie-blue-stained gel is shown in the bottom panel, demonstrating loading of equivalent amounts of GST-fusion proteins.

partner was removed by proteolytic cleavage with thrombin (2 units enzyme/mg protein, 4 h at 22°C), and further purified by glutathione-agarose and ion-exchange chromatography using Q-Sepharose resin (Pharmacia, Sweden). Protein concentration was calculated from the UV absorbance using  $A_{278} = 8400 \text{ M}^{-1} \text{ cm}^{-1}$ . BAG1 (residues 90–219) and Hsc70 ATPase domain (Hsc70 $\Delta$ E) were expressed as GST-fusion and His<sub>6</sub>-tagged proteins, respectively, and purified as described (17, 19).

**Circular dichroism.** CD spectra of Hsc70min (26.4  $\mu$ M in 250 mM NaF, 20 mM KH<sub>2</sub>PO<sub>4</sub>, 1 mM DTT, pH 6.8) were recorded on an AVIV 62A spectrometer (Aviv, New Jersey). Each spectrum was collected at 1 nm intervals. Mean residue molar ellipticities were calculated using Igor Pro 3.0 (Wavemetrics Inc., Oregon). The secondary structure content was predicted from the data by a least squares fit to reference protein sets using DicroProt 2.5 (27) (<http://dicroprot-pbil.ibcp.fr>). The best fits were obtained using the protein set of Chen *et al.* (28).

**In vitro protein interaction assays.** GST-fusion proteins were immobilized on glutathione-Sepharose beads (5  $\mu$ g) and mixed in a volume of 0.1 ml of binding buffer (20 mM HEPES pH 7.7, 142 mM KCl, 5 mM MgCl<sub>2</sub>, 2 mM EGTA, 0.5% NP40) with 1  $\mu$ l of *in vitro*-translated <sup>35</sup>S-L-methionine-labeled BAG1 (pBluescript SKII+). After 1 h incubation at 4°C, the beads were washed three times with 1 ml of ice-cold binding buffer. Following SDS-PAGE separation, autoradiography was used to visualize the proteins.

**Surface plasmon resonance.** Binding affinity and kinetics were studied with a Biacore 3000 (Biacore AB, Sweden) surface plasmon resonance instrument. Anti-GST monoclonal antibodies (Biacore AB) were immobilized (7000 RU) to a CM5 sensor chip by a standard amine coupling procedure. Non-specific binding of Hsc70 $\Delta$ E and Hsc70min to the chip was reduced by preadsorption of the Hsc70min at 10  $\mu$ l/min for 120 sec before each capture of GST-BAG1 (250–450 RU, 10  $\mu$ l/min) on the surface in one of two flow cells. Hsc70 $\Delta$ E or Hsc70min were injected for 12 sec over the surfaces at high flow rate (100  $\mu$ l/min) to minimize mass transport effects. Each injection se-

ries at four concentrations (Hsc70 $\Delta$ E: 3.0, 1.0, 0.33 and 0.11  $\mu$ M; Hsc70min: 110, 36.7, 12.2 and 4.1 nM) and a blank injection was measured three times for each series and the GST-BAG1 surface was regenerated after each round. Low concentrations of the analyte and low surface density of GST-BAG were necessary for the Hsc70min experiments due to the high association rates. Dissociation of GST-BAG1 from the anti-GST surface is negligible as shown previously (19). The running buffer for all experiments was 10 mM HEPES, pH 7.4, 150 mM NaCl, 50  $\mu$ M EDTA, 1 mM  $\beta$ -mercaptoethanol and 0.005% P20 surfactant (Biacore AB). Data from the control cell were subtracted from the GST-BAG1 binding data, and blank buffer sensorgrams from all series were averaged and subtracted from each sensorgram. The data were globally fit to a 1:1 binding model with BIAevaluation 3.1 software (Biacore). Error limits were estimated from the deviations from the mean rate constants of the three individual experiments. Dissociation constants were calculated by the relationship  $K_d = k_d/k_a$ .

**NMR spectroscopy.** All data were recorded on a Varian Unity Plus 500 MHz spectrometer (Varian, Palo Alto). A 1-dimensional spectrum of 2 mM Hsc70min in 20 mM potassium phosphate buffer, pH 6.8, 150 mM KCl, 1 mM DTT, 0.1 mM EDTA was acquired at 37°C. <sup>1</sup>H-<sup>15</sup>N HSQC spectra of <sup>15</sup>N-labeled BAG1 alone or mixed with Hsc70min (0.6 mM) in 1:1 or 2:3 molar ratios (Hsc70min:BAG1) in the same buffer were collected at 37°C. The data were processed and analyzed using Vnmr (Varian) and Felix2000 (Molecular Simulations, Inc). In order to estimate minimal backbone amide resonance shifts of BAG1 upon Hsc70min binding, each peak in the <sup>1</sup>H-<sup>15</sup>N HSQC spectrum of free BAG1 was matched with the closest peak in the spectrum of the complex. The chemical shift change upon Hsc70min binding was then defined as a sum of median-normalized <sup>1</sup>H and <sup>15</sup>N peak shifts.

## RESULTS AND DISCUSSION

To evaluate binding of BAG1 to the molecular chaperone Hsc70, we previously demonstrated that BAG1 binds tightly to the ATPase domain of Hsc70 (19) and that other members of the BAG family also bind to this molecular chaperone (5). BAG proteins contact Hsc70 through residues in helices  $\alpha$ 2 and  $\alpha$ 3 in the three-helix

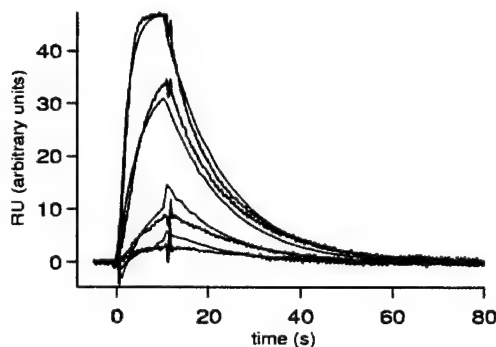


**FIG. 3.** Binding of Hsc70min to BAG1 determined with surface plasmon resonance. The sensorgrams illustrate the relative response for interactions of the minimal BAG1-binding domain Hsc70min at 110, 36.7, 12.2, 4.1, and 0 nM to immobilized GST-BAG1 $\Delta$ N. Rate constants were globally fitted to all four curves within each of the three runs, and the solid lines show the simulated curve from the averaged rate constants. Global fitting of 1:1 binding kinetics yields an estimated equilibrium dissociation constant of  $K_D = 22 (\pm 0.1)$  nM for Hsc70min/BAG1 as compared with 500 ( $\pm 48$ ) nM for Hsc70 $\Delta$ E/BAG1 (Stuart *et al.*, 1998).

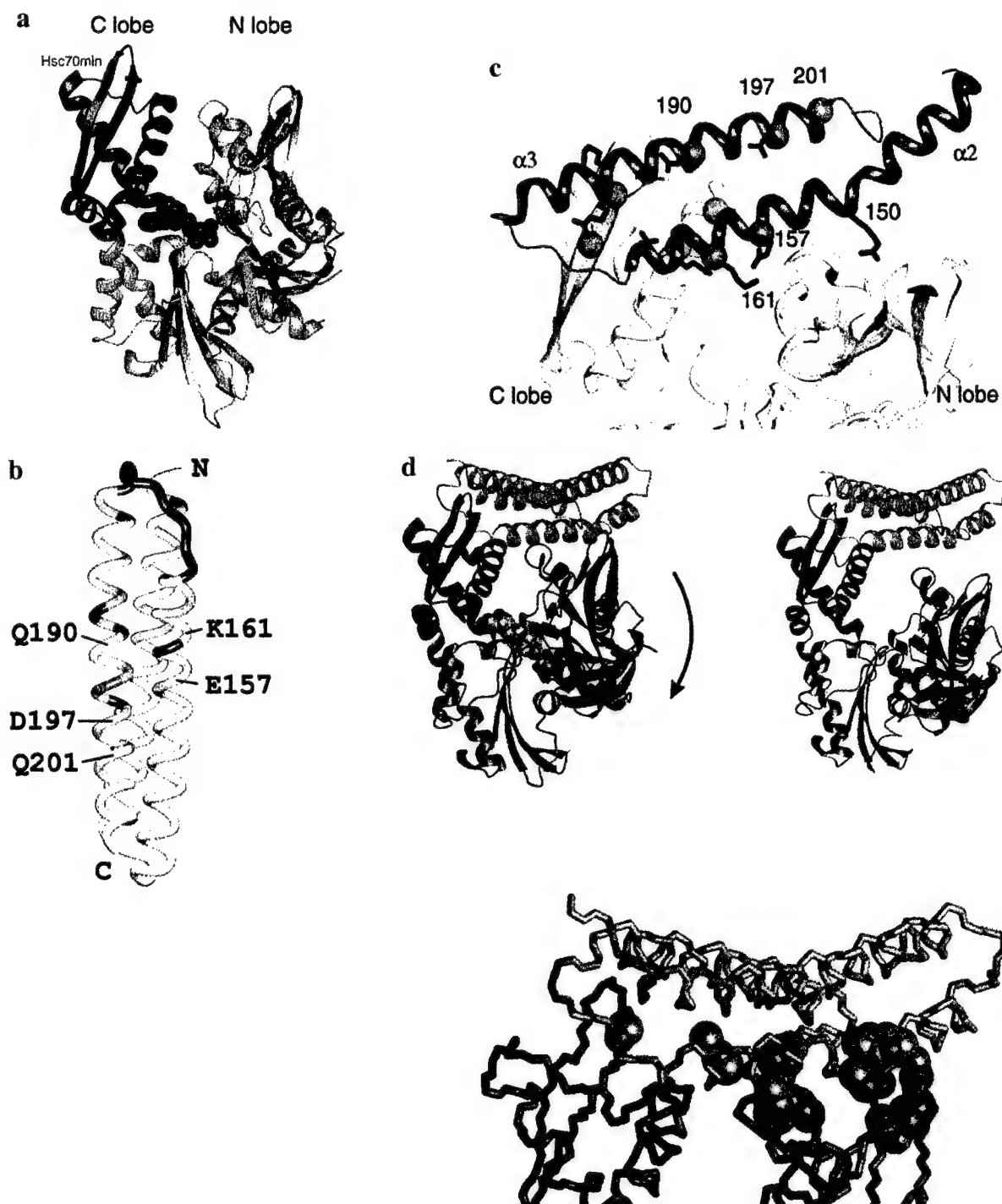


**FIG. 4.** The Hsc70min region is a functional subdomain of the Hsc70 ATPase structure. (a) The ATPase domain of Hsc70 (29) is shown schematically as a ribbon with the N- and C-terminal lobes labeled. The backbone for Hsc70min used in the present study is highlighted in red. The ADP nucleotide, shown as blue spheres, is bound in the deep crevice between the two lobes of the domain. (b) Hsc70min binds to  $\alpha 2$  and  $\alpha 3$  of BAG1. Tube model of BAG1 residues 99–210 (PDB code 1H6Z) (17) is colored according to estimated  $^1\text{H}$  and  $^{15}\text{N}$  chemical shift changes of the individual residues upon binding of Hsc70min. The color intensity is proportional to the change. The sites of mutation that abolish binding to Hsc70 (17) are labeled. (c) Intermolecular contacts between BAG1 and Hsc70 ATPase domain are made predominately with the C-terminal lobe. BAG1 helices  $\alpha 2$ – $\alpha 3$  are shown as an orange ribbon in the upper region of the figure and the interacting regions of the ATPase domain are shown in gray (coordinates taken from PDB 1HX1) (18). Side chains of BAG1 residues that interact through hydrogen bonds or salt bridges with Hsc70 are shown in stick representation. Those that contact the N-terminal lobe are colored blue and those that contact the C-terminal lobe are colored red. Superimposed on this model, spheres mark the residues where mutation to alanine caused loss of binding to Hsc70 (17). (d) BAG1 contacts promote conformational rearrangement in the ATPase domain of Hsc70. Schematic representation of the BAG domain of BAG1 bound to the nucleotide-bound or nucleotide-free form of the Hsc70 ATPase domain. The view of each

bundle, i.e., the conserved BAG domain (17, 18). The contact is made with the ATPase domain of Hsc70. The ATPase domain is bi-lobed with an N-terminal lobe (residues 1–189) and C-terminal lobe (residues 190–373) each consisting of separately folded units. In fact, the C-terminal lobe is encoded by a single exon. A deep nucleotide binding crevice exists between the two lobes and ATP/ADP exchange occurs through this crevice. Our earlier studies suggested that residues in the N-terminal lobe of the ATPase domain (residues 1–186) are not required for binding BAG1 (5). In the course of defining the contact interface between BAG1 and the ATPase domain, we realized that there is a sub-domain of the C-terminal lobe called IIB (25) that contains the contacts required for binding to BAG proteins. All of the residues shown by mutagenesis to be necessary for BAG1 binding (17) were contained in this 80-residue sub-domain. Therefore, we designed and generated this portion of the ATPase domain (Fig. 4a) as a protein tool to probe the interactions between BAG1 and Hsc70.

The residues to be included in the sub-domain were selected by inspection of the three-dimensional structure of the bovine Hsc70 ATPase domain (PDB accession code 1nga; 30). This sub-domain represents  $\frac{1}{4}$  of the ATPase domain in mass and molecular surface. In this study we have demonstrated that this fragment of Hsc70 is the minimal BAG1-binding domain. The sub-domain (Hsc70min) was cloned as a GST fusion protein and transformed into BL21(DE3) cells. The protein was purified to homogeneity by affinity separation and ion-exchange chromatography as shown in Fig. 1. The molecular size was confirmed by SDS-PAGE electrophoresis, gel filtration, and by sedimentation equilibrium. The isolated domain is soluble and well-folded as judged by a narrow thermal denaturation interval and a well-dispersed  $^1\text{H}$  NMR spectrum (Fig. 1). To evaluate whether Hsc70min was correctly folded, the secondary structure of this 80 residue sub-domain was analyzed by circular dichroism (see Fig. 2). The CD measurements indicated that the Hsc70min fragment contains approximately 58%  $\alpha$ -helix, 31%  $\beta$ -sheet and 11% random coil, which is consistent with the secondary structure of the same region in the crystal structure of the intact ATPase domain (29).

Binding of Hsc70min to BAG1 was examined by *in vitro* protein interaction assays. GST-fusion-proteins representing the Hsc70min domain (residues 229–309) or full-length Hsc70 ATPase domain (residues 1–377)

were immobilized on glutathione-Sepharose beads and tested for binding to *in vitro*-translated  $^{35}\text{S}$ -BAG1.  $^{35}\text{S}$ -BAG1 bound to both the Hsc70min and Hsc70 ATPase proteins but not to control proteins (see Fig. 2), indicating that Hsc70min retained the capacity to bind BAG1, apparently including the necessary contact residues. This is consistent with our previous results from deletion analysis indicating that the contact region in Hsc70 for BAG1 recognition is contained within residues 186–377 (5). Our results indicate that an independently folded sub-domain encompassing residues 229–309 from the Hsc70 ATPase domain is sufficient for binding to BAG1. This was verified by NMR spectroscopy. Addition of Hsc70min to  $^{15}\text{N}$ -labeled BAG1 induced pronounced shifts in the  $^1\text{H}$ - $^{15}\text{N}$  HSQC spectrum as shown in Fig. 4b. These shifts correlated well with the results of mutagenesis which identified essential residues for binding the whole ATPase domain (17).

The interaction of Hsc70min with BAG1 was further characterized with surface plasmon resonance spectroscopy. Purified GST-BAG1 was immobilized on the biosensor surface by binding to a covalently-linked high affinity anti-GST antibody. Binding of Hsc70min to BAG1 from solution flowing over the surface was monitored and quantified by a change in refractive index at the surface (see Fig. 3). The response was corrected for contributions from bulk solvent and non-specific binding and the kinetic rate constants were determined. The results confirm that Hsc70min binds to BAG1. The association and dissociation rates for the BAG1/Hsc70min interactions were  $k_a = (3.8 \pm 0.4) \times 10^6 \text{ M}^{-1} \text{ s}^{-1}$  and  $k_d = (8.3 \pm 0.7) \times 10^{-2} \text{ s}^{-1}$ . We previously reported that an Hsc70 construct that contains the ATPase domain and part of the substrate binding domain (Hsc70 $\Delta\text{E}$ ) binds to BAG1 with an equilibrium dissociation constant of 500 nM (Stuart *et al.*, 1998). The estimated equilibrium dissociation constant ( $K_D$ ) for Hsc70min binding to GST-BAG1 was determined in this study to be 22 nM and represents a 10-fold increase in the affinity of the interaction when compared to the interaction with Hsc70 $\Delta\text{E}$ .

The increase in binding affinity observed with the minimal BAG1-binding domain was unexpected. This result may indicate that the binding process is less complex when only a part of the ATPase domain is present. Moreover, comparison of the binding kinetics for Hsc70min vs Hsc70 $\Delta\text{E}$  suggests a mechanism for the interaction. Our results indicate that the dissocia-

complex is the same as that shown for the ATPase domain alone shown in (a). The ribbon models were adapted directly from the co-crystal structure (PDB file 1HX1) (18) with BAG1 in orange and the ATPase domain shown in blue. This conformation represents the nucleotide-free configuration. At upper left, the nucleotide-bound ATPase domain is shown (PDB file 3HSC) (29). The ADP nucleotide is displayed as gray spheres. For this comparison, the coordinates for the C-terminal lobe of the nucleotide-bound ATPase conformer were superimposed on the corresponding residues in the nucleotide-free conformer. Twenty-six intermolecular contacts  $<1.7\text{\AA}$  were noted and shown in the lower panel as colored spheres. With the exception of one close contact, all of the sterically disallowed contacts fall between BAG1 and the N-terminal lobe of the ATPase domain. The proposed conformational shift necessary to prevent this steric hindrance is indicated by an arrow (upper left).

tion rate constants of Hsc70 $\Delta$ E and Hsc70min are similar, whereas the Hsc70min/BAG1 association rate is increased 10-fold, comparable with the increase in binding affinity. The surface area on Hsc70 ATPase domain that is buried when BAG1 binds is  $\sim 1160 \text{ \AA}^2$  (18). However, contacts with the C-terminal lobe at the interface predominate since the surface area buried in the C-terminal lobe is  $870 \text{ \AA}^2$  as compared to  $200 \text{ \AA}^2$  in the N-terminal lobe.

The fact that Hsc70min consists of only the C-terminal lobe of the ATPase domain raises the question of essential contacts for binding of BAG1 to Hsc70 and relates directly to functional implications for nucleotide exchange and substrate release. Our earlier results with deletion mapping (5), combined with the binding analyses using Hsc70min in this study, shows that interactions of BAG1 with the N-terminal lobe of the heat shock ATPase domain are not necessary to form the complex. It has been proposed that BAG1 may act as a nucleotide exchange factor for Hsc70 in a manner homologous to the prokaryotic GrpE. Based on the crystal structure of the complex of BAG1 with a nucleotide-free form of the ATPase domain, Sondermann *et al.* (18) extend the analogy to suggest that, like GrpE, BAG1 promotes a conformational change in the ATPase domain that influences nucleotide exchange. GrpE binds to DnaK, an *E. coli* homologue of Hsc70, contacting both lobes of the homologous ATPase domain (30). GrpE facilitates the ADP/ATP exchange and may influence a conformational change, opening the nucleotide binding crevice. The mechanism may be complex since there are associated conformational changes in DnaK that influence ATP binding/peptide release (31) and temperature-induced structural changes in GrpE itself that shift DnaK toward the ADP-bound state (32).

Structural analysis revealed 13 residues from BAG1 and 11 residues from Hsc70 that are involved in intermolecular interactions at the contact interface between BAG1 and the ATPase domain (18). Importantly, removal of only one or two of these interactions by mutation results in complete loss of binding of BAG1 to Hsc70 (17). For example, as shown in Fig. 6, substitution of alanine for residues E157, Q190 and D197 in BAG1 or R258, R262, and E283 in Hsc70 that are involved in intermolecular salt bridges or hydrogen bonds abolishes binding.<sup>2</sup> The results suggest that a few precise contacts are critical for stabilizing the complex. In the crystal structure, the intermolecular contacts are made predominately with the C-terminal lobe of the ATPase domain. Only two residues in BAG1 (K161 and R150) are closer than  $3.5 \text{ \AA}$  to residues in

the N-terminal lobe of the Hsc70 domain (Fig. 4c). The side chain of R150 forms a salt-bridge with D46 in the N-terminal lobe (18). Interestingly, in our study, substitution of alanine for BAG1 residue R150 did not abolish binding to Hsc70 (17), indicating that this contact is not critical for binding.

The findings reported here provide further insight into the interaction between BAG1 and Hsc70. A portion of the Hsc70 ATPase domain has been defined that is structurally and functionally sufficient for strong binding to BAG1. The observation that Hsc70min binds to BAG1 with higher affinity than the full-length ATPase domain suggests that a portion of the binding energy is used to produce a structural rearrangement in Hsc70, altering the configuration of the nucleotide crevice. This may represent the structural basis for the functional role of BAG1 as a nucleotide exchange factor. Without this conformational rearrangement, steric hindrance with the N-terminal lobe would impede binding of BAG1 to the nucleotide-bound form of the ATPase domain, as illustrated in Fig. 4d. The contacts made with the C-terminal lobe could represent the primary recognition interactions with subsequent close contacts to the surface of the N-terminal lobe being made only after the initial docking to the C-terminal lobe.

## ACKNOWLEDGMENTS

The authors are grateful to M. Havert for purification of the BAG1 protein, N. Preece for assistance with the NMR spectrometer, C. Lombardo for advice with the surface plasmon resonance experiments, and S. Hammond for preparation of the manuscript for publication. This study was funded by grants from the Human Frontier Science Program (to L.B.), The California Breast Cancer Research Program (to K.R.E.), CaP CURE (to K.R.E.), the National Institutes of Health (to J.C.R.), the State of California Cancer Research Program (to S.T.) and the USAMRDC Breast Cancer Research Program (to S.T.).

## REFERENCES

1. Bukau, B., and Horwich, A. L. (1998) The Hsp70 and Hsp60 Chaperone Machines. *Cell* **92**, 351–366.
2. Hartl, F.-U. (1996) Molecular chaperones in cellular protein folding. *Nature* **381**, 571–580.
3. Palleros, D. R., Welch, W. J., and Fink, A. L. (1991) Interaction of hsp70 with unfolded proteins: Effects of temperature and nucleotides on the kinetics of binding. *Proc. Natl. Acad. Sci. USA* **88**, 5719–5723.
4. Freeman, B. C., Myers, M. P., Schumacher, R., and Morimoto, R. I. (1995) Identification of a regulatory motif in Hsp70 that affects ATPase activity, substrate binding and interaction with HDJ-1. *EMBO J.* **14**, 2281–2292.
5. Takayama, S., Bimston, D. N., Matsuzawa, S., Freeman, B. C., Aime-Sempe, C., Xie, Z., Morimoto, R. J., and Reed, J. C. (1997) BAG-1 modulates the chaperone activity of Hsp70/Hsc70. *EMBO J.* **16**, 4887–4896.
6. Bimston, D., Song, J., Winchester, D., Takayama, S., Reed, J. C., and Morimoto, R. I. (1998) BAG-1, a negative regulator of Hsp70

<sup>2</sup> Except for R262, these residues are partly surface-exposed. The fact that mutation of these residues abolishes binding is interesting in light of the study of intermolecular interfaces (32) that showed that mutations with substantial effect on binding affinity are almost exclusively limited to positions that are well-protected from solvent.

- chaperone activity, uncouples nucleotide hydrolysis from substrate release. *EMBO J.* **17**, 6871–6878.
7. Höhfeld, J., and Jentsch, S. (1997) GrpE-like regulation of the Hsc70 chaperone by the anti-apoptotic protein BAG-1. *EMBO J.* **16**, 6209–6216.
  8. Höhfeld, J., Minami, Y., and Hartl, F. U. (1995) Hip, a Novel Cochaperone Involved In the Eukaryotic Hsc70/Hsp40 Reaction Cycle. *Cell* **83**, 589–598.
  9. Terada, K., and Mori, M. (2000) *J. Biol. Chem.* **275**, 24728–24734.
  10. Raynes, D. A., and Guerriero, V. (1998) Inhibition of Hsp70 ATPase activity and protein renaturation by a novel Hsp70-binding protein. *J. Biol. Chem.* **273**, 32883–32888.
  11. Takayama, S., Zhihua, X., and Reed, J. C. (1999) An evolutionarily conserved family of Hsp70/Hsc70 molecular chaperone regulators. *J. Biol. Chem.* **274**, 781–786.
  12. Tschopp, J., Martinon, F., and Hofmann, K. (1999) Apoptosis: Silencing the death receptors. *Curr. Biol.* **R9**, 381–384.
  13. Doong, H., Price, J., Kim, Y. S., Gasbarre, C., Probst, J., Liotta, L. A., Blanchette, J., Rizzo, K., and Kohn, E. (2000) CAIR-1/BAG-3 forms an EGF-regulated ternary complex with phospholipase C- $\gamma$  and Hsp70/Hsc70. *Oncogene* **19**, 4385–4395.
  14. Lee, J. H., Takahashi, T., Yasuhara, N., Inazawa, J., Kamada, S., and Tsujimoto, Y. (1999) Bis, a Bcl-2-binding protein that synergizes with Bcl-2 in preventing cell death. *Oncogene* **18**, 6183–6190.
  15. Jiang, Y., Woronicz, J. D., Liu, W., and Goeddel, D. V. (1999) Prevention of constitutive TNF receptor 1 signaling by silencer of death domains. *Science* **283**, 543–546.
  16. Thress, K., Song, J., Morimoto, R. I., and Kornbluth, I. (2001) Reversible inhibition of Hsp70 chaperone function by Scythe and Reaper. *EMBO J.* **20**, 1033–1041.
  17. Briknarová, K., Takayama, S., Brive, L., Havert, M. L., Knee, D. A., Velasco, J., Homma, S., Cabezas, E., Stuart, J., Hoyt, D. W., Satterthwait, A. C., Llinás, M., Reed, J. C., and Ely, K. R. (2001) Structural analysis of BAG1 Co-chaperone and its interactions with Hsc70 Heat Shock protein. *Nat. Struct. Biol.* **8**, 349–352.
  18. Sondermann, H., Scheufler, C., Schneider, C., Höhfeld, J., Hartl, F.-U., and Moarefi, I. (2001) Structure of a Bag/Hsc70 Complex: Convergent Functional Evolution of Hsp70 Nucleotide Exchange Factors. *Science* **291**, 1553–1557.
  19. Stuart, J. K., Myszk, D. G., Joss, L., Mitchell, R. S., McDonald, S. M., Xie, Z., Takayama, S., Reed, J. C., and Ely, K. R. (1998) Characterization of BAG-1 interactions with Hsc70 molecular chaperones. *J. Biol. Chem.* **273**, 22506–22514.
  20. Froesch, B. A., Takayama, S., and Reed, J. C. (1998) BAG-1L protein enhances androgen receptor function. *J. Biol. Chem.* **273**, 11660–11666.
  21. Knee, D. A., Froesch, B. A., Nuber, U., Takayama, S., and Reed, J. C. (2001) Structure-Function Analysis of BAG1 Proteins: Effects on Androgen Receptor Transcriptional Activity. *J. Biol. Chem.* In Press.
  22. Lüders, J., Demand, J., and Höhfeld, J. (2000) The Ubiquitin-related BAG-1 Provides a Link between the Molecular Chaperones Hsc70/Hsp70 and the Proteasome. *J. Biol. Chem.* **275**, 4613–4617.
  23. Flaherty, K. M., DeLuca-Flaherty, C., and McKay, D. B. (1990) Three-dimensional structure of the ATPase fragment of a 70K heat-shock cognate protein. *Nature* **346**, 623–628.
  24. Sriram, M., Osipiuk, J., Freeman, B. C., Morimoto, R. L., and Joachimiak, A. (1997) Human Hsp70 molecular chaperone binds two calcium ions within the ATPase domain. *Structure* **5**, 403–414.
  25. Osipiuk, J., Walsh, M. A., Freeman, B. C., Morimoto, R. I., and Joachimiak, A. (1999) Structure of a new crystal form of human Hsp70 ATPase domain. *Acta Cryst.* **D55**, 1105–1107.
  26. Petersen, G., Hahn, C., and Gehring, U. (2000) Dissection of the ATP binding domain of the chaperone hsc70 for interaction with the cofactor Hsp46. *J. Biol. Chem.* **276**, 10178–10184.
  27. Deléage, G., and Geourjon, C. (1993) SOMPA: Significant improvements in protein secondary structure prediction by prediction from multiple alignments. *Comp. Appl. Biosc.* **9**, 197–199.
  28. Chen, Y. H., Yang, J. T., and Chau, K. H. (1974) Determination of the helix and  $\beta$ -form of proteins in aqueous solution by circular dichroism. *Biochemistry* **13**, 3350–3359.
  29. Flaherty, K. M., Wilbanks, S. M., DeLuca-Flaherty, C., and McKay, D. B. (1994) Structural basis of the 70-kilodalton heat shock cognate protein ATP hydrolytic activity. II. Structure of the active site with ADP or ATP bound to wild type and mutant ATPase fragment. *J. Biol. Chem.* **269**, 12899–12907.
  30. Harrison, C. J., Hayer-Hartl, M., Liberto, M. C., Hartl, F.-U., and Kuriyan, J. (1997) Crystal Structure of the Nucleotide Exchange Factor GrpE Bound to the ATPase Domain of the Molecular Chaperone DnaK. *Science* **276**, 431–435.
  31. Grimshaw, J. P. A., Jelesarov, I., Shönfeld, H.-J., and Christen, P. (2001) Reversible thermal transition in GrpE, the nucleotide exchange factor of the DnaK heat-shock system. *J. Biol. Chem.* **276**, 6098–6104.
  32. Mally, A., and Witt, S. N. (2001) GrpE accelerates peptide binding and release from the high affinity state of DnaK. *Nature Struct. Biol.* **8**, 254–257.
  33. Bogan, A. A., and Thorn, K. S. (1998) Anatomy of Hot Spots in Protein Interfaces. *J. Mol. Biol.* **280**, 1–9.

# BAG-1: A Novel Biomarker Predicting Long-Term Survival in Early-Stage Breast Cancer

By Bruce C. Turner, Stanislaw Krajewski, Maryla Krajewska, Shinichi Takayama, Andrew A. Gumbs, Darryl Carter, Timothy R. Rebbeck, Bruce G. Haffey, and John C. Reed

**Purpose:** Among women with early-stage breast cancer treated with lumpectomy and radiation therapy, 30% to 40% will develop metastatic disease, which is often fatal. A need exists therefore for biomarkers that distinguish patients at high risk of relapse. We performed a retrospective correlative analysis of BAG-1 protein expression in breast tumors derived from a cohort of early-stage breast cancer patients.

**Patients and Methods:** Archival paraffin blocks from 122 women with stages I to II breast cancer treated with lumpectomy and radiation therapy (median follow-up, 12.1 years) were analyzed by immunohistochemical methods using monoclonal antibodies recognizing BAG-1 and other biomarkers, including Bcl-2, estrogen receptor, progesterone receptor, p53, and HER2/Neu. Immunostaining data were correlated with distant metastasis-free survival (DMFS) and overall survival (OS).

**Results:** Cytosolic immunostaining for BAG-1 was upregulated in 79 (65%) of 122 invasive breast cancers ( $P < .001$ ) compared with normal breast. Elevated BAG-1 was significantly associated with longer DMFS and OS, overall (stages I and II) and in node-negative (stage I only) patients, on the basis of univariate and multivariate analyses (DMFS,  $P = .005$ ; OS,  $P = .01$ , in multivariate analysis of all patients; DMFS,  $P = .005$ ; OS,  $P = .001$ , in multivariate analysis of node-negative patients). All other biomarkers failed to reach statistical significance in multivariate analysis. Clinical stage was an independent predictor of OS ( $P = .04$ ) and DMFS ( $P = .02$ ).

**Conclusion:** These findings provide preliminary evidence that BAG-1 represents a potential marker of improved survival in early-stage breast cancer patients, independent of the status of axillary lymph nodes.

*J Clin Oncol* 19:992-1000. © 2001 by American Society of Clinical Oncology.

ONE OF EVERY nine women currently develops breast cancer. Among women with early-stage breast cancers treated with lumpectomy and local radiotherapy, 10% to 20% will experience local recurrences and 30% to 40% will develop distant metastatic disease, which is often fatal.<sup>1-6</sup> A need exists for identifying prognostic markers that accurately predict long-term outcome in these patients, thus permitting rational choices among therapeutic options such as adjuvant chemotherapy, surgical resection, radiation therapy, hormonal therapy, and application of newly discovered experimental therapeutics. This is especially important for women with axillary lymph node-negative breast cancer, where the use of systemic chemotherapy and hormonal therapy

remains controversial, and thus, decisions regarding clinical management are especially problematic.<sup>7,8</sup>

Several biomarkers have been shown to provide prognostic information for patients with breast cancer. Overexpression of the HER2/Neu oncoprotein, for example, has been shown to predict breast cancer patients at risk for metastatic disease and shorter survival in some studies.<sup>9-11</sup> The overexpression of the HER2/Neu protein is also used to identify patients that may be candidates for treatment with the humanized monoclonal antibody to HER2/Neu, trastuzumab (Herceptin; Genentech, South San Francisco, CA).<sup>12</sup> Somatic mutations that inactivate the p53 gene, with resulting overexpression of p53 protein, have been identified as predictors of poor prognosis in many subgroups of breast cancer patients.<sup>13-16</sup> Conversely, the expression of estrogen receptor (ER) and the Bcl-2 protein have been associated with favorable outcome in early-stage breast cancer.<sup>17-19</sup> However, among the many biomarkers studied, only the use of ER, progesterone receptor (PR) status, and perhaps immunostaining to detect mutant p53 provides sufficiently reliable information for clinical decision making.

BAG-1 is a multifunctional protein that contains a domain that binds tightly to Heat Shock 70-kd (Hsp70) family molecular chaperones and appears to modulate stress-responses through interactions with a variety of intracellular proteins, thereby regulating diverse cellular processes relevant to cancer, including cell division, cell survival, and cell migration.<sup>20-27</sup> Nuclear and cytosolic isoforms of the

---

From Thomas Jefferson University, Department of Radiation Oncology and Kimmel Cancer Center; University of Pennsylvania School of Medicine, Department of Epidemiology and Biostatistics, Philadelphia, PA; The Burnham Institute, La Jolla, CA; and Yale University School of Medicine, Departments of Therapeutic Radiology and Pathology, New Haven, CT.

Submitted December 8, 1999; accepted October 25, 2000.

Supported by grants no. CA67329 and CA30199 from the National Institutes of Health, Bethesda, MD, and by grant no. DAMD17-99-1-9094 from the United States Army.

Address reprint requests to John C. Reed, MD, PhD, The Burnham Institute, 10901 North Torrey Pines Rd, La Jolla, CA 92037; email: jreed@burnham.org.

© 2001 by American Society of Clinical Oncology.

0732-183X/01/1904-992

BAG-1 protein are produced from a common mRNA by use of alternative translation initiation sites.<sup>28-30</sup> Interestingly, longer nuclear isoforms of BAG-1 reportedly bind to several types of steroid hormone receptors, including ER, and modulate the activities of some of these transcription factors.<sup>30-32</sup> The expression and prognostic significance of BAG-1 expression in breast cancers has not been fully examined, but a recent study suggests that BAG-1 may be unregulated in invasive breast cancer and associated with compromised survival.<sup>33</sup> Using monoclonal antibodies that allow specific detection of human BAG-1 proteins, we have examined the expression patterns of the BAG-1 protein in normal mammary tissues and invasive breast cancers, revealing associations of BAG-1 with patient survival in early-stage breast cancer patients.

## PATIENTS AND METHODS

### Patient Population

We identified 122 early-stage (stage I;  $n = 78$ ; 64%) (stage II;  $n = 44$ ; 36%) breast cancer patients treated at Yale University School of Medicine between 1978 and 1993, representing 20% of the breast cancer database registry at that time and for whom the primary paraffin tumor blocks were available for analysis (Table 1). Patients were excluded from molecular analysis if the breast tumor blocks were unavailable. Staging was performed according to the American Joint

Committee on Cancer, and all patients underwent bone scans to evaluate for metastatic disease. All patients were treated by lumpectomy, with or without axillary dissection, followed by radiation therapy to the intact breast using a median dose of 48 Gy followed by an electron boost to the lumpectomy site to yield a total median dose of 64 Gy. Of the 122 patients, 18 (15%) were treated with adjuvant systemic chemotherapy and 20 (16%) were treated with tamoxifen therapy (Table 1). Treatment was verified by chart review. Of the cohort, 63 of 122 (52%) underwent axillary lymph node dissection with a minimum of six sampled lymph nodes (Table 1). Lymph node biopsies were histologically negative for cancer in 49 (78%) of 63 women, whereas 14 (22%) of 63 had histologic evidence of metastatic spread to axillary lymph nodes (Table 1). The median follow-up for the patient cohort was 12.1 years. The start of the follow-up interval commenced at time of diagnosis, and failure required clinical or radiographic evidence of metastatic disease. Survival was ascertained from the breast cancer database that is updated yearly and maintained by full-time staff. Overall survival (OS) was defined as the time of diagnosis to last follow-up date or time of death for all patients, distant metastasis-free survival (DMFS) as time of diagnosis to development of first evidence of clinical or radiographic metastatic disease, and cause-specific survival (CSS) as the time of diagnosis to death with breast cancer. All patients with deaths not related to breast cancer were included up until the time of their death, after which they were excluded. We defined follow-up period as the time between the beginning of follow-up at diagnosis and a failure event (OS, DMFS, or CSS). If none of these events occurred, individuals were censored at the time of their death from other causes or at the end of the follow-up period. The study was approved by the Human Investigations Committee at the Yale University School of Medicine.

### Immunohistochemical Analysis of BAG-1 and Other Proteins

Paraffin-embedded blocks containing primary tumor specimens fixed in 10% neutral-buffered formalin were evaluated for invasive ductal carcinoma by hematoxylin-eosin staining and processed for immunohistochemical analysis as described previously.<sup>28,34</sup> Tissue sections were deparaffinized in xylene, rehydrated in ethanol, rehydrated with water, and washed in 1% phosphate-buffered saline. After blocking sections with 10% (vol/vol) goat serum, primary antibodies were applied to slides and incubated overnight, using a Dako Universal Staining System automated immunostainer (Dako, Carpinteria, CA). These primary antibodies included a mouse monoclonal antibody specific for human BAG-1 (KS6C8; 0.1% vol/vol ascites) and a rabbit polyclonal for Bcl-2, previously developed in our laboratory.<sup>28,35</sup> The specificity of these antibody reagents has been demonstrated by immunoblotting, immunoprecipitation, peptide-competition, and other methods.<sup>28,35</sup> After washing, the slides were incubated for 30 minutes with either antimouse or antirabbit biotinylated antibody (1:500 vol: vol) followed by either an avidin-biotin HRPase complex reagent (Vector Laboratories, Burlingame, CA), or the Envision-Plus-HRP system (Dako), with diaminobenzidine-based colorimetric detection. Among the other proteins analyzed using immunohistochemistry were several biomarkers previously suggested to provide prognostic information for breast cancer patients. These other biomarkers were detected using monoclonal antibodies to ER and PR (Abbott Laboratories, Abbott Park, IL) using the previously described ER immunohistochemical assay method, monoclonal antibody to HER2/Neu (1:1000 dilution; Dako), and a monoclonal antibody (DO7; 1:750 vol:vol) that recognizes mutant p53 (Oncogene; Cambridge, MA). We also stained

Table 1. Characteristics of Breast Cancer Patients and Tumors

Data	No.	%
Total patients	122	NA
Age at presentation, years		NA
Mean	54	
Range	28-82	
Infiltrating ductal cancer, n	109	89
Infiltrating lobular cancer, n	9	8
Infiltrating medullary cancer, n	4	3
Follow-up, years		NA
Median	12.1	
Range	2-18	
Stage, n		
I/II	122	100
I	78	64
II	44	36
Mean pathologic size, cm	1.7	NA
Axillary dissection, n	63	52
Lymph nodes, n		
Positive	14	12
Negative	49	40
Unknown	59	48
ER positive, n	50	41
PR positive, n	45	37
Adjuvant chemotherapy, n	18	15
Adjuvant tamoxifen, n	20	16

NOTE. Metastatic disease indicates patients who developed clinical or radiographic evidence of detectable metastatic disease.

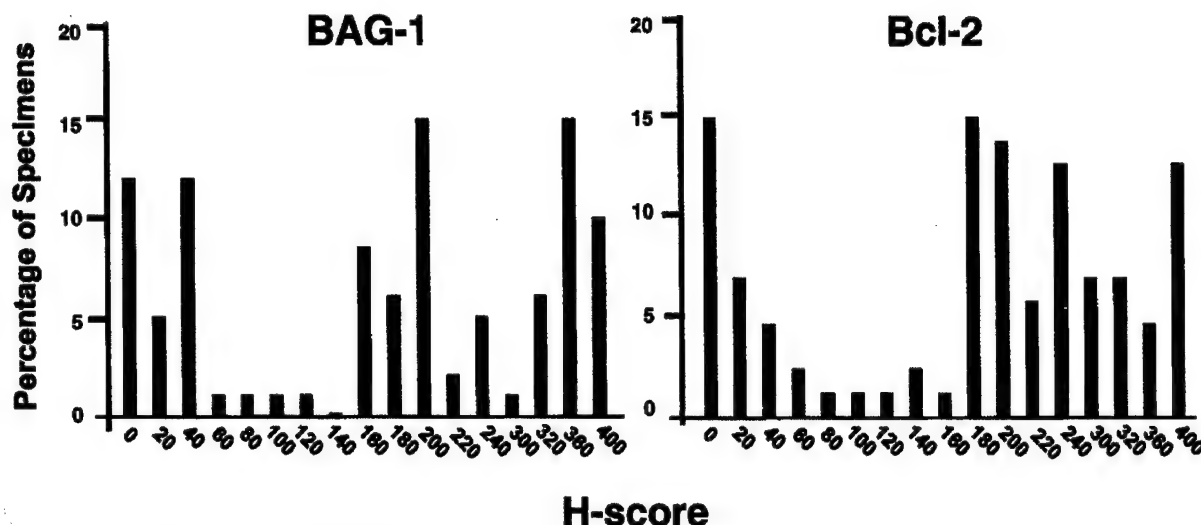


Fig 1. Distribution of BAG-1 and Bcl-2 immunostaining data in invasive breast cancers. The H-score data for invasive breast cancers are presented with H-score on the abscissa and the number of specimens having a particular H-score on the ordinate.

the cohort with an additional monoclonal antibody to ER (6F11; Novocastra Laboratories, Newcastle, United Kingdom, Newcastle-Upon-Tyne, United Kingdom).<sup>17</sup> Immunoscoring was performed separately for both invasive and benign components. The intensity of immunostaining on each slide was rated on a four-point scale: 0, none; 1+, light; 2+, moderate; 3+, heavy; and 4+, intense. The percentage of immunopositive tumor cells was determined by counting a minimum of 200 cells from at least three representative high-power fields. H-scores were then calculated as the product of intensity (0 to 4) X distribution (0% to 100%), with H-scores ranging from 0 to 400. Two tumor sections from each tumor specimen were immunostained and scored separately to minimize any effects of immunohistochemical heterogeneity. However, BAG-1 immunostaining patterns did not significantly differ among pairs of sections from the same breast tumors (data not shown). The pathologist (D.C.) scoring the stained specimens was blinded to the clinical histories of the patients. All samples were reread in a blinded fashion by the pathologist, and the mean H-score of both tumor sections was determined. To set cutoffs for dichotomization of data into high (positive) and low (negative) expression groups, the mean H-score data for the entire data set were displayed as bar-histograms (Fig 1), with H-score on the x-axis and the number of patient samples having a given H-score on the y-axis. A H-score  $\geq 150$  was determined by this approach to be appropriate for use as a cutoff for BAG-1 positivity. Individual H-scores were also determined for Bcl-2 (H-score  $> 180$ ), HER2/Neu (H-score  $\geq 25$ ), p53 (H-score  $\geq 50$ ), ER (H-score  $\geq 75$ ), and PR (H-score  $\geq 75$ ), as previously described.<sup>16,17,36</sup>

#### Statistical Analysis

All patient data, including clinical, pathologic, and outcome measures were entered into a computerized database using the PRODATA database management system (Conceptual Software, Inc, Houston, TX). Multivariate Cox proportional hazards models were fitted to assess whether elevated levels of biomarkers, clinical variables, or pathologic parameters were associated with DMFS, CSS, and OS. Separate models were fitted to assess the effect of cytoplasmic BAG-1 in the total patients sample, those with negative axillary lymph nodes,

and those with positive axillary lymph nodes. All multivariate models contained candidate variables including nuclear BAG-1, Bcl-2, ER, and stage. OS, CSS, and DMFS curves were calculated by the life-table method, with differences between the curves tested by the Mantel-Haenszel statistics test. Variables were included in the model using a stepwise variable selection procedure. A two-sided *P* value of  $\leq .05$  was considered statistically significant.

#### RESULTS

##### *BAG-1 Expression Patterns in Normal Breast Epithelium (NBE) and Malignant Breast Cancers*

BAG-1 immunostaining was compared in the invasive components of breast tumors and adjacent normal breast epithelium present in the same breast cancer biopsy sections. The monoclonal BAG-1 antibody demonstrated specific immunoreactivity in both NBE and invasive breast cancers as demonstrated in Fig 2. Depending on the particular tissue specimen, BAG-1 immunoreactivity in normal and neoplastic mammary cells was found in cytosol, nucleus, or both, consistent with prior studies of BAG-1 immunolocalization in normal tissues.<sup>28</sup> In NBE, BAG-1 immunostaining was generally weak (Fig 2A and B). When present, BAG-1 immunostaining was typically found in the nuclei of NBE cells but not the cytosol, with 25 (28%) of 88 NBE specimens having H-scores  $\geq 150$  for nuclear immunostaining (Table 2). In contrast, although the frequency of invasive cancers with high levels of nuclear BAG-1 immunostaining was not significantly different from NBE (Table 2), cytosolic BAG-1 immunostaining was clearly elevated in many tumors compared with adjacent NBE. Analysis of the immunostaining scores (H-scores) for cytosolic BAG-1

## BAG-1 Upregulation in Breast Cancer

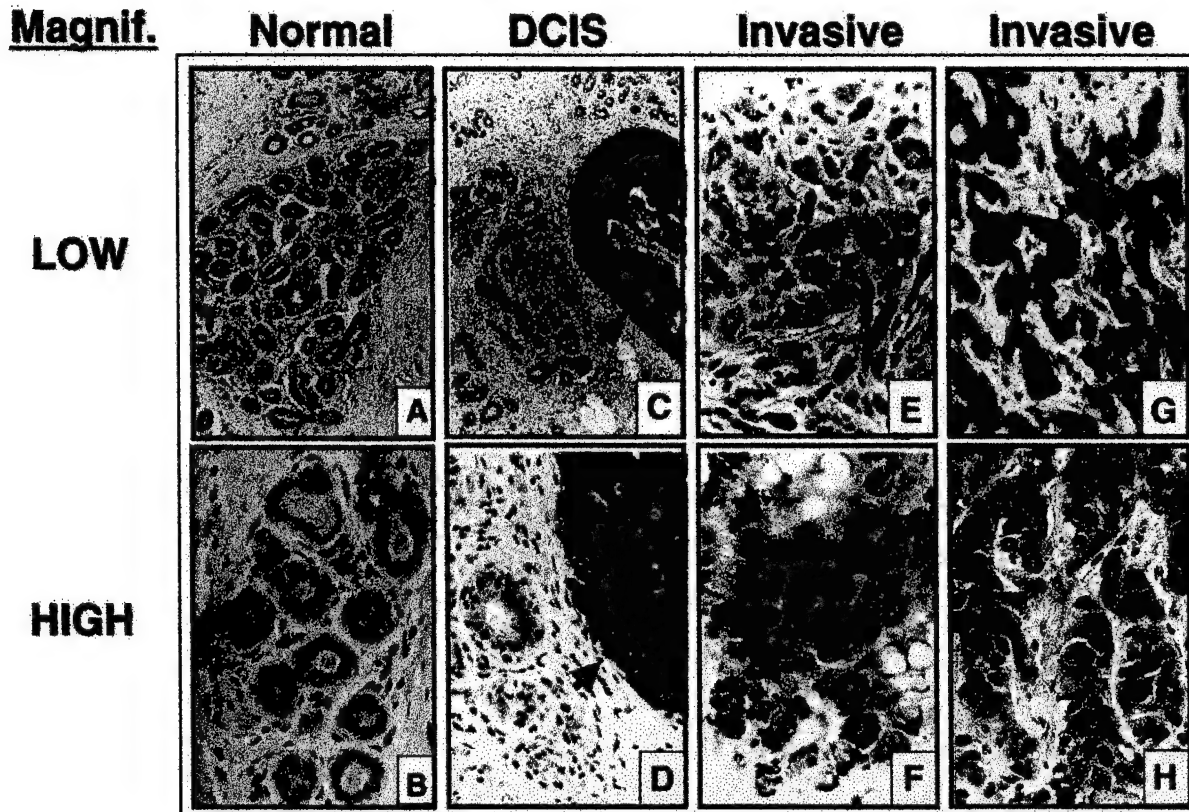


Fig 2. BAG-1 Immunostaining. Abbreviation: DCIS, ductal carcinomas in situ.

demonstrated a bimodal distribution, with invasive cancers having H-scores  $\geq 150$  representing a subgroup having clearly higher levels of this protein (Fig 1). Among the 122 tumor biopsies analyzed, 79 (65%) had invasive cancer

Table 2. Expression of BAG-1 and Bcl-2 in Normal Breast Epithelium and Invasive Cancer Components

Protein	NBE		Cancer		P
	No.	%	No.	%	
BAG-1, cytosolic	10/88	11	79/122	65	< .001
BAG-1, nuclear	25/88	28	28/122	23	NS
Bcl-2	18/106	17	70/106	66	< .001

NOTE. NBE and invasive cancer components were compared with regards to immunointensity. Specimens having an H-score (intensity  $\times$  distribution)  $\geq 150$  for BAG-1 and  $\geq 180$  for Bcl-2 protein positivity were considered positive. Data represent the fraction of immunopositive specimens as determined by mean H-score system. Statistical significance was determined by Fisher  $\chi^2$  analysis.

Abbreviations: NBE, normal breast epithelium; NS, not significant.

components that contained high-level (H-score  $\geq 150$ ) cytosolic BAG-1 immunostaining (Table 2), compared with only 10 (11%) of 88 of NBE specimens ( $P < .001$ ). Thus, roughly two thirds of early-stage breast cancers contained elevated levels of BAG-1 protein in their cytosol, suggesting that upregulation of cytosolic BAG-1 represents a tumor-specific event for a subset of these malignancies. Some of the same tumor specimens also contained histologically evident ductal carcinomas in situ (DCIS) lesions. High levels of cytoplasmic and nuclear BAG-1 immunostaining were present in nine (64%) of 14 and seven (50%) of 14 DCIS specimens, respectively, suggesting that upregulation of BAG-1 can occur as a relatively early event in tumorigenesis (Fig 2C and D; data not shown).

### Bcl-2 Expression in Breast Cancer

It has been shown that the antiapoptotic protein Bcl-2 becomes upregulated during the transition from benign to

malignant epithelium in the breast (reviewed in<sup>37</sup>). Overexpression of the Bcl-2 protein has been correlated with improved survival in both node-negative and node-positive breast cancer patients.<sup>18,19</sup> Analysis of Bcl-2 immunoscores revealed a bimodal distribution, with invasive cancers having H-scores  $\geq 180$  representing a subgroup with distinctly higher levels of this antiapoptotic protein (Fig 1). Of the 106 tumor specimens successfully stained for Bcl-2, 70 (66%) had H-scores  $\geq 180$  (Table 2). Comparison of Bcl-2 and BAG-1 immunostaining data revealed that 62 (82%) of 76 breast tumors had overexpression of both proteins, demonstrating a statistically significant positive correlation of cytosolic BAG-1 immunostaining with Bcl-2 expression ( $P = .0005$ ). Thus, expression of BAG-1 and Bcl-2 may be coregulated to some extent in early-stage invasive breast cancers.

#### Univariate Analysis of BAG-1

Life-table analysis revealed that elevated levels of BAG-1 were statistically significantly associated with longer DMFS ( $P < .001$ ) and OS ( $P < .001$ ) (Fig 3, Table

3). The 10-year DMFS for breast cancer patients with BAG-1 protein overexpression was 79% compared with 34% for those whose tumors scored low for BAG-1 immunoreactivity (Fig 3, Table 3). Likewise, the 10-year OS for women with high BAG-1 protein levels was 82% compared with 42% for patients with breast tumors having low levels of this protein (Fig 3, Table 3). There were 79 (65%) of 122 of breast tumors that were BAG-1 positive and 43 (35%) of 122 BAG-1 negative that were used for the analysis of OS and DMFS (Table 2, Fig 3). The 10-year OS for all 122 breast cancer patients in the study was 68% (data not shown), compared with 82% for patients with early-stage breast cancer that overexpresses the BAG-1 protein ( $P = .01$ ) (Table 3). A strong relationship between the overexpression of cytoplasmic BAG-1 protein and improved survival in breast cancer patients was also detected using several alternative H-score cutoffs, including 25 and 75, in addition to the optimized cutoff of 150 (data not shown). We also found that elevated levels of BAG-1 were associated with improved DMFS ( $P < .01$ ) and OS ( $P < .01$ )

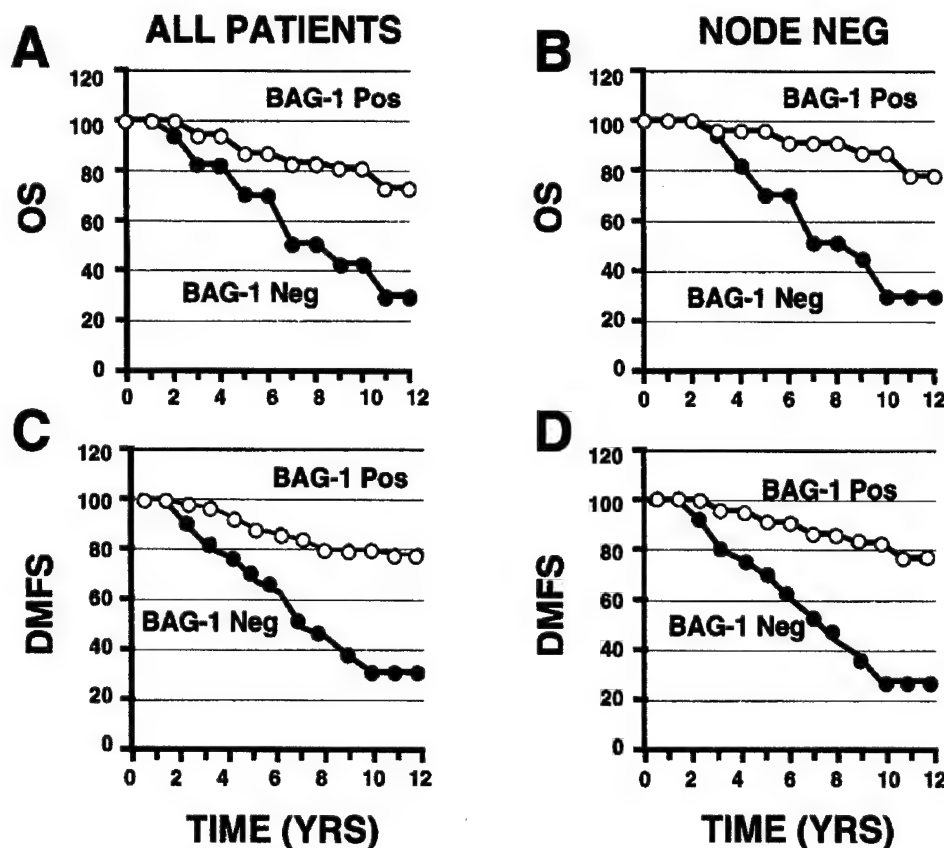


Fig 3. High BAG-1 protein levels associated with improved OS. Abbreviations: Neg, negative; Pos, positive; YRS, years; OS, overall survival; DMFS, distant metastasis-free survival.

when examining levels of intensity of BAG-1 immunoreactivity (intensity  $\geq 2$ ; data not shown).

Because the identification of prognostic biomarkers has a potentially greater role in axillary lymph node-negative breast cancer patients, we performed subgroup analysis examining the importance of BAG-1 cytoplasmic expression in 63 women who underwent axillary lymph node dissection (Table 1). In 49 breast cancer patients with pathologically determined negative axillary lymph nodes, the 10-year OS for women with cytoplasmic expression of BAG-1 was 87% compared with 30% for those patients with low levels of BAG-1 protein ( $P = .001$ ) (Table 3). We also found that elevated levels of BAG-1 protein were associated with significantly improved DMFS and CSS in breast cancer patients whose axillary lymph nodes were not involved with breast cancer ( $P = .002$ ) (Table 3). Although the expression of Bcl-2 often correlates with ER and PR positivity,<sup>18,19,34</sup> we found no correlations between the levels of nuclear or cytoplasmic BAG-1 protein and ER or PR positivity using several different monoclonal antibodies in breast cancer specimens used for this study (data not shown).

**Table 3. Comparison of Biomarkers With 10-Year Survival Parameters**

Marker	OS		DMFS		CSS	
	%	P	%	P	%	P
Cytoplasmic BAG-1						
Neg	42		34		48	
Pos	82	< .001	79	< .001	84	< .001
Cytoplasmic BAG-1, lymph node negative						
Neg	30		29		37	
Pos	87	.001	81	.002	87	.002
Nuclear BAG-1						
Neg	71		64		70	
Pos	79	NS	71	NS	86	.05
Bcl-2						
Neg	40		43		40	
Pos	86	< .001	84	< .001	92	< .001
p53						
Neg	69		70		78	
Pos	55	NS	50	NS	55	.05
HER2/Neu						
Neg	64		62		70	
Pos	73	NS	65	NS	73	NS
ER						
Neg	65		66		69	
Pos	70	NS	74	NS	76	NS
PR						
Neg	66		62		72	
Pos	62	NS	59	NS	68	NS

NOTE. The 10-year survival rates were estimated by the life-table method and differences determined by Mantel-Haenszel. Immunostaining was analyzed by the H-scoring method, using cutoffs of 150, 180, 50, and 75 for BAG-1, Bcl-2, p53, and ER, respectively.<sup>17</sup>

Abbreviations: Neg, negative; Pos, positive.

### Univariate Analysis of Bcl-2

Among the other biomarkers evaluated, Bcl-2 was statistically significant in univariate analysis as a predictor of CSS ( $P < .001$ ), DMFS ( $P < .001$ ), and OS ( $P < .001$ ) (Table 3). The 10-year OS in early-stage breast cancer patients with high levels of Bcl-2 protein immunoreactivity was 86% compared with 40% for women with breast tumors having low levels of the Bcl-2 protein ( $P < .001$ ) (Fig 3, Table 3). The statistically significant relationship with Bcl-2 expression and improved survival was also demonstrated at alternative H-scores, including 25 and 75 (not shown). Our findings are consistent with prior studies demonstrating an important relationship between expression of Bcl-2 protein and improved survival (reviewed in<sup>38,39</sup>). We also found that Bcl-2 positive breast tumors were more likely to be ER positive ( $P = .01$ ) but were not associated with PR positivity ( $P =$  not significant), consistent with prior reports (reviewed in<sup>38,39</sup>).

### Correlations of Other Markers and Survival

In the same cohort of patients, immunohistochemical overexpression of mutant p53 protein was associated with poor CSS ( $P = .05$ ) but not OS or DMFS in univariate analysis (Table 3). Although ER, PR, and HER2/Neu were not of statistical significance as far as predicting survival for this cohort of patients, we did observe a trend to better survival rates in women with breast tumors that expressed ER (Table 3). Among clinical, pathologic, and molecular variables (age, tumor size, stage, tumor histology, PR, p53, HER2/Neu), only stage (I v II) was significant in univariate analysis for predicting OS ( $P = .006$ ; data not shown). There were 38 (31%) of 122 breast cancer patients treated with adjuvant chemotherapy or hormonal therapy, and no significant correlation was seen with respect to OS, DMFS, or CSS in this limited cohort of patients using univariate analysis (data not shown).

### Multivariate Analysis of BAG-1 and Bcl-2

In multivariate analysis using Cox proportional hazards models with variables including BAG-1, Bcl-2, ER, and stage, only the expression of cytoplasmic BAG-1 protein was a statistically significant predictor of OS ( $P = .01$ ), DMFS ( $P = .005$ ), and CSS ( $P = .008$ ) in all 122 breast cancer patients (Table 4). Elevated BAG-1 protein was also statistically significant in a separate multivariate analysis in women with negative axillary lymph nodes for OS ( $P = .001$ ), DMFS ( $P = .005$ ), and CSS ( $P = .002$ ) (Table 4). We did not find any significant relationships between BAG-1 protein and survival in women with positive axillary lymph node, which maybe related to the small size of this sub-

Table 4. Multivariate Analysis of Prognostic Factors With 10-Year Survival Parameters

Marker	OS P	DMFS P	CSS P
Cytoplasmic BAG-1			
All breast cancer patients	.01	.005	.008
Lymph node-negative breast cancer patients	.001	.005	.002
Lymph node-positive breast cancer patients	NS	NS	NS
Nuclear BAG-1, all breast cancer patients	NS	NS	NS
Bcl-2, all breast cancer patients	.07	.11	.007
ER, all breast cancer patients	NS	NS	NS
Stage, all breast cancer patients	.04	.02	.05

NOTE. Data were dichotomized into high versus low groups using H-scores of  $\geq 150$ ,  $\geq 180$ ,  $\geq 75$ , and  $\geq 25$  for BAG-1, Bcl-2, and ER, respectively. Staging was performed using American Joint Committee on Cancer criteria. Multivariate analysis was performed using a Cox proportional hazards regression model, which included BAG-1, Bcl-2, ER, and stage in three multivariate models including all breast cancer patients, lymph node-negative breast cancer patients, and lymph node-positive breast cancer patients.

group. The expression of Bcl-2 was an independent predictor for CSS ( $P = .007$ ) but not DMFS or OS (Table 4). Use of alternative H-scores for BAG-1 and Bcl-2 as described above did not change these conclusions (not shown). There were 38 (31%) of 122 of patients who received systemic therapy, and multivariate analysis revealed that elevated levels of BAG-1 remained a strong predictor of OS when these patients were removed from the analysis, which suggests these findings are not dependent on adjuvant therapy ( $P = .02$ ; data not shown). All other biomarkers including ER and nuclear BAG-1 failed to reach statistical significance. In multivariate analysis of all 122 patients, stage was significant for DMFS ( $P = .02$ ) and OS ( $P = .04$ ) (Table 4).

## DISCUSSION

This is the first study to address the potential prognostic significance of BAG-1 using highly specific immunohistochemical reagents in early-stage breast cancer patients treated uniformly with breast-conserving therapy. The data presented here demonstrate that overexpression of BAG-1 correlates with improved survival in early-stage breast cancer patients, including patients with pathologically-documented negative axillary lymph node biopsies. The *bag-1* gene encodes two major proteins, including BAG-1 and a longer nuclear-targeted isoform BAG-1L.<sup>28,29</sup> Although BAG-1 is preferentially found in the cytosol, the BAG-1L protein is exclusively nuclear.<sup>28,29</sup> However, the shorter BAG-1 protein can also be found in the nucleus under some circumstances, probably as a result of its association with

other proteins that enter nuclei.<sup>24,28</sup> Interestingly, although both normal and malignant mammary epithelial cells sometimes contained prominent nuclear BAG-1 immunoreactivity, cytosolic BAG-1 immunostaining was rarely present at high levels in normal mammary epithelium, whereas cytosolic BAG-1 was clearly elevated in 66% of the invasive breast carcinomas evaluated when compared with normal mammary epithelium.

A recent report of BAG-1 immunostaining in a diverse cohort of breast cancer patients, including women with early- and late-stage disease undergoing a wide variety of therapies, demonstrated upregulation of both nuclear and cytoplasmic BAG-1 immunostaining in 77% of breast cancers studied and increases in cytoplasmic staining without concomitant nuclear staining in 57% of patient tumor specimens.<sup>33</sup> Thus, although that recent study is in agreement with our observations concerning upregulation of cytosolic BAG-1 immunostaining, our findings differ from those of Tang et al<sup>33</sup> with respect to nuclear BAG-1 immunoreactivity. Moreover, Tang et al found that high levels of nuclear BAG-1 immunostaining were associated with shorter, rather than longer, disease-free and overall survival in their collection of heterogeneous patient tumor specimens. Several factors could contribute to differences in the results obtained recently by others and those reported here. For example, the study by Tang et al used a polyclonal anti-BAG-1 antibody that recognizes several isoforms of the BAG-1 protein. The anti-BAG-1 monoclonal antibody chosen for our study, however, has been confirmed to lack cross-reactivity with other BAG-family proteins, including BAGL2, BAGL3, BAGL4, and BAGL5.<sup>40</sup> In contrast, the reactivity of polyclonal antisera with other members of the BAG family has not been addressed. Thus, differences in antibody reagents may play a role in the differences observed. In addition, the cohort of patients examined in our study consisted entirely of early-stage breast cancer patients (stages I and II), whereas the recent report by others included 27% of patients with either metastatic disease or unknown stage.<sup>33</sup> Finally, we correlated nuclear and cytosolic BAG-1 immunoreactivity separately with patient outcome, whereas the method used by Tang et al combined nuclear and cytosolic staining data.

The BAG-1 protein has been shown to form complexes with and modulate the activities of a variety of proteins involved in cell proliferation, survival, and differentiation, including the antiapoptotic protein Bcl-2, the kinase Raf-1, the tyrosine kinase growth factor receptors for platelet-derived growth factor and hepatocyte growth factor, the growth regulator Siah-1, and retinoic acid receptors.<sup>4,21,22,24,25,27</sup> In every instance evaluated so far in cultured cells, overexpression of BAG-1 has been associated with enhanced cell proliferation and survival. Thus, contrary to expectations, higher levels of

cytosolic BAG-1 immunostaining were paradoxically associated with longer OS in the cohort of early-stage breast cancer patients used for this study. The molecular basis for this observation can only be speculated, but it may be related to either (a) the recent realization that BAG-1 is only one member of a family of at least five similar Hsc70/Hsp70-binding proteins that potentially compete for binding to these molecular chaperones<sup>40</sup> or (b) the role of Hip and related cochaperones that also compete with BAG-1 for binding to Hsc70/Hsp70 and that have opposing effects compared with BAG-1 on the Hsc70/Hsp70-mediated peptide refolding cycle.<sup>30,40,42-44</sup> Thus, the ratio of BAG-1 protein relative to other BAG-family members or relative to Hip and its related cochaperones may be the ultimate arbiter of biologic responses, rather than the absolute levels of BAG-1 alone.<sup>45</sup>

The utility of Bcl-2 as a marker of favorable outcome in breast cancer has been established by prior studies, which have included cohorts of breast cancer patients with node-negative or node-positive disease.<sup>18,19</sup> In agreement with these studies, we also found that overexpression of Bcl-2 protein in breast cancer specimens was associated with improved survival characteristics in univariate but not multivariate analysis. Given that Bcl-2 is a potent blocker of apoptosis, higher levels of this antiapoptotic protein would not be expected to correlate with better clinical outcome. However, Bcl-2 is also an antiproliferative protein, at least in some cellular contexts,<sup>46,47</sup> and its antiapoptotic and antiproliferative functions are separable.<sup>48</sup> Moreover, the activity of Bcl-2 can be either positively or negatively modulated by phosphorylation,<sup>49,50</sup> which is not detected by immunohistochemical assays. Thus, the functional status of the Bcl-2 protein in breast cancers remains undefined. Furthermore, ratios of Bcl-2 relative to other members of the Bcl-2 family may play a role in dictating the ultimate phenotypes conferred by this protein, because (a) high levels of Bcl-2 have even been associated with enhanced rather than suppressed sensitivity to apoptosis in some

cellular contexts<sup>51</sup> and (b) the ratio of Bcl-2 to Bax can influence the antiproliferative effects of Bcl-2.<sup>47</sup>

Approximately 30% to 40% of patients with apparently localized breast cancer probably have micrometastatic disease, which is clinically undetectable at the time of diagnosis and which accounts for most instances of distant relapses and disease-related deaths.<sup>1,3</sup> Predictive biomarkers are greatly needed that can help guide clinicians and patients in treatment-related decisions about the necessity (or lack thereof) for adjuvant chemotherapy, hormonal therapy, and new treatments as they become available. The results reported herein indicate that a large proportion of early-stage primary breast cancers arise through a pathway that includes upregulation of BAG-1 protein expression, in agreement with a recent report.<sup>33</sup> The axillary lymph node-negative patients whose breast tumors contain elevated levels of cytosolic BAG-1 protein were found to be more likely to enjoy long-term survival and freedom from distant metastases, compared with those with BAG-1 negative tumors. Moreover, these findings are independent of systemic therapy. Because many of the patients did not undergo axillary dissection or were axillary lymph node-negative, the predictive value of BAG-1 protein in node-positive breast cancer patients remains to be determined and the importance of BAG-1 in predicting survival in lymph node-negative breast cancer patients will now need to be confirmed. Additional studies that seek to establish optimal methods for quantifying expression of specific isoforms of BAG-1 and that involve larger cohorts of patients in prospective trials are needed to firmly establish the overall prognostic utility of BAG-1 testing for women with early-stage breast cancer.

#### ACKNOWLEDGMENT

We thank S.E. Turner, S.R. Turner, E. Smith, and R. Cornell for article preparation. B.C.T. is the recipient of an Radiological Society of North America Scholar Award.

#### REFERENCES

1. Fisher B, Anderson S, Fisher E, et al: Significance of ipsilateral breast tumour recurrence after lumpectomy. *Lancet* 338:327-331, 1991
2. Veronesi U, Saccozzi R, Del Vecchio M: Comparing radical mastectomy with quadrantectomy, axillary dissection, and radiotherapy in patients with small cancers of the breast. *N Engl J Med* 305:6-11, 1981
3. Fischer B, Redmond C, Poisson R: Eight-year results of a randomized clinical trial comparing total mastectomy and lumpectomy with or without irradiation in the treatment of breast cancer. *N Engl J Med* 320:822-828, 1989
4. Stotter A, McNeese M, Ames F: Predicting the rate and extent of locoregional failure after breast conservation therapy for early breast cancer. *Cancer* 64:217-2225, 1989
5. Haffty B, Fischer D, Beinfeld M: Prognosis following local recurrence in the conservatively treated breast cancer patient. *Int J Radiat Oncol Biol Phys* 21:293-298, 1991
6. Haffty B, Reiss M, Beinfeld M: Ipsilateral breast tumor recurrence as a predictor of distant disease: implications for systemic therapy at the time of local relapse. *J Clin Oncol* 14:52-57, 1996
7. Fischer B, Dignam J, Wolmark N: Tamoxifen and chemotherapy for lymph node-negative, estrogen receptor-positive breast cancer. *J Natl Cancer Inst* 89:1673-1682, 1997
8. Group EBCTC: Systematic treatment of early breast cancer by hormonal, cytotoxic, or immune therapy: 133 randomized trials involving 31,000 recurrences and 24,000 deaths among 75,000 women. *Lancet* 339:71-85, 1992
9. Slamon D, Godolphin W, Jones L, et al: Studies of the HER-2/*neu* proto-oncogene in human breast and ovarian cancer. *Science* 244:707-712, 1989
10. Paik S, Hazan R, Fischer E: Pathologic findings from the national surgical adjuvant breast and bowel project: prognostic signifi-

- icance of erbB-2 protein overexpression in primary breast cancer. *J Clin Oncol* 8:103-112, 1990
11. Gusterson B, Gelber R, Goldhirsch A: Prognostic importance of c-erbB-2 expression in breast cancer. *J Clin Oncol* 10:1049-1056, 1992
  12. Carter P, Presta L, Gorman CM: Humanization of an anti-p185 HER2 antibody for human cancer therapy. *Proc Natl Acad Sci U S A* 89:4285-4289, 1992
  13. Thor AD, Moore II DH, Edgerton SM, et al: Accumulation of p53 tumor suppressor gene protein: An independent marker of prognosis in breast cancers. *J Natl Cancer Inst* 84:845-855, 1992
  14. Bergh J, Norberg T, Sjogren S, et al: Complete sequencing of the p53 gene provides prognostic information in breast cancer patients, particularly in relation to adjuvant systemic therapy and radiotherapy. *Nat Med* 1:1029-1034, 1995
  15. Kovach J, Hartmann A, Blaszyck H, et al: Mutation detection by highly sensitive methods indicates that p53 gene mutation in breast cancer can have important prognostic value. *Proc Natl Acad Sci U S A* 93:1093-1096, 1996
  16. Turner BC, Gumbs AA, Carbone CJ, et al: Mutant p53 protein overexpression in women with ipsilateral breast tumor recurrence following lumpectomy and radiation therapy. *Cancer* 88:1091-1098, 2000
  17. King W, DeSombre E, Jensen E, et al: Comparison of immunocytochemical and steroid-binding assays for estrogen receptor in human breast tumors. *Cancer Res* 45:293-304, 1985
  18. Silvestrini R, Veneroni S, Daidone MG, et al: The Bcl-2 protein: a prognostic indicator strongly related to p53 protein in lymph node-negative breast cancer patients. *J Natl Cancer Inst* 86:499-504, 1994
  19. Silvestrini R, Benini E, Veneroni S, et al: p53 and bcl-2 expression correlates with clinical outcome in a series of node-positive breast cancer patients. *J Clin Oncol* 14:1604-1610, 1996
  20. Takayama S, Bimston DN, Matsuzawa S, et al: BAG-1 modulates the chaperone activity of Hsp70/Hsc70. *EMBO J* 16:4887-4896, 1997
  21. Takayama S, Sato T, Krajewski S, et al: Cloning and functional analysis of BAG-1: A novel Bcl-2 binding protein with anti-cell death activity. *Cell* 80:279-284, 1995
  22. Wang H-G, Takayama S, Rapp UR, et al: Bcl-2 interacting protein, BAG-1, binds to and activates the kinase Raf-1. *Proc Natl Acad Sci U S A* 93:7063-7068, 1996
  23. Clevenger CV, Thiekman K, Ngo W, et al: Role of Bag-1 in the survival and proliferation of the cytokine-dependent lymphocyte lines, Ba/F3 and Nb2. *Mol Endocrinol* 11:608-618, 1997
  24. Liu R, Takayama S, Zheng Y, et al: Interaction of BAG-1 with retinoic acid receptor and its inhibition of retinoic acid-induced apoptosis in cancer cells. *J Biol Chem* 273:16985-16992, 1998
  25. Matsuzawa S, Takayama S, Froesch BA, et al: p53-inducible human homologue of Drosophila seven in absentia (Siah) inhibits cell growth: Suppression by BAG-1. *EMBO J* 17:2736-2747, 1998
  26. Naishiro Y, Adachi M, Okuda H, et al: BAG-1 accelerates cell motility of human gastric cancer cells. *Oncogene* 18:3244-3251, 1999
  27. Bardelli A, Longati P, Alberio D, et al: HGF receptor associates with the anti-apoptotic protein BAG-1 and prevents cell death. *EMBO J* 15:6205-6212, 1996
  28. Takayama S, Krajewski S, Krajewska M, et al: Expression and location of Hsp70/Hsc-binding anti-apoptotic protein BAG-1 and its variants in normal tissues and tumor cell lines. *Cancer Res* 58:3116-3131, 1998
  29. Packham G, Brimmell M, Cleveland JL: Mammalian cells express two differently localized Bag-1 isoforms generated by alternative translation initiation. *Biochem J* 328:807-813, 1997
  30. Zeiner M, Gebauer M, Gehring U: Mammalian protein RAP46: An interaction partner and modulator of 70 kDa heat shock proteins. *EMBO J* 16:5483-5490, 1997
  31. Froesch BA, Takayama S, Reed JC: BAG-1L protein enhances androgen receptor function. *J Biol Chem* 273:11660-11666, 1998
  32. Kullmann M, Schneikert J, Moll J, et al: RAP46 is a negative regulator of glucocorticoid receptor action and hormone induced apoptosis. *J Biol Chem* 273:14620-14625, 1998
  33. Tang S-C, Shaheta N, Chernenko G, et al: Expression of BAG-1 in invasive breast carcinomas. *J Clin Oncol* 17:1710-1719, 1999
  34. Krajewski S, Blomqvist C, Franssila K, et al: Reduced expression of pro-apoptotic gene Bax is associated with poor response rates to combination chemotherapy and shorter survival in women with metastatic breast adenocarcinoma. *Cancer Res* 55:4471-4478, 1995
  35. Krajewski S, Thor AD, Edgerton SM, et al: Immunohistochemical analysis of Bax and Bcl-2 in p53-immunopositive breast cancers. *Clin Cancer Res* 3:199-208, 1997
  36. Turner BC, Haffty B, Narayanan L, et al: Insulin-like growth factor-I receptor overexpression mediates cellular radioresistance and local breast cancer recurrence after lumpectomy and radiation. *Cancer Res* 57:3079-3083, 1997
  37. Reed JC: Balancing cell life and death: Bax, apoptosis, and breast cancer. *J Clin Invest* 97:2403-2404, 1996
  38. Schorr K, Li M, Krajewski S, et al: The Bcl-2 gene family and related proteins in mammary gland involution and breast cancer. *J Mammary Gland Biol Neoplasia* 4:153-164, 1999
  39. Zhang GJ, Kimijima J, Tsuchiya A, et al: The role of bcl-2 expression in breast carcinomas. *Oncol Rep* 5:1211-1216, 1998
  40. Takayama S, Xie Z, Reed J: An evolutionarily conserved family of Hsp70/Hsc70 molecular chaperone regulators. *J Biol Chem* 274:781-786, 1999
  41. Yawata A, Adachi M, Okuda H, et al: Prolonged cell survival enhances peritoneal dissemination of gastric cancer cells. *Oncogene* 16:2681-2686, 1998
  42. Gebauer M, Zeiner M, Gehring U: Proteins interacting with the molecular chaperone hsp70/hsc70: Physical associations and effects on refolding activity. *FEBS Lett* 417:109-113, 1997
  43. Gebauer M, Zeiner M, Gehring U: Interference between proteins Hsp46 and Hsp/p60, which bind to different domains of the molecular chaperone hsp70/hsc70. *Mol Cell Biol* 18:6238-6244, 1998
  44. Hohfeld J, Jentsch S: GrpE-like regulation of the Hsc70 chaperone by the anti-apoptotic protein BAG-1. *EMBO J* 16:6209-6216, 1997
  45. Frydman J, Hohfeld J: Chaperones get in touch: The hip-hop connection. *Trends Biochem Sci* 22:87-92, 1997
  46. Pietenpol JA, Papadopoulos N, Markowitz S, et al: Paradoxical inhibition of solid tumor cell growth by bcl-2. *Cancer Res* 54:3714-3717, 1994
  47. Borner C: Diminished cell proliferation associated with the death-protective activity of Bcl-2. *J Biol Chem* 271:12695-12698, 1996
  48. Huang DCS, O'Reilly LA, Strasser A, et al: The anti-apoptosis function of Bcl-2 can be genetically separated from its inhibitory effect on cell cycle entry. *EMBO J* 16:4628-4638, 1997
  49. Haldar S, Chintapalli J, Croce CM: Taxol induces Bcl-2 phosphorylation and death of prostate cancer cells. *Cancer Res* 56:1253-1255, 1996
  50. Itoh T, Deng X, Carr B, et al: Bcl-2 phosphorylation required for anti-apoptosis function. *J Biol Chem* 272:11671-11673, 1997
  51. Chen J, Flannery JG, LaVail MM, et al: bcl-2 overexpression reduces apoptotic photoreceptor cell death in three different retinal degenerations. *Proc Natl Acad Sci U S A* 93:7042-7047, 1996

# Structural analysis of BAG1 cochaperone and its interactions with Hsc70 heat shock protein

Klára Briknarová<sup>1,2</sup>, Shinichi Takayama<sup>1,2</sup>, Lars Brive<sup>1</sup>, Marnie L. Havert<sup>1</sup>, Deborah A. Knee<sup>1</sup>, Jesus Velasco<sup>1</sup>, Sachiko Homma<sup>1</sup>, Edelmira Cabezas<sup>1</sup>, Joan Stuart<sup>1</sup>, David W. Hoyt<sup>3</sup>, Arnold C. Satterthwait<sup>1</sup>, Miguel Llinás<sup>4</sup>, John C. Reed<sup>1</sup> and Kathryn R. Ely<sup>1</sup>

<sup>1</sup>The Burnham Institute, La Jolla, California 92037, USA. <sup>2</sup>These two authors contributed equally to this work. <sup>3</sup>EMSL, Pacific Northwest National Laboratory, Richland, Washington 99352, USA. <sup>4</sup>Department of Chemistry, Carnegie Mellon University, Pittsburgh, Pennsylvania 15213, USA.

BAG-family proteins share a conserved protein interaction region, called the 'BAG domain', which binds and regulates Hsp70/Hsc70 molecular chaperones. This family of cochaperones functionally regulates signal transducing proteins and transcription factors important for cell stress responses, apoptosis, proliferation, cell migration and hormone action. Aberrant overexpression of the founding member of this family, BAG1, occurs in human cancers. In this study, a structure-based approach was used to identify interacting residues in a BAG1-Hsc70 complex. An Hsc70-binding fragment of BAG1 was shown by multidimensional NMR methods to consist of an antiparallel three-helix bundle. NMR chemical shift experiments marked surface residues on the second ( $\alpha 2$ ) and third

( $\alpha 3$ ) helices in the BAG domain that are involved in chaperone binding. Structural predictions were confirmed by site-directed mutagenesis of these residues, resulting in loss of binding of BAG1 to Hsc70 *in vitro* and in cells. Molecular docking of BAG1 to Hsc70 and mutagenesis of Hsc70 marked the molecular surface of the ATPase domain necessary for interaction with BAG1. The results provide a structural basis for understanding the mechanism by which BAG proteins link molecular chaperones and cell signaling pathways.

Both *in vitro* and *in vivo*<sup>1-3</sup>, the BAG domain of BAG1 suppresses refolding of peptide substrates by the molecular chaperone Hsc70. This suppression apparently uncouples ATP-hydrolysis from peptide release<sup>4</sup> and acts as an antagonist of the cochaperone protein Hsc70 interacting protein<sup>2,5</sup> (Hip). BAG-family proteins are conserved throughout evolution, with homologs<sup>5</sup> found in humans, mice, *Drosophila*, *Caenorhabditis elegans*, *Schizosaccharomyces pombe*, *Saccharomyces cerevisiae* and plants. The human members of this family include BAG1, BAG2, BAG3 (CAIR-1/Bis), BAG4 (SODD), BAG5 and BAG6 (BAT3/Scythe)<sup>5-10</sup>. In addition to the BAG domain near the C-terminal end of the molecules, BAG proteins also contain diverse N-terminal regions that target cellular locations and interact with other proteins involved in numerous cellular processes<sup>11,12</sup>. It is speculated that BAG proteins serve as bridging molecules that recruit Hsc70 to specific target proteins, thus creating a novel mechanism to alter cell signaling by conformational change rather than post-translational modification<sup>5-8,10</sup>.

## Structure of BAG domain

NMR experiments indicate that the C-terminal region of BAG1 is highly helical (Fig. 1a), consistent with the results of circular dichroism (CD) analysis and secondary structure prediction<sup>13</sup>.

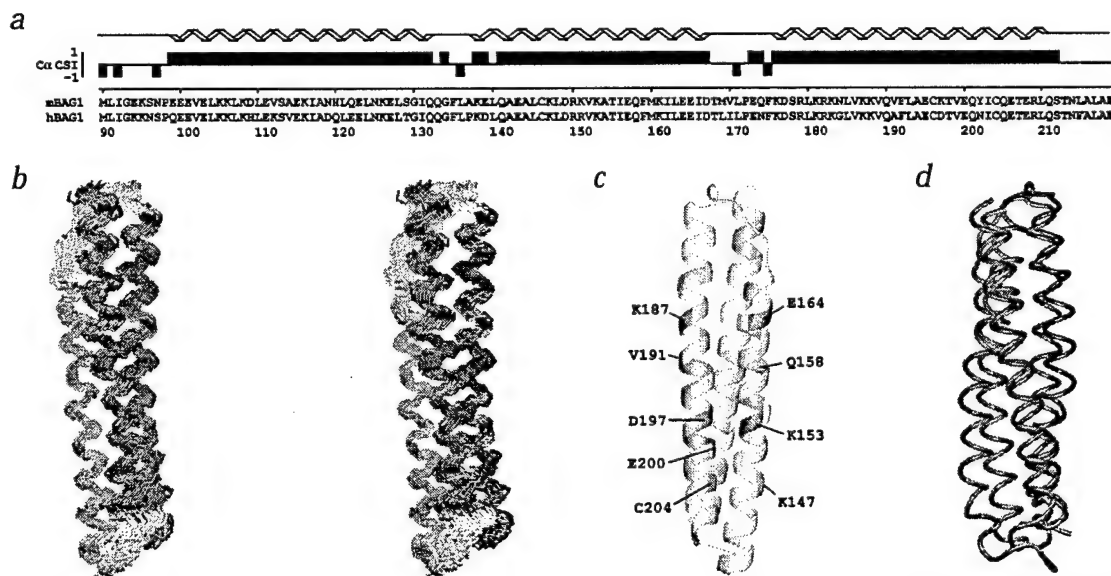


**Fig. 1** C-terminal region of BAG1 is a three-helix bundle. **a**,  $\alpha$  chemical shift index<sup>33</sup> (CSI) of residues 90–219 of murine BAG1 (mBAG1). The sequence of the murine BAG1 fragment used in this study is indicated to scale below the CSI data and aligned with human BAG1L. The  $\alpha$ -helices are defined schematically at the top of the figure. **b**, Stereo image of superimposed backbone traces of a family of 25 final structures of BAG1 residues 99–210. The first helix ( $\alpha 1$ ) is colored blue, the second one ( $\alpha 2$ ) green and the third one ( $\alpha 3$ ) orange; the connecting loops are white. The images were generated with the program MOLMOL<sup>34</sup>. **c**, Ribbon representation of BAG1 residues 99–210 colored according to <sup>1</sup>H- and <sup>15</sup>N-chemical shift changes of the individual residues upon binding of Hsc70 peptide (Asn 256–Cys 267). The color intensity is proportional to the change. Gray indicates residues for which no data are available. Some of the residues with the most pronounced changes are labeled. The model depicted here is rotated 180° relative to the orientation in (b). **d**, Comparison of BAG1 with syntaxin (view as in (a)). Tube models of the  $\alpha$  atoms of residues 101–212 of BAG1 (orange) and residues 27–146 of syntaxin (blue; PDB code 1BRO)<sup>23</sup> are superimposed. Note the similar configuration of helices in these two antiparallel three-helix bundles.

## letters



**Fig. 2** Mutational analysis of BAG1 binding to Hsc70. **a**, GST fusion proteins representing wild type BAG1 (WT; residues 90–219) or mutants were tested. Mutants were made by substituting Ala for surface residues in the central region of the elongated BAG1 molecule at residues on adjacent turns of each  $\alpha$ -helix. The mutations were: H1A (E115A, K116A, N119A); H1B (E123A, K126A); H2A (D149A, R150A); H2B (E157A, K161A); H3A (Q190A); and H3B (D197A, Q201A). Proteins were immobilized on glutathione-Sepharose beads and tested for *in vitro* binding to *in vitro* translated (IVT)  $^{35}$ S-L-Met-labeled Hsc70 ATPase domain (residues 67–377). GST-CD40 (cytoplasmic domain) was included as a negative control. Samples were analyzed by SDS-PAGE and autoradiography to detect bound Hsc70-ATPase (upper panel) and with Coomassie blue staining to verify loading of equivalent amounts of GST-fusion proteins (lower panel). IVT  $^{35}$ S-Hsc70-ATPase was also loaded directly in the gel for comparisons of the amount of input versus bound Hsc70 ATPase. **b**, GST-fusion proteins representing wild type Hsc70 (WT; residues 1–377) or mutant Hsc70 molecules with substitutions at sites predicted to bind BAG1 were tested. The mutations were: B1 (R258A, R262A), B2 (E283A, D285A) and C (E318A, R322A). The proteins were immobilized on glutathione-Sepharose beads and mixed with *in vitro* translated  $^{35}$ S-L-Met-labeled mouse BAG1. The assay to detect bound BAG1 was performed and monitored as described for (a).

The structure of the BAG1 fragment studied here comprises three distinct helical regions —  $\alpha$ 1 (residues Glu 99–Gln 132),  $\alpha$ 2 (residues Lys 138–Asp 167) and  $\alpha$ 3 (residues Lys 176–Leu 210) — arranged in an antiparallel bundle (Fig. 1). Sequence similarities and secondary structure predictions<sup>5,10</sup> suggest that most BAG family proteins may contain a similar three-helix structure.

### Interactions of BAG1 with Hsc70

We predicted regions of direct contact between BAG1 and the ATPase domain (residues 1–377) of Hsc70 (ref. 13) based on homology with a complex of GrpE and the ATPase domain of DnaK (the bacterial counterpart of Hsc70)<sup>14</sup>. To test this model experimentally, synthetic peptides representing two helices (residues Ala 54–Pro 63 and Asn 256–Cys 267), which flank the predicted binding crevice in Hsc70, were used in NMR-monitored titrations of BAG1. The latter peptide, Asn 256–Cys 267, induced pronounced chemical shift changes in the central region of  $\alpha$ 2 and  $\alpha$ 3 of BAG1 (Fig. 1c). These results demonstrated that residues interacting with Hsc70 lie on adjacent turns of  $\alpha$ 2 and  $\alpha$ 3 and are located on the same face of the conserved BAG domain.

Sites for mutagenesis in BAG1 were selected based on the results of these chemical shift experiments and used to evaluate the role of residues at predicted interacting surfaces between the BAG domain and Hsc70. In contrast to wild type protein, mutant BAG molecules with Ala substituted at residues Glu 157 and Lys 161 in  $\alpha$ 2 and Gln 190, Asp 197 and Gln 201 in  $\alpha$ 3 failed to bind Hsc70 ATPase domain in yeast two hybrid (data not shown) and *in vitro* binding assays (Fig. 2). These mutant molecules retained wild type folding patterns, as verified by CD (data not shown). Consistent with the model, mutant proteins with Ala substituted in the central region of  $\alpha$ 1 at residues Glu 115, Lys 116, Asn 119 or Lys 126 retained the ability to bind to Hsc70. The contact surfaces suggested by mutagenesis correlate well with those predicted by the chemical shifts (Fig. 1c). Thus, a region of BAG1 that is essential for binding to the ATPase domain of Hsc70 has been defined.

To test the predicted molecular surface of the ATPase domain of Hsc70 contacting BAG1, the BAG domain was docked interac-

tively to the atomic model of Hsc70 (ref. 15). Our previous studies defined the minimal BAG1-binding region (residues 186–377) of Hsc70 (ref. 1). This region lacks the N-terminal lobe of the bi-lobed ATPase domain. Docking strategies optimized geometric and electrostatic charge complementarity of the central part of the electronegative BAG domain with the C-terminal lobe of the ATPase domain. Residues on the surface of the ATPase domain oriented to contact critical residues in the BAG domain were selected as sites for Ala substitution mutagenesis, including Arg 258, Arg 262, Glu 283 and Asp 285. Unlike the wild type ATPase domain, all of these mutants failed to bind BAG1 when tested in yeast two hybrid (data not shown) and *in vitro* binding assays (Fig. 2). In contrast, substitution of Ala for residues Glu 318 and Arg 322 on the opposite face of this lobe did not inhibit interaction with BAG1. These results define a surface region on Hsc70 that is the site for binding BAG1. This surface differs from that predicted by homology modeling<sup>13</sup> because the contact surface involves only one lobe of the ATPase domain.

The BAG1 and Hsc70 recognition surfaces predicted by these studies are shown in Fig. 3. The interacting region in Hsc70 is located on one face of the C-terminal lobe adjacent to a deep crevice in the bi-lobed ATPase domain. ATP binds at the bottom of this crevice<sup>15,16</sup>. Members of the Hsc70/Hsp70 heat shock family interact with linear peptide folding intermediates. This interaction is mediated by cycles of ATP binding and hydrolysis followed by ADP/ATP exchange and peptide release. The prokaryotic homologue of BAG1, GrpE, binds to both lobes of

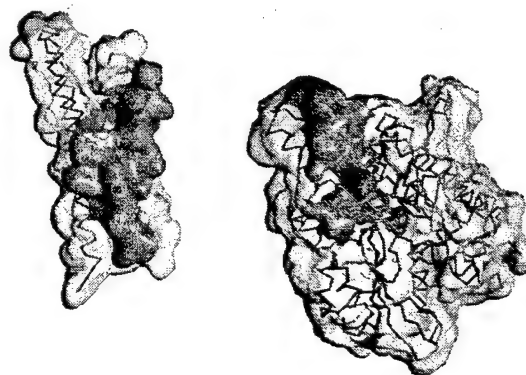
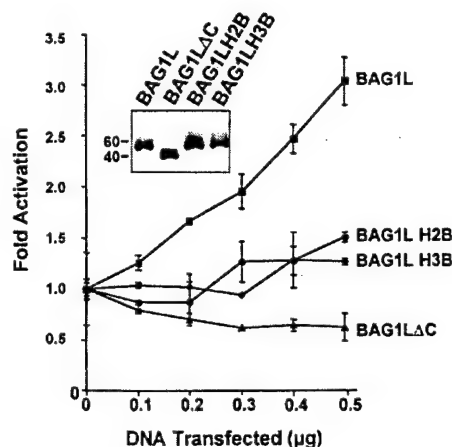


**Fig. 3** Contact regions of the BAG1–Hsc70 ATPase complex. The proteins are represented by red  $\alpha$  traces and transparent surfaces of BAG1 on the left and Hsc70 ATPase domain<sup>15</sup> on the right. An ADP molecule that binds in the cleft between the two lobes of the ATPase domain is shown in red as van der Waals spheres. The complex has been 'opened up' by a 180° rotation of BAG1 to reveal the contact surfaces predicted from mutagenesis and molecular docking. The sites of mutation that abolish binding are colored yellow and adjacent contact sites suggested from molecular docking are colored cyan. This image was produced with the program SPOCK<sup>25</sup>.

**Fig. 4** BAG domain is necessary for transactivation of AR by BAG1L. Mutant BAG1L proteins containing Ala substitutions within the BAG domain that ablated Hsc70 binding *in vitro* and a BAG1L truncation mutant lacking  $\alpha 3$  of the BAG domain ( $\Delta C$ ) were tested. Mutant proteins are H2B (E157A, K161A in  $\alpha 2$ ) and H3B (D197A, Q201A in  $\alpha 3$ ). (These sites are numbered 283, 287, 323 and 327 in human BAG1L). Cos-7 cells were transfected with fixed amounts of pSG5-AR, pLCI, pCMV- $\beta$ Gal and increasing amounts of pcDNA3-BAG1L, wild type and mutants. Cell extracts were prepared and assayed for CAT and  $\beta$ -galactosidase activity at 40 h after transfection. Data are expressed as fold transactivation relative to cells transfected with reporter gene alone (mean  $\pm$  S.E.;  $n = 2$ ).



the Hsp70 homolog DnaK ATPase domain<sup>14,17</sup> and stimulates dissociation of ADP from DnaK by inducing a conformational change in the nucleotide-binding cleft, including the N-terminal lobe of the domain<sup>14</sup>. BAG1 is also known to promote dissociation of ADP<sup>2</sup>, but the mechanism may differ and remains to be elucidated. In contrast to GrpE, our results suggest that contact with the N-terminal lobe of the ATPase domain may not be critical for binding of BAG1.

#### Analysis of the BAG1-Hsc70 contacts *in vivo*

The significance of the structural analyses was tested in intact cells, comparing the bioactivity of wild type and mutant BAG1 proteins. At least four isoforms of BAG1 are produced in many cells, including BAG1 and a longer isoform BAG1L. The unique N-terminal region of BAG1L contains both SV40 large T-like and nucleoplasm-like candidate nuclear localization signals, which target BAG1L to the nucleus<sup>5</sup>. BAG1L has been shown to form complexes with and coactivate steroid hormone receptors<sup>18-22</sup>, such as androgen receptor<sup>11</sup> (AR), in a manner requiring the BAG domain-containing C-terminal region of BAG1. We therefore engineered the same mutations described above for BAG1 into plasmids encoding the BAG1L protein and tested them for the ability to enhance the transcriptional activity of AR. As shown in Fig. 4, wild type BAG1L caused a concentration-dependent increase in AR-mediated transactivation of a reporter gene promoter containing androgen response elements (AREs)<sup>11</sup>. However, mutant BAG1L proteins containing the same Ala substitutions within the BAG domain that ablated Hsc70 binding demonstrated diminished capacity to affect

AR transactivation in these assays. Immunoblot analysis confirmed that the differences in activity of wild type and mutant BAG1L proteins were not attributable to differences in levels of expression. We conclude therefore that the contact residues required for interaction of BAG1 with Hsc70 are critical for the function of this protein in cells.

#### Structural similarity of BAG1 and syntaxin

BAG-family members bind to a variety of intracellular proteins and regulate diverse cellular processes including cell division, survival and migration. Members of this family link cell signaling to molecular chaperones, altering cellular pathways by changing protein conformation. Using the BAG1 structure, the database of known three-dimensional structures was searched with the program DALI<sup>23</sup> for similar folding patterns. A striking similarity (see Fig. 1d) was noted with the syntaxin protein<sup>24,25</sup>. Syntaxins are members of a large family of related proteins that are key components in protein trafficking. The N-terminal region of syntaxin is an independently folded antiparallel three-helix bundle that participates in protein-protein interactions. A hydrophobic groove between helices 2 and 3 on the surface of syntaxin lined by conserved residues can accommodate interactions with another helix in a distal portion of the molecule. This helix is 'swapped' when the molecule associates with SNARE complexes at the plasma membrane<sup>25</sup>. The structural similarities with BAG1 suggest that BAG domains may participate in similar protein-protein interactions, adapting to molecular exchange of  $\alpha$ -helices. Future studies may reveal molecular interfaces in BAG-binding proteins that are complementary with BAG domains, and which may modulate Hsc70/BAG1 interactions.

*Note added in proof:* While this manuscript was under review, a study of the BAG1-interacting surface of Hsc70 ATPase domain using peptide libraries was reported<sup>26</sup>. Also, the crystal structure of BAG1 in complex with nucleotide-free Hsc70 ATPase domain was published<sup>27</sup>. BAG1 residues that interact with the ATPase domain in the crystal structure are located on  $\alpha 2$  and  $\alpha 3$ , as suggested by chemical shift experiments in the present study. The contact surfaces colored here in Fig. 3 include most of the residues seen at the interface in the crystal structure, with the exception of residues in the N-terminal lobe of the ATPase domain. For direct comparison with the crystal structure, the reader should add 55 to the BAG1 sequence number used in our NMR study.

**Table 1** Structural statistics for BAG1

Ensemble	
R.m.s. deviation from experimental restraints <sup>1</sup>	
NOE distance restraints (Å)	0.030 $\pm$ 0.001
Dihedral angle restraints (°)	0.42 $\pm$ 0.03
R.m.s. deviation from idealized geometry	
Bonds (Å)	0.0031 $\pm$ 0.0002
Angles (°)	0.46 $\pm$ 0.01
Impropers (°)	0.36 $\pm$ 0.01
R.m.s. deviation from mean coordinates <sup>2</sup>	
Backbone atoms (N, C $\alpha$ , C) (Å)	1.1 $\pm$ 0.4
Heavy atoms (Å)	1.6 $\pm$ 0.3
Ramachandran plot <sup>2</sup>	
Most favored regions (%)	94.2
Additional allowed regions (%)	4.4
Generously allowed regions (%)	1.0
Disallowed regions (%)	0.4

<sup>1</sup>No NOE distance and dihedral angle restraint was violated by more than 0.5 Å or 5°, respectively, in any of the structures.

<sup>2</sup>Residues 99–210; mean coordinates were obtained by averaging coordinates of the 25 calculated structures, which were first superposed using backbone atoms (N, C $\alpha$ , C) of residues 99–210.

## letters

## Methods

**NMR spectroscopy.** A recombinant fragment containing residues 90–219 of murine BAG1 was purified essentially as described for a longer construct<sup>13</sup>. NMR samples contained 1–2 mM <sup>15</sup>N-, <sup>13</sup>C/<sup>15</sup>N- or <sup>2</sup>H/<sup>15</sup>N-labeled protein in 10 mM potassium phosphate buffer, pH 7.2, 25 mM KCl, 1 mM DTT and 1 mM EDTA in 90% H<sub>2</sub>O/10% D<sub>2</sub>O. Spectra were acquired at 37 °C on a Bruker 500MHz and Varian 500, 600 and 750 MHz spectrometers. The data were processed and analyzed with Felix 98.0 (Molecular Simulations, Inc.). <sup>1</sup>H, <sup>15</sup>N and <sup>13</sup>C assignments were established based on CBCA(CO)NH, HNCACB, HNCO, CBCACOHA, C(CO)NH, H(CCO)NH, HCCH-TOCSY (HB)CB(CGCD)HD, <sup>13</sup>C/<sup>15</sup>N-edited NOESY, 4D <sup>15</sup>N-edited NOESY and HNCACB optimized for Asn and Gln NH<sub>2</sub> groups. Distance restraints were obtained from 3D <sup>15</sup>N-edited NOESY and 3D <sup>13</sup>C/<sup>15</sup>N-edited NOESY.  $\phi$  and  $\psi$  dihedral angle restraints were generated with TALOS<sup>28</sup>. Structures were calculated with the torsion angle dynamics simulated annealing protocol implemented in CNS 1.0 (ref. 29) using restraints for 1,567 interproton distances (98 long range,  $5 \leq |i - j|$ , 267 medium range,  $2 \leq |i - j| \leq 4$ , 363 sequential and 839 intraresidual), 168 hydrogen bond distances, and 88  $\phi$  and 86  $\psi$  dihedral angles. Statistics for 25 final structures are summarized in Table 1.

**Chemical shift experiments and computer modeling.** Helix-nucleated peptides representing helical regions of the ATPase domain of human Hsc70 predicted to bind to BAG1 were synthesized using a protocol described in ref. 30. Helix-nucleation was introduced to stabilize the helical nature of the synthetic peptides, corresponding with the known conformation in the protein<sup>15,16</sup>. The CD spectra for the nucleated peptides were consistent with enhanced helicity<sup>30</sup> relative to control linear peptides. <sup>1</sup>H-<sup>15</sup>N HSQC spectra were recorded for <sup>15</sup>N-labeled BAG1 solutions containing varying concentrations of peptide. Most pronounced resonance shifts of BAG1 amides were noted and mapped onto the structure. To model the binding surfaces in a BAG1–Hsc70 complex, docking of BAG1 to Hsc70 ATPase domain (PDB accession number 1NGA)<sup>15</sup> was performed manually to visually optimize geometric fit and intermolecular distance between contact residues identified from the HSQC experiments and surface residues on the ATPase domain. Docking was directed to contact regions predicted from homology modeling<sup>13</sup>.

**Plasmids.** Mutations in BAG1 were generated by two-step PCR-based mutagenesis using a full length murine BAG1 cDNA (SN 245–9) (ref. 31) as template. Products were purified by QiaQuick gel extraction kit (Qiagen), subcloned into the TOPO TA vector (Invitrogen) and sequenced. The fragments were subcloned into either pGEX4T-1 for expression as mutant GST-fusion proteins or into pJG4-5 for yeast two-hybrid assays. Mutations in Hsc70 were made by the same methods, using a cDNA encoding the ATPase domain<sup>1</sup>.

**Protein interaction assays.** For yeast two hybrid assays<sup>32</sup>, the yeast EGY48 strain was cotransformed with pJG4-5 plasmids encoding wild type or mutant BAG1/B42 transactivation domain fusion proteins, pGilda plasmids encoding Hsc70 ATPase/LexA DNA-binding domain fusion proteins and a  $\beta$ -galactosidase reporter gene (pSH18-34 or pRB1840).

For *in vitro* binding assays, DH5 $\alpha$  cells were transformed with pGEX4T-1 plasmids encoding wild type or mutant GST-BAG1 fusion proteins. After induction at room temperature with 0.1 mM IPTG, cells were lysed by sonication, and expressed proteins were isolated from lysates by affinity purification on glutathione-Sepharose (Pharmacia). *In vitro* translated <sup>35</sup>S-methionine labeled Hsc70 ATPase domain<sup>1</sup> (1  $\mu$ l) was mixed with 5  $\mu$ g immobilized mutant GST-BAG1 fusion proteins, along with negative controls. Alternatively, GST-Hsc70 ATPase domain was produced and immobilized on glutathione-Sepharose and then mixed with *in vitro*-translated <sup>35</sup>S-BAG1 or negative control proteins. After 1 h incubation at

4 °C, beads were washed extensively and then subjected to SDS-PAGE electrophoresis to detect bound protein.

**Reporter gene assays.** Cos-7 cells ( $3 \times 10^4$  cells/well in 12-well plates) were transfected as described<sup>31</sup> with fixed amounts of 0.06  $\mu$ g of pSG5-AR, 0.5  $\mu$ g of pLCl, 0.04  $\mu$ g of pCMV- $\beta$ Gal and increasing amounts of pcDNA3-BAG1L, wild type and mutant plasmids. Total DNA was maintained at 1.1  $\mu$ g by the addition of empty plasmid. After 30 hrs, cells were stimulated with 1 nM R1881 for 10 h. Cell extracts were prepared and assayed for CAT and  $\beta$ -galactosidase activity at 40 h after transfection, expressing data as a ratio of CAT: $\beta$ -galactosidase.

**Coordinates.** The coordinates have been deposited in the Protein Data Bank with accession code 1I6Z.

## Acknowledgments

This research was performed in part at the Environmental Molecular Sciences Laboratory (a national scientific user facility sponsored by the U.S. DOE Office of Biological and Environmental Research) located at Pacific Northwest National Laboratory, operated by Battelle for the DOE. The authors are grateful to the staff at the HFMR facility at EMSL for useful discussions. We also thank K. Baker for protein purification and characterization, X. Jia for assistance with the Varian 500 MHz spectrometer and P. Crescenti for manuscript preparation. This work was funded by the National Institutes of Health NCI, NCIHL, USAMRDC Breast Cancer Program, the University of California Breast Cancer Research Program, the State of California Cancer Research Program, the Susan G. Komen Breast Cancer Foundation, the Human Frontier Science Program and CaPCURE.

Correspondence should be addressed to K.R.E. email: [ely@burnham.org](mailto:ely@burnham.org)

Received 30 November, 2000; accepted 2 March, 2001.

1. Takayama, S. et al. *EMBO J.* **16**, 4887–4896 (1997).
2. Hohfeld, J. & Jentsch, S. *EMBO J.* **16**, 6209–6216 (1997).
3. Nollen, E.A., Brunsting, J.F., Song, J., Kampinga, H.H. & Morimoto, R.I. *Mol. Cell. Biol.* **20**, 1083–1088 (2000).
4. Bimston, D. et al. *EMBO J.* **17**, 6871–6878 (1998).
5. Takayama, S., Zhihua, X. & Reed, J.C. *J. Biol. Chem.* **274**, 781–786 (1999).
6. Doong, H. et al. *Oncogene* **19**, 4385–4395 (2000).
7. Lee, J. H. et al. *Oncogene* **18**, 6183–6190 (1999).
8. Jiang, Y., Woronicz, J. D., Liu, W. & Goeddel, D.V. *Science* **283**, 543–546 (1999).
9. Thress, K., Song, J., Morimoto, R.I. & Kornbluth, L. *EMBO J.* **20**, 1033–1041 (2001).
10. Tschopp, J., Martinon, F. & Hofmann, K. *Curr. Biol.* **9**, 381–384 (1999).
11. Froesch, B.A., Takayama, S. & Reed, J.C. *J. Biol. Chem.* **273**, 11660–11666 (1998).
12. Crocchi, A., Schneikert, J., Hubner, S., Martin, E. & Cato, A. C. *Kidney Int.* **57**, 1265–1269 (2000).
13. Stuart, J.K. et al. *J. Biol. Chem.* **273**, 22506–22514 (1998).
14. Harrison, C.J., Hayer-Hartl, M., Di Liberto, M., Hartl, F.-U. & Kuriyan, J. *Science* **276**, 431–435 (1997).
15. Flaherty, K.M., Wilbanks, S.M., DeLuca-Flaherty, C. & McKay, D.B. *J. Biol. Chem.* **269**, 12899–12907 (1994).
16. Flaherty, K.M., DeLuca-Flaherty, C. & McKay, D.B. *Nature* **346**, 623–628 (1990).
17. Liberrek, K., Marszałek, J., Ang, D., Georgopoulos, C. & Zyllicz, M. *Proc. Natl. Acad. Sci. USA* **88**, 2874–2878 (1991).
18. Zeiner, M. & Gehring, U. *Proc. Natl. Acad. Sci. USA* **92**, 11465–11469 (1995).
19. Liu, R. et al. *J. Biol. Chem.* **273**, 16985–16992 (1998).
20. Schneikert, J., Hubner, S., Martin, E. & Cato, A.C.B. *J. Cell Biol.* **146**, 929–940 (1999).
21. Kne, D.A., Froesch, B.A., Nuber, U., Takayama, S. & Reed, J.C. *J. Biol. Chem.* in the press (2001).
22. Schneikert, J. et al. *EMBO J.* **19**, 6508–6516 (2000).
23. Holm, L. & Sander, C. *J. Mol. Biol.* **233**, 123–138 (1993).
24. Fernandez, I. et al. *Cell* **94**, 841–849 (1998).
25. Misura, K.M.S., Scheller, R.H. & Weiss, W.I. *Nature* **404**, 355–362 (2000).
26. Petersen, G., Hahn, C. & Gehring, J. *Biol. Chem.* in the press (2001).
27. Sondermann, H. et al. *Science* **291**, 1553–1557 (2001).
28. Cornilescu, G., Delaglio, F. & Bax, A. *J. Biomol. NMR* **13**, 289–302 (1999).
29. Brünger, A.T. et al. *Acta Crystallogr. D* **54**, 905–921 (1998).
30. Cabezas, E. & Satterthwait, A.C. *J. Am. Chem. Soc.* **121**, 3862–3875 (1999).
31. Takayama, S. et al. *Cell* **80**, 279–284 (1995).
32. Golemis, E.A., Gyuris, J. & Brent, R. In *Current protocols in molecular biology* (eds. Asubel, F.M. & Struhl, K. J.) 1–17 (Wiley & Sons, Inc. New York: 1994).
33. Wishart, D.S. & Sykes B.D. *J. Biomol. NMR* **4**, 171–180 (1994).
34. Koradi, R., Billeter, M. & Wüthrich, K. *J. Mol. Graph.* **14**, 51–55 (1996).
35. Christopher, J.A. *The structural properties observation and calculation kit* (The Center for Macromolecular Design, Texas A&M University, College Station, Texas: 1998).

## **BAG4/SODD Protein Contains a Short BAG Domain**

Klára Briknarová<sup>‡</sup>, Shinichi Takayama<sup>‡</sup>, Sachiko Homma<sup>‡</sup>, Kelly Baker<sup>‡</sup>, Edelmira Cabezas<sup>‡</sup>,  
David W. Hoyt<sup>§</sup>, Zhen Li<sup>‡</sup>, Arnold C. Satterthwait<sup>‡</sup>, and Kathryn R. Ely<sup>‡¶</sup>

*From <sup>‡</sup>The Burnham Institute, 10901 N. Torrey Pines Rd., La Jolla, CA 92037 and*

*<sup>§</sup> EMSL, Pacific Northwest National Laboratory, 3335 Q Avenue, Richland, WA 99352*

Running title: BAG4/SODD BAG Domain

<sup>¶</sup> *To whom correspondence should be addressed:*

*Tel: 858-646-3135*

*Fax: 858-646-3191*

*E-mail: [ely@burnham.org](mailto:ely@burnham.org)*

## SUMMARY

BAG proteins are molecular chaperone regulators that affect diverse cellular pathways. All members share a conserved motif, called the "BAG domain" (BD), which binds to Hsp70/Hsc70 family proteins and modulates their activity. We have determined the solution structure of BD from BAG4/SODD (Bcl-2 – Associated Athanogene / Silencer of Death Domains) by multidimensional nuclear magnetic resonance methods and compared it to the corresponding domain in BAG1 (Briknarová et al., *Nature Struct. Biol.* 8:349-352). The difference between BDs from these two BAG proteins is striking and the structural comparison defines two subfamilies of mammalian BD-containing proteins. One subfamily includes the closely related BAG3, BAG4 and BAG5 proteins, and the other is represented by BAG1 which contains a structurally and evolutionarily distinct BD. BDs from both BAG1 and BAG4 are three-helix bundles; however, in BAG4, each helix in this bundle is three to four turns shorter than its counterpart in BAG1, which reduces the length of the domain by one-third. BAG4 BD thus represents a prototype of the minimal functional fragment that is capable of binding to Hsc70 and modulating its chaperone activity.

## INTRODUCTION

BAG proteins are conserved throughout eukaryotes, with homologues found in vertebrates, insects, nematodes, yeast and plants (1-3). The human members of this family include BAG1 (4), BAG2 (1), BAG3 (CAIR-1/Bis) (1,5,6), BAG4 (SODD) (1,7), BAG5 (1) and BAG6 (BAT3/Scythe) (8-10) (Fig. 1). BAG proteins contain diverse N-terminal sequences but share a conserved protein interaction module near the C-terminal end called the BAG domain (BD). The BD binds to the ATPase domain of Hsp70/Hsc70 and modulates activity of these molecular chaperones (11,12). The BD of BAG1 also interacts with the C-terminal catalytic domain of Raf-1 and activates the kinase (13). It has been proposed that BAG-family members serve as "toggles" in cell signaling pathways (10). For example, Raf-1 and Hsp70 may compete for binding to BAG1 (14). When levels of Hsp70 are elevated after cell stress, the BAG1/Raf-1 complex is replaced by BAG1/Hsp70 and DNA synthesis is inhibited (14). Thus, BAG1 serves as a molecular switch between cell proliferation and growth arrest. BAG4 (SODD), on the other hand, may play a role as a cellular "adaptor". It has been speculated that BAG4 recruits Hsc70 to tumor necrosis factor receptor 1 (TNFR1) and death receptor 3 (DR3) (2,7), inducing conformational changes that prevent receptor signaling in the absence of ligand.

Each of the human BAG proteins binds to Hsp70/Hsc70 and modulates their chaperone activity. The conserved BD is necessary and sufficient for this interaction (1,11, and S. Takayama, unpublished results). Here we report the solution structure of the BD of BAG4 and its comparison with the BD of BAG1 (3,15). The BD in BAG4 is significantly shorter than its counterpart in BAG1 and may define a minimal structural unit that binds Hsp70/Hsc70. Our comparison reveals two subfamilies of BAG proteins that are structurally and evolutionarily distinct.

## EXPERIMENTAL PROCEDURES

*NMR spectroscopy and structure calculation* - BAG4 BD (residues 376-457) was expressed in *E. coli* as a glutathione transferase (GST) fusion construct. After initial purification of the recombinant protein by affinity chromatography on glutathione-agarose resin, the GST moiety was removed by thrombin cleavage and the digest was separated using glutathione-agarose. Remaining impurities were eliminated by affinity chromatography on a benzamidine-agarose column, and by ion-exchange chromatography on a Q-Sepharose column. NMR samples contained 1-2 mM  $^{15}\text{N}$ - or  $^{13}\text{C}/^{15}\text{N}$ -labeled protein, 10 mM potassium phosphate buffer, pH 7.2, 100 mM KCl, 1 mM DTT and 1 mM EDTA in 90%  $\text{H}_2\text{O}/10\% \text{D}_2\text{O}$ . Spectra were acquired at 30°C on Varian 500, 600 and 750 MHz spectrometers. The data were processed and analyzed with Felix 2000 (Molecular Simulations, Inc., San Diego).  $^1\text{H}$ ,  $^{15}\text{N}$  and  $^{13}\text{C}$  assignments were established based on CBCA(CO)NH, HNCACB, HNCO, C(CO)NH, H(CCO)NH, HCCH-TOCSY and 3D  $^{15}\text{N}$ -edited NOESY. Distance restraints were obtained from 3D  $^{15}\text{N}$ -edited NOESY and 3D  $^{13}\text{C}/^{15}\text{N}$ -edited NOESY.  $\phi$  and  $\psi$  dihedral angle restraints were generated with TALOS (16). Structures were calculated with standard torsion-angle dynamics (TAD) simulated annealing protocol implemented in CNS 1.0 (17) using restraints for 1153 interproton distances (120 long-range,  $5 \leq |i-j|$ , 199 medium-range,  $2 \leq |i-j| \leq 4$ , 195 sequential and 639 intraresidual), 92 hydrogen bond distances, and 61  $\phi$  and 61  $\psi$  dihedral angles. The protocol consisted of high temperature TAD, followed by TAD and cartesian slow cooling stages and final minimization. The scale factor for dihedral angle energy term was doubled throughout the calculation; otherwise, default parameters were employed. Out of 28 structures, 25 structures were selected that had no distance and dihedral angle restraint violated by more than 0.5 Å or 5°, respectively. The statistics are summarized in Table 1. The structure with the lowest energy was used for illustrations and discussion. All figures were generated with MOLMOL 2K.1 (18).

*Peptide synthesis and binding study* - The peptide corresponding to helical region Asn256-Cys267 of the ATPase domain of human Hsc70, which was predicted to bind to BAG4, was synthesized in a helix-nucleated form to stabilize helicity (19) and characterized as described previously (15). <sup>1</sup>H-<sup>15</sup>N HSQC spectra were recorded for <sup>15</sup>N-labeled BAG4 solutions containing varying concentrations of peptide, and most pronounced resonance shifts of BAG4 amides were noted and mapped onto the structure.

*Mutational analysis of BAG4 binding to Hsc70* - Mutations in BAG4 were generated by two-step PCR-based mutagenesis using a full length human BAG4 cDNA (1) as a template (15). The following forward (f) and reverse (r) primers were used:  
GGGAATTCACTCCTCCGAGTATTAATAAAATC (f),  
GCGCTCGAGTCATAATCCTTTTTTTTCTAATTTTCCAGTATGGC (r),  
CATGTGCTGGCGGCGGTCCAGTATC (E388A E389A f),  
GATACTGGACCGCCGCCAGCACATG (E388A E389A r),  
GCTTCTGGAAGCAATGCTAACC (E414A f), GGTTAGCATTGCTTCCAGAAGC (E414 r),  
GGAAGTGGCTTCAGTTGAAAC (D424 f),  
GTTTCAACTGAAGCCAGTTCC (D424A r), CGGCAGGCCGCAGCAGAGGCTG (R438A K439A f),  
CAGCCTCTGCTGCGGCCTGCCG (R438A K439A r),  
GTTTGTAAGATTGCGGCCATACTGG (Q446A f),  
CCAGTATGGCCGCAATCTTACAAAC (Q446A r),  
CCTCGAGTCATAATCCTTTTTTTTGCTAATTTTCC (E453A r). The products were purified by QiaQuick gel extraction kit (Qiagen), subcloned into the TOPO TA vector (Invitrogen) and sequenced. For in vitro binding assays, the fragments comprising wild type or mutant BAG4 BD were subcloned into pGEX4T-1 vector and expressed in BL21(DE3) cells as GST-fusion proteins. After induction at room temperature with 0.1 mM IPTG, cells were lysed by sonication, and expressed proteins were isolated from lysates by affinity purification on glutathione-Sepharose (Pharmacia). GST fusion proteins (5 µg)

were immobilized on glutathione-Sepharose and incubated for 1 hr at 4°C in a volume of 0.1 ml of binding buffer (20 mM HEPES, pH 7.7, 142 mM KCl, 5mM MgCl<sub>2</sub>, 2 mM EGTA, 0.5 % NP40) with 1 µl of in vitro translated <sup>35</sup>S-L-methionine-labeled Hsc70 (pcDNA3-HA-Hsc70 (67-377),(11)). The beads were then washed three times with 1 ml of ice-cold binding buffer, bound proteins were separated by SDS-PAGE and visualized by autoradiography.

*Computer modeling* - The homology models of BDs from BAG3 and BAG5 were created with SwissModel (22-24) using the sequence alignment shown in Fig. 2c. The coordinates were used to visualize charge and hydrophobicity distribution on molecular surfaces.

## RESULTS AND DISCUSSION

*Structure of the BAG domain from BAG4* - We have determined the solution structure of BAG4 BD, using multidimensional NMR methods. Similar to its BAG1 counterpart (3,15), the BAG4 BD is a three-helix bundle (Fig. 2a). However, a striking difference between the BDs of BAG4 and BAG1 is obvious. The three helices in BAG4 BD, which correspond to residues 380-399 ( $\alpha$ 1), 407-423 ( $\alpha$ 2) and 432-456 ( $\alpha$ 3), are substantially shorter than those in BAG1 (Fig. 2b).

*Comparison of BAG domains from BAG1 and BAG4* - In order to compare the BDs of BAG4 and BAG1, we first superimposed their structures using only residues that are identical in the most conserved helix  $\alpha$ 3. Once  $\alpha$ 3 was overlaid, structurally equivalent residues were matched in the whole domain. The resulting structure-based sequence alignment is shown in Fig. 2c. As the alignment illustrates, BAG4 BD, relative to BAG1, contains a deletion of 19 residues between  $\alpha$ 1 and  $\alpha$ 2. This deletion results in shortening of  $\alpha$ 1 and  $\alpha$ 2 by 2.5 and 3.5 turns, respectively. BAG4 BD also lacks three turns of  $\alpha$ -helix at the C-terminal end of  $\alpha$ 3. All three helices in BAG4 BD are truncated at one end of the

structure, making the BD of BAG4 significantly shorter (26 x 12 x 11 Å) than the BD of BAG1 (37 x 14 x 10 Å).

After the two domains were superimposed,  $\alpha 1$ ,  $\alpha 2$  and  $\alpha 3$  in BAG4 BD matched closely with their BAG1 counterparts (3,15). The root mean square deviation (rmsd) of BAG4 backbone atoms in the three  $\alpha$ -helices from equivalent atoms in murine and human BAG1 BD is 1.7 Å and 1.4 Å, respectively. (For comparison, rmsd between the same atoms of human and murine BAG1 is 1.2 Å). Also, the conformation of the loop between helices  $\alpha 2$  and  $\alpha 3$  is very similar in BAG4 and BAG1, even though it contains a single insertion, Met 169<sup>1</sup>, in the latter. Overall, the structure of BD from BAG4 closely resembles the upper two thirds of BAG1 BD (Fig. 2b).

*Hsc70 binding interface on BAG4 BD* - Most BAG1 residues that interact with Hsc70 (3) are conserved or conservatively substituted in BAG4 BD (Fig. 2c). Hence, it can be predicted that BAG4 binds Hsc70 in a manner analogous to BAG1 (3,15). This was tested experimentally by NMR-monitored titrations of BAG4 BD with a synthetic peptide corresponding to an  $\alpha$ -helix (residues Asn256-Cys267) from the BAG1-binding interface on the ATPase domain of Hsc70. This helix contributes several predominantly basic residues to the intermolecular contacts with BAG1. In particular, Arg258, Arg261, Arg262 and Thr265 from Hsc70 form salt bridges with Glu157, Glu164, Asp167 from  $\alpha 2$  and

---

<sup>1</sup> The sequence numbering for murine BAG1 is the same as that used in our previous NMR study reporting the solution structure of mBAG1 [15]. Human BAG1 is numbered accordingly for clarity. When the crystal structure of human BAG1 was published [3], a different numbering scheme was used based on the sequence of BAG1M, a longer isoform of BAG1. For direct comparison with the sequence numbers for human BAG1 in the crystal structure, the reader should add 55 to the BAG1 sequence numbers used in the present study.

Asp197 from  $\alpha 3$  of BAG1 (3). The peptide interacted with BAG4 BD; the most pronounced  $^1\text{H}/^{15}\text{N}$  chemical shift changes in BAG4 BD induced by peptide binding were localized in  $\alpha 2$  (Fig. 3a,c). This is consistent with the expected peptide contact sites and with the results of NMR titrations of BAG1 with the same peptide (15).

To further define the binding interface in BAG4 BD across the conserved helices  $\alpha 2$  and  $\alpha 3$ , we used site-directed mutagenesis of the predicted contact residues within these helices. The results indicated that Glu414 and Asp424 from  $\alpha 2$ , as well as Arg438, Lys439 and Gln446 from  $\alpha 3$  are important for interaction of BAG4 with Hsc70, since mutating these residues to alanine abolished or weakened the binding (Fig. 3b,c). The equivalents of these residues in BAG1 each make direct contact with Hsc70 (3). As expected, mutations in  $\alpha 1$  (E388A, E389A) had no effect, since this helix does not interact with Hsc70. Thus the results indicate that the binding surface for the heat shock chaperone is similar in BAG4 and BAG1, involving  $\alpha 2$ - $\alpha 3$  and extending through an area of approximately  $10 \times 30 \text{ \AA}$  across one face of the domain.

While most intermolecular interactions between BAG4 and Hsc70 are identical to those in the BAG1/Hsc70 complex (3), the contributions and relative importance of some residues differ. For example, the BAG4 E453A mutant still interacted with Hsc70, even though mutation of the equivalent residue in BAG1 (D197A, made as a double mutant with Q201A) resulted in a failure to bind Hsc70 (15). In BAG1, Asp197 forms a salt bridge with Arg258 in Hsc70 while Gln201 is not involved in direct contact (3). Aspartic or glutamic acid is found at this position in all human BDs. It is possible that the longer aliphatic side chain of glutamic acid precludes formation of a stable intermolecular salt bridge as seen in the BAG1/Hsc70 complex, and consequently, this residue is not critical for BAG4/Hsc70 recognition.

*Structure-based sequence alignment of human BAG domains* - The sequence similarity between BDs of BAG4 and BAG1 is strongest in  $\alpha 3$  (30% identical) and somewhat weaker in  $\alpha 2$  (24% identical), so the alignment was clear for these two helices. However, until now, low levels of homology for the sequences in  $\alpha 1$  obscured alignments of this region, even with knowledge of the BAG1 structure (1-3). In some cases, this segment of BDs was excluded from sequence alignments. Now, with the structures of two BDs in hand, it is possible to evaluate the conserved folding pattern of  $\alpha 1$  and to more accurately predict sequence homology for the BDs. A structure-based sequence alignment is presented in Fig. 2c. The most significant correction to previous alignment attempts is the relative position of  $\alpha 1$ : BAG4  $\alpha 1$  spans residues 380-399, corresponding to structurally equivalent residues 104-123 in BAG1.

While the sequence alignment of more distantly related BAG4 and BAG1 BDs required comparison of their structures, sequences of BDs from BAG3, BAG4 and BAG5 can be aligned with a high degree of confidence (Fig. 2c, compare with (2,3)). BDs from BAG3 and BAG4 are the most closely related among human BDs, being 60% identical. BAG5 was shown previously to contain four BDs (20-40% identical to BAG3 and BAG4) (1,2), arranged in tandem and accounting for most of the protein. Now, our alignment has revealed that another segment in BAG5, located immediately after the first BD and predicted to contain three  $\alpha$ -helices, is yet another BD, which we termed BAG5/BD2. For the alignment in Fig. 2c, we renumbered the remaining BDs from the identifiers cited previously (2,10) to BAG5/BD3, BAG5/BD4 and BAG5/BD5. The role of these linked BDs in BAG5 is not yet understood.

Alignment of the putative BDs from BAG2 and BAG6/Scythe was not straightforward, and therefore we did not include their sequences in Fig. 2c. Even though both proteins bind to Hsc70 and inhibit its refolding activity (1,9), they are obvious outliers and their structures are

likely to be different from other BDs. In BAG2, the C-terminus of the protein itself terminates the putative BD shortly after the segment with homology to  $\alpha 2$ . Thus, if the folding pattern were retained for the first part of the domain, BD in BAG2 would lack most of  $\alpha 3$ . In contrast, the BD of BAG6 may lack the structural equivalent of  $\alpha 1$  since the corresponding sequence contains several prolines that are likely to disrupt the helix. Only half of the residues whose counterparts in BAG1 contact the chaperone are conserved in BAG6. The region with  $\alpha 2$ - $\alpha 3$  homology is necessary for binding of BAG6 to Hsc70 (9). It remains to be seen whether this segment forms a structural domain *per se* or is part of a novel larger domain, together with the preceding proline-rich region or other parts of the protein.

*Implications for human BAG proteins* - To consider conserved structure/function relationships in the human BAG family, we used BAG4 BD as a template to construct three-dimensional homology models for the BDs from BAG3 and BAG5. The sequence identity is 60%, 39%, 29%, 22%, 23% and 43% for BAG3 BD, BAG5/BD1, BAG5/BD2, BAG5/BD3, BAG5/BD4, and BAG5/BD5, respectively. The BDs from BAG2 and BAG6 were excluded from this comparison because they lack the clear homology seen in the other members of the family. Thus, a "gallery" of BDs was generated consisting of three experimentally determined structures (BAG4, murine BAG1 (15) and human BAG1 (3)) and six homology models (Figs. 4, and 5). This gallery was used to compare overall globular shape as well as surface features and protein interaction interfaces across the family. It should be noted for the homology models that the main chain conformation is likely to be accurate but the positions of the side chains are less well-defined. Our models provide a reasonable representation of overall surface feature distribution and can be useful in the absence of experimental structures of other members of the BAG family. BAG1, BAG3 and BAG4 interact with Hsc70 (1,2,6,11,20), and, consistent with that, the Hsc70-binding faces (helices  $\alpha 2$  and  $\alpha 3$ ) of BDs from these family members are very similar with

respect to charge distribution (Fig. 5, top row). Acidic residues (Glu413 and Glu414 from  $\alpha 2$ , Asp424 and Glu427 from the connecting loop and Glu450 and Glu453 from  $\alpha 3$  in BAG4) dominate diagonally across the surface (Fig. 4a). The N-terminal portion of  $\alpha 3$  presents a cluster of basic residues (Arg435, Arg438 and Lys439 in BAG4), seen in the upper left corner of the domain (Fig. 4a). Some of the acidic residues and the basic cluster on the  $\alpha 2$ - $\alpha 3$  face are shared by all the BDs. Similarly, a central hydrophobic region (Leu420 and Leu421 from  $\alpha 2$  and Val442, Ile445 and Leu449 from  $\alpha 3$  in BAG4) is conserved through the family (Fig. 5).

Among the BAG5 BDs, BAG5/BD5 is the most canonical while BAG5/BD2 is the least. In fact, the charge distribution in BAG5/BD2 is rather unusual, resulting in a large dipolar moment on the  $\alpha 2$ - $\alpha 3$  face of the domain. In BAG5/BD3 and BAG5/BD4, the cluster of acidic residues on  $\alpha 2$  and  $\alpha 3$  is not conserved, which could impede the interaction with Hsc70. In particular, the equivalents of the critical contact residue Glu414 in BAG4 are cysteine in BAG5/BD3 and threonine in BAG5/BD4. When this glutamic acid is mutated to alanine in BAG4 or BAG1, binding to Hsc70 is abolished. The putative Hsc70 contact interfaces in BAG5/BD5 and also BAG5/BD1 are more closely similar to that in BAG4. In BAG5/BD5, this critical glutamate residue is conserved but an arginine is present at this site in BAG5/BD1. Interestingly, both of these BDs bind Hsc70 in *in vitro* assays (S. Takayama, unpublished results). Future studies are needed to reveal how BAG5 is organized, whether its five BDs act independently or interact with one another, and to identify the molecular targets of BAG5/BDs that do not bind Hsc70.

*Short versus long BAG domains* - In our comparison of BDs from human BAG family members, we have demonstrated the presence of two structurally distinct BAG domains that divide the family into two subfamilies, characterized by the presence of "short" (BAG3, BAG4 and BAG5) or "long" (BAG1) BAG domains. Gene structure of these two BD

types also differs and reflects separate evolutionary history. While the BDs in BAG3, BAG4 and BAG5 are neither flanked by nor contain any introns, there are several phase 0 introns in the BD region of human BAG1 gene. The existence of short and long varieties raises numerous questions about evolution and function of BDs. Since the short BD is sufficient for binding to Hsc70 and modulating its activity, what is the advantage of having each  $\alpha$ -helix extended at one end of the long BD by three turns? Does the long BD represent the original form, and did the short BD arise by elimination of the part of the molecule which was not required for its function? Alternatively, did the long BD evolve from an ancestral short BD, with the extra residues enabling it to gain a new function?

To learn more about short and long BDs, we investigated which types are present in other species. Sequences similar to BDs are found in fungi, plants and animals (1-3). Proteins containing the long BD, homologous to human BAG1, have been identified in various vertebrates (mouse, *Mus musculus* (4); rat, *Rattus norvegicus*, BI280304, BF407193, AI045819; cow, *Bos taurus*, AV601527; frog, *Xenopus laevis*, AW640566, BJ036536; fish, *Oryzias latipes*, BJ021354) and in nematodes (*Caenorhabditis elegans* (1); *Meloidogyne arenaria*, BI746004, BI501569; *Meloidogyne javanica*, BI324599; *Heterodera glycines*, BF249474). All the nematode BDs contain an insertion of 6 residues between  $\alpha 2$  and  $\alpha 3$ . Short BDs, similar to those in human BAG4, have been found throughout vertebrates (mouse, *Mus musculus*, BAB27167; rat, *Rattus norvegicus*, BF392489; cow, *Bos taurus*, BM104841, AW416999; chicken, *Gallus gallus*, AJ396368; zebrafish, *Danio rerio*, BM071126, BG303781, BM095203) and in chordates (tunicate, *Ciona intestinalis*, AV841356, AV881072). Short BDs are also present in insects (silkworm, *Bombyx mori* (21); fruitfly, *Drosophila melanogaster* (3); bee, *Apis mellifera*, BI515842, BI508980; mosquito, *Anopheles gambiae*, AJ280648) in a set of proteins distinct from BAG3, BAG4 and BAG5. In BDs from fungi (Sn1p in *Saccharomyces cerevisiae* (2); BAG1A and BAG1B in *Saccharomyces pombe* (1); *Neurospora crassa*,

CAB88563), homology is limited to the Hsc70-binding region of  $\alpha 2$  and  $\alpha 3$ , which is common to both short and long BDs. However, C-termini of the proteins limit  $\alpha 3$  to a size typical of a short BD. Consistent with this observation, secondary structure prediction indicates that the three  $\alpha$ -helices span a region of approximately ninety residues. Altogether, BDs in fungi are likely to be "short". Also in plant BDs (2,3), only the chaperone-binding sequence of  $\alpha 2$  and  $\alpha 3$  is conserved. In this case, however, protein termini do not limit size of the BDs and secondary structure prediction is not straightforward. Classification as short or long may therefore require knowledge of three-dimensional structure of these proteins.

Presence of the short BD in at least two kingdoms, animals and fungi, suggests that this form of BD is of ancient origin. It is not clear if the long BD is limited only to a part of the animal kingdom, or if it will be found elsewhere as well. Interestingly, nematodes possess an orthologue of BAG1, which contains the long BD, but short BD has not yet been identified in the completed genome of *C. elegans*. Does this imply that the short BD is absent in some animal species? Obviously, many open questions remain. The origin of short and long BDs, point of their divergence, diversity of BDs within eukaryotes and significance of their different lengths are still obscure. Also, even though the structures of BAG domains from human and mouse BAG1 (3,15) and from human BAG4 have been determined, it is not straightforward to predict structures of BDs from distantly related BAG family members whose sequence similarity is limited to Hsc70-binding regions of  $\alpha 2$  and  $\alpha 3$ . Once structures of BDs from yeast and plant proteins, as well as those from BAG2 and BAG6, are known they will provide new insights into the structure-function relationship in this diverse family of molecular regulators.

*Coordinates* - The atomic coordinates have been deposited in the Protein Data Bank, Research Collaboratory for Bioinformatics, Rutgers University, New Brunswick, NJ (<http://www.rcsb.org/>) with accession code \_\_\_\_\_.

*Acknowledgments* - This research was performed in part at the Environmental Molecular Sciences Laboratory (a national scientific user facility sponsored by the U.S. DOE Office of Biological and Environmental Research) located at Pacific Northwest National Laboratory, operated by Battelle for the DOE. We thank N. E. Preece for assistance with the Varian 500 MHz spectrometer, D. Kedra for help with sequence database searches, J. C. Reed for helpful discussions and critical review of the manuscript and S. Hammond for assistance in preparing the manuscript for publication. This work was funded by the National Institute of Health NCI (CA 67329), USAMRMC Prostate Cancer Program (DAMD 17-99-1-9094 and PC010678), and the University of California Breast Cancer Research Program (7FB-0084).

## REFERENCES

1. Takayama, S., Xie, Z., and Reed, J. (1999). *J. Biol. Chem.* **274**, 781-786.
2. Tschopp, J., Martinon, F., and Hofmann, K. (1999). *Curr. Biol.* **9**, R381-384.
3. Sondermann, H., Scheufler, C., Schneider, C., Höhfeld, J., Hartl, F.-U. and Moarefi, I. (2001). *Science* **291**, 1553-1557.
4. Takayama, S., Sato, T., Krajewski, S., Kochel, K., Irie, S., Millan, J.A., and Reed, J.C. (1995). *Cell* **80**, 279-284.
5. Lee, J.H., Takahashi, T., Yasuhara, N., Inazawa, J., Kamada, S. and Tsujimoto, Y. (1999). *Oncogene* **18**, 6183-6190.
6. Doong, H., Price, J., Kim, Y. S., Gasbarre, C., Probst, J., Liotta, L. A., Blanchette, J., Rizzo, K. and Kohn, E. (2000). *Oncogene* **19**, 4385-4395.

7. Jiang, Y., Woronicz, J.D., Liu, W., and Goeddel, D.V. (1999). *Science* **283**, 543-546.
8. Thress, K., Henzel, W., Shillinglaw, W., and Kornbluth, S. (1998). *EMBO J.* **17**, 6135-6143.
9. Thress, K., Song, J., Morimoto, R.I., and Kornbluth, S. (2001). *EMBO J.* **20**, 1033-1041.
10. Takayama, S., and Reed, J.C. (2001). *Nat. Cell Biol.* **3**, E237-E241.
11. Takayama, S., Bimston, D.N., Matsuzawa, S., Freeman, B.C., Aime-Sempe, C., Xie, Z., Morimoto, R.J. and Reed, J. C. (1997). *EMBO J.* **16**, 4887-4896.
12. Stuart, J.K., Myszka, D.G., Joss, L., Mitchell, R.S., McDonald, S.M., Zhihua, X., Takayama, S., Reed, J.C. and Ely, K.R. (1998). *J. Biol. Chem.* **273**, 22506-22514.
13. Wang, H.G., Takayama, S., Rapp, U.R., and Reed, J.C. (1996). *Proc. Natl. Acad. Sci. USA* **93**, 7063-7068.
14. Song, J., Takeda, M., and Morimoto, R.I. (2001). *Nat. Cell Biol.* **3**, 276-282.
15. Briknarová, K., Takayama, S., Brive, L., Havert, M.L., Knee, D.A., Velasco, J., Homma, S., Cabezas, E., Stuart, J., Hoyt, D.W., Satterthwait, A.C., Llinás, M., Reed, J.C. and Ely, K.R. (2001). *Nat. Struct. Biol.* **8**, 349-352.
16. Cornilescu, G., Delaglio, F., and Bax, A. (1999). *J. Biomol. NMR* **13**, 289-302.
17. Brünger, A.T., Adams, P. D., Clore, G. M., DeLano, W. L., Gros, P., Grosse-Kunstleve, R. W., Jiang, J. S., Kuszewski, J., Nilges, M., Pannu, N. S., Read, R. J., Rice, L. M., Simonson, T., and Warren, G. L. (1998). *Acta Crystallogr. D*, **54**, 905-921.
18. Koradi, R., Billeter, M., and Wuthrich, K. (1996). *J. Mol. Graph.* **14**, 51-55.
19. Cabezas, E., and Satterthwait, A.C. (1999). *J. Am. Chem. Soc.* **121**, 3862-3875.
20. Antoku, K., Maser, R.S., Scully, W.J. Jr., Delach, S.M., and Johnson, D.E. (2001). *Biochem. Biophys. Res. Commun.* **286**, 1003-1010.
21. Moribe, Y., Niimi, T., Yamashita, O., and Yaginuma, T. (2001). *Eur. J. Biochem.* **268**, 3432-3442.
22. Guex, N., Diemand, A., and Peitsch, M.C. (1999). *TIBS* **24**, 364-367.

23. Guex, N., and Peitsch, M.C. (1997). *Electrophoresis* **18**, 2714-2723.
24. Peitsch M.C. (1995). *Bio/Technology* **13**, 658-660.
25. Takayama, S., Krajewski, S., Krajewska, M., Kitada, S., Zapata, J. M., Kochel, K., Knee, D., Scudiero, D., Tudor, G., Miller, G. J., Miyashita, T., Yamada, M., and Reed, J.C. (1998). *Cancer Res.* **58**, 3116-3131.
26. Yang, X., Chernenko, G., Hao, Y., Ding, Z., Pater, M.M., Pater, A., and Tang, S.C. (1998). *Oncogene* **17**, 981-989.
27. Thompson, J.D., Gibson, T.J., Plewniak, F., Jeanmougin, F., and Higgins, D.G. (1997). *Nucleic Acids Res.* **24**, 4876-4882.
28. Laskowski, R.A., MacArthur, M.W., Moss, D.S., and Thornton, J.M. (1993). *J. Appl. Cryst.* **26**, 283-291.

## FIGURE LEGENDS

Fig. 1. Domain structure of human BAG-family proteins. The positions of the BAG domain (red), ubiquitin-like domain (yellow), WW domain (blue), nuclear localization sequence (cyan) and TXSEEX repeats (green) in human BAG-family members are indicated. Boundaries of the putative BAG domains in BAG2 and BAG6 are not known. Four isoforms of BAG1 protein have been identified (25,26) and are denoted BAG1-L, BAG1-M, BAG1 and BAG1-S.

Fig. 2. BAG domain from BAG4 is a short triple-helix bundle. **a**, Stereo view of ten superimposed backbone traces of human BAG4 BD (residues 376-457).  $\alpha 1$  is colored blue,  $\alpha 2$  green,  $\alpha 3$  red; connecting loops are yellow and termini white. **b**, Comparison of BAG domains from BAG4 and BAG1. Tube models of C $^{\alpha}$  atoms from human BAG4 (red; residues 376-457), murine BAG1 (blue; PDB ID 1I6Z, residues 99-210) and human BAG1 (green; PDB ID 1HX1, residues 99-205) are shown<sup>1</sup>; the structures were

superimposed using BAG4 backbone atoms located in  $\alpha$ -helices (residues 380-399, 407-423, 432-456) and their counterparts in BAG1 proteins. Orientation of the molecules is the same as in Panel a. **c**, Structure-based sequence alignment of BAG domains. BDs from human BAG4 (hBAG4), human BAG3 (hBAG3), human BAG5 (hBAG5/1, hBAG5/2, hBAG5/3, hBAG5/4 and hBAG5/5), human BAG1 (hBAG1) and murine BAG1 (mBAG1) were aligned, as described in the text. Homology is highlighted by the default ClustalX coloring scheme (27). Position of residues in hBAG1 that interact with N- and C-terminal lobes of Hsc70 are indicated with open and filled circles, respectively. hBAG4 and mBAG1 residue numbers are marked above or below the respective sequences. Secondary structure of hBAG4 and mBAG1 BDs is outlined on top.

Fig. 3. Analysis of BAG4 binding to Hsc70. **a**, Effect of Hsc70 peptide Asn256-Cys267 on  $^1\text{H}$ - $^{15}\text{N}$  HSQC spectra of BAG4 BD. Spectra of ligand-free BAG4 BD (black) and BAG4 BD in the presence of 30-fold molar excess of the peptide (red) are superimposed; several noticeable crosspeak shifts are labeled. **b**, Mutational analysis of the interaction between human BAG4 BD and Hsc70. GST fusion proteins representing wild type BAG4 BD, mutants or CD40 negative control were immobilized on glutathione-Sepharose beads and tested for *in vitro* binding to *in vitro* translated  $^{35}\text{S}$ -L-methionine labeled Hsc70 (67-377). Samples were analyzed by SDS-PAGE and autoradiography to detect bound Hsc70 (upper panel) and with Coomassie blue staining to verify loading of equivalent amounts of GST fusion proteins (lower panel). Substitutions for residues 388-389 were made as control mutations, since they are located in  $\alpha 1$ , on the opposite side of the molecule from the Hsc70 contact interface, and were not expected to affect binding. Input lane shows 1/5 of total *in vitro* translated protein, which was mixed with GST fusion protein. **c**, Tube model of BAG4 BD (residues 376-457) colored according to  $^1\text{H}$ - and  $^{15}\text{N}$ -chemical shift changes of the individual residues upon binding of Hsc70 peptide Asn256-Cys267. Color intensity is proportional to the observed change. Sites of alanine

substitution, which are described in Panel a, are depicted as spheres. Black, gray or white spheres indicate mutations which abolished, weakened or did not affect binding to Hsc70, respectively. The chemical shifts and mutations that affect binding were located in  $\alpha 2$ - $\alpha 3$ , marking an interaction interface that is closely similar to that seen in BAG1 (3,15). Orientation of the molecule is the same as in Fig. 2a.

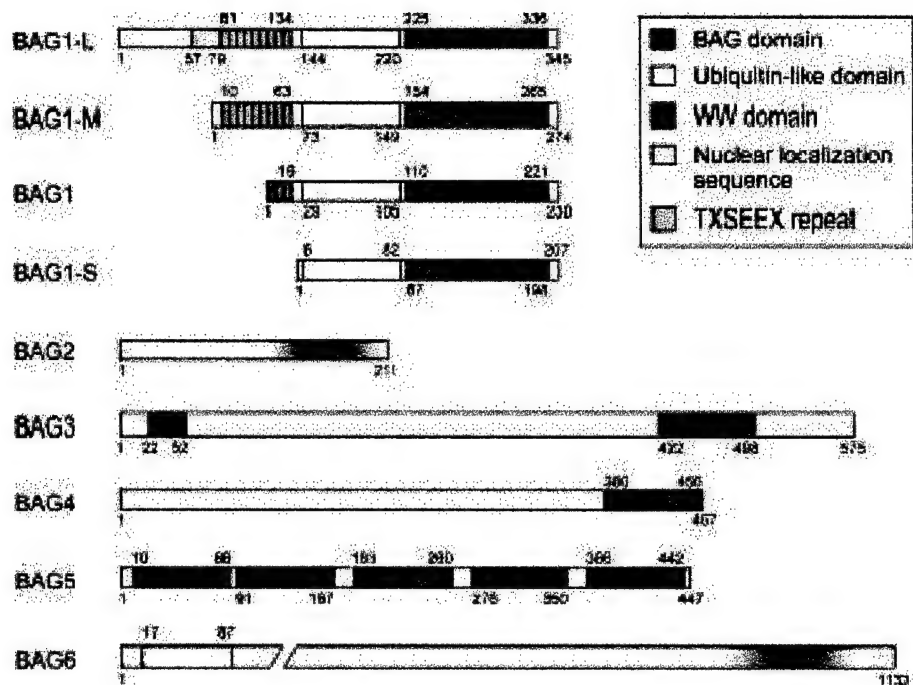
Fig. 4. Surface maps of BAG4 BD. In Panels a and b, the solvent accessible surface of the domain is colored according to electrostatic potential. Areas with negative, positive or neutral character are depicted in red, blue or white, respectively. In Panel a, The view is the same as in Fig. 2a, with helices 2 and 3 and the Hsc70 binding site facing forward. In Panel b, the molecule is rotated 180° around a vertical axis relative to the view in Panel a, thus revealing the opposite side with helix 1 in front. In Panels c and d, the surface is colored according to hydrophobicity. Yellow color intensity is proportional to increasing hydrophobic character, and the “front” and “back” views of the molecule are displayed as in Panels a and b. Charged and hydrophobic residues are labeled in the appropriate panels.

Fig. 5. A comparative gallery of BAG domains. Contact surfaces of BDs from BAG1, BAG3, BAG4 and BAG5 (columns 1-9), whose sequences are aligned in Fig. 2c, are colored according to electrostatic potential (rows 1-2) and hydrophobicity (rows 3-4). Residues 99-210 of murine BAG1 (PDB ID 1I6Z), residues 99-205 of human BAG<sup>1</sup> (PDB ID 1HX1), residues 376-457 of human BAG4 and corresponding residues from homology models of BAG3 and BAG5 BDs are shown. Coloring and orientation are the same as in Fig. 4 to permit direct comparison. Front views are shown in rows 1 and 3, while back views are presented in rows 2 and 4.

**TABLE 1**

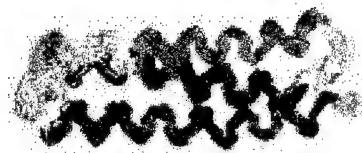
<b>Structural statistics for BAG4</b>	
Root mean square deviation (RMSD)	
from experimental restraints	
NOE distance restraints (Å)	0.016±0.001
dihedral angle restraints (°)	0.26±0.02
RMSD from idealized geometry (17)	
bonds (Å)	0.0018±0.0001
angles (°)	0.38±0.02
impropers (°)	0.28±0.02
RMSD of residues 380-399, 407-423, 432-456	
(helical regions) from mean coordinates <sup>a</sup>	
backbone atoms (N, C <sup>α</sup> , C) (Å)	0.58±0.14
heavy atoms (Å)	1.21±0.10
RMSD of residues 376-457 from mean	
coordinates <sup>a</sup>	
backbone atoms (N, C <sup>α</sup> , C) (Å)	0.82±0.18
heavy atoms (Å)	1.32±0.11
Distribution of $\phi$ , $\psi$ dihedral angles of	
residues 99-210 in Ramachandran plot (28)	
the most favored regions (%)	94.3
additional allowed regions (%)	4.3
generously allowed regions (%)	0.6
disallowed regions (%)	0.7

<sup>a</sup>Mean coordinates were obtained by averaging coordinates of 25 calculated structures, which were first superposed using backbone atoms (N, C<sup>α</sup>, C) of the helical regions (residues 380-399, 407-423 and 432-456).

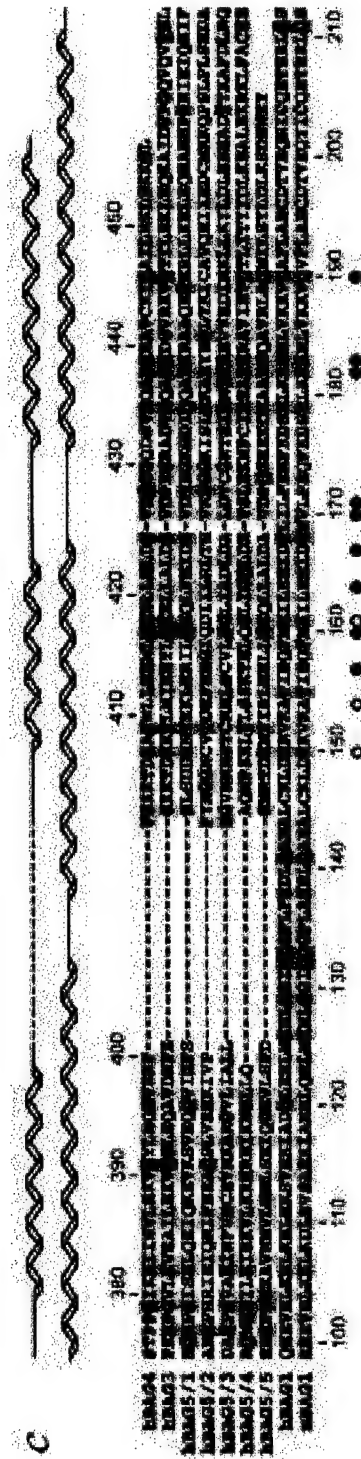




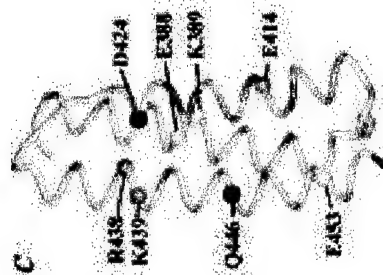
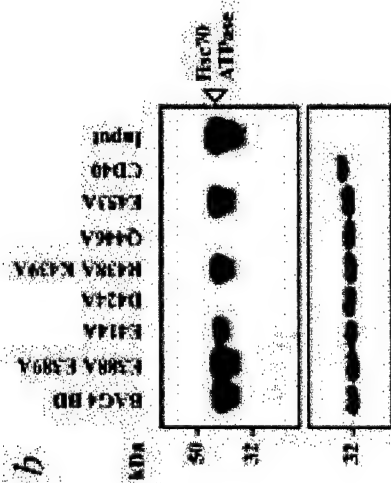
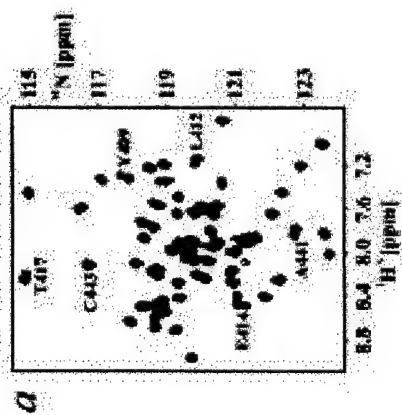
b

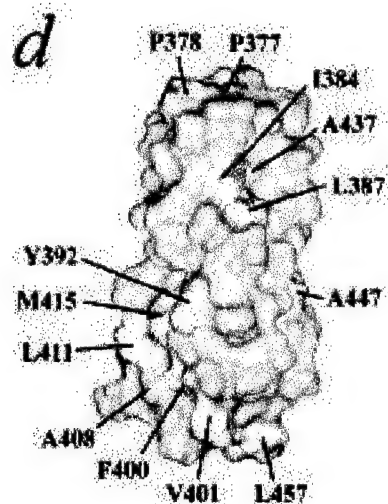
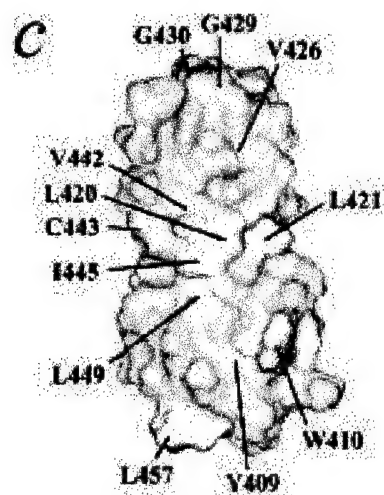
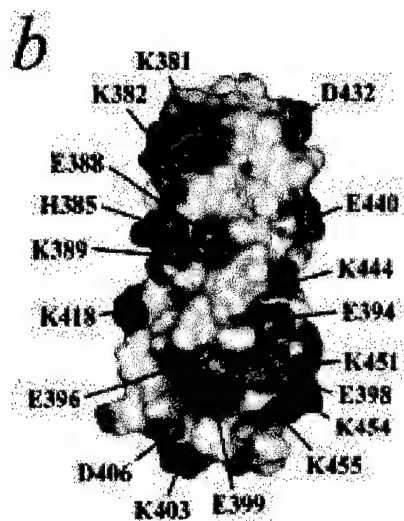
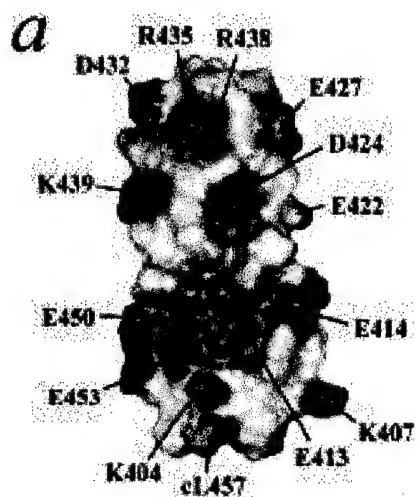


a



c

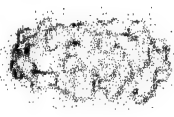
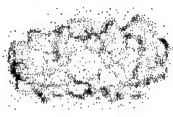
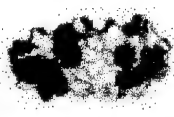




hBAG5/5



hBAG5/4



hBAG5/3



hBAG5/2



hBAG5/1



hBAG4



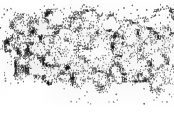
hBAG3



hBAG1



mBAG1



## Nucleotide and Amino acid sequence

### 1. BAG3 nucleotide sequence and predicted amino acid sequence.

LOCUS AF095193 2534 bp mRNA PRI 10-SEP-1999  
DEFINITION Homo sapiens BAG-family molecular chaperone regulator-3 mRNA,  
complete cds.  
ACCESSION AF095193  
NID g4322821  
KEYWORDS .  
SOURCE human.  
ORGANISM Homo sapiens  
Eukaryota; Metazoa; Chordata; Craniata; Vertebrata; Mammalia; Eutheria;  
Primates; Catarrhini; Hominidae; Homo. REFERENCE 1 (bases 1 to 2534)  
AUTHORS Takayama, S., Xie, Z. and Reed, J.C. TITLE An evolutionarily  
conserved family of Hsp70/Hsc70 molecular  
chaperone regulators  
JOURNAL J. Biol. Chem. 274 (2), 781-786 (1999) MEDLINE 99091615  
REFERENCE 2 (bases 1 to 2534)  
AUTHORS Takayama, S. and Reed, J.C.  
TITLE BAG-family regulators of Hsp70/Hsc70  
JOURNAL Unpublished  
REFERENCE 3 (bases 1 to 2534)  
AUTHORS Takayama, S. and Reed, J.C.  
TITLE Direct Submission  
JOURNAL Submitted (28-SEP-1998) The Burnham, 10901 N. Torrey Pines Rd., La  
Jolla, CA 92037, USA  
REFERENCE 4 (bases 1 to 2534)  
AUTHORS Takayama, S. and Reed, J.C.  
TITLE Direct Submission  
JOURNAL Submitted (10-SEP-1999) The Burnham, 10901 N. Torrey Pines Rd., La  
Jolla, CA 92037, USA  
REMARK Sequence update by submitter  
FEATURES Location/Qualifiers  
source 1..2534  
/organism="Homo sapiens"  
/db\_xref="taxon:9606"  
/cell\_line="Jurkat"  
/cell\_type="T lymphocyte"  
CDS 307..2034  
/note="member of the molecular chaperone regulator BAG  
family proteins; BAG-3"  
/codon\_start=1  
/product="BAG-family molecular chaperone regulator-3"  
/db\_xref="PID:g4322822"  
/translation="MSAATHSPMMQVASGNGDRDPLPPGWEIKIDPQTGWPFVVDHNS  
RTTTWNDPRVPSEGPKEPTSSANGPSREGSRLPPAREGHPVYPQLRPGYIPIPVLHEG  
AENRQVHPFHVYPQGMQRFRTAAAAAPQRSQSPLRGMPETTQPDKQCGQVAAAAAA  
QPPASHGPERSQSPAASDCSSSSSSASLPSSGRSSLGSHQLPRGYISIPVIEQNVTR  
PAAQPSFHKAKQTHYPAQRGEYQTHQPVYHKIQGDDWEPRPLRAASPFSSVQGASSR  
EGSPARSSTPLHSPSPIRVHTVVDRPQQPMTHRETAPVSQPENKPKPGVGPVPELPP  
GHIPIQVIRKEVDSKPVSQKPPPPSEKVEVKVPPAPVPCPPSPGSPSAVPSSPKSVAT  
EERAAPSTAPAEATPPKPGEAAPKHPGVLEKVEAILEKVQGLEQAVDNFEGKKTDDK  
YLMIEEYLTKEALLDSVDPEGRADVRRQARRDGVRRKVTILEKLEQKVIDVPGQVQVY  
ELQPSNLEADQPLQAIMEMGAADKGGKNAGNAEDPHTETQQPEATAAATSNPSSMT  
DTPGNPAAP"  
BASE COUNT 596 a 806 c 653 g 479 t  
ORIGIN  
1 g c g g a g c t c c g c a t c c a a c c c g g g c c g c g g c c a a c t t c t c t g g a c t g g a c c a g a g t t t 61  
c t a g c c g g c c a g t t g c t a c c t c c t t t a t c t c t c c t t c c c t c t g g c a g c g a g g a g g c t 121  
a t t t c c a g a c a c t t c c a c c c c t c t c t g g c c a c g t c a c c c c g c c t t t a a t t c a t a a a g g t 181  
g c c c g g c c c g g c t t c c c g g a c a c g t c g g c g g c g g a g a g g g g c c c a c g g c g g c g g c c c g g 241  
c c a g a g a c t c g g c g c c c g g a g c c a g c g c c c g c a c c c g c g c c c a g c g g c a g a c c c c a a 301

```

cccagcatga  gcgcgcgcac  ccactcgccc  atgatgcagg  tggcgtccgg  caacgggtgac  361
cgcgaccctt  tgccccccgg  atgggagatc  aagatcgacc  cgcagaccgg  ctggcccttc  421
ttcgtggacc  acaacagccg  caccactacg  tggaacgacc  cgcgcggtgc  ctctgagggc  481
cccaaggaga  ctccatcctc  tgccaatggc  ccttcccggg  agggctctag  gctgccgcct  541
gctagggaag  gccaccctgt  gtacccccag  ctccgaccag  gctacattcc  cattcctgtg  601
ctccatgaag  gcgctgagaa  ccggcaggtg  cacccttttc  atgtctatcc  ccagcctggg  661
atgcagcgat  tccgaactga  ggcggcagca  gcggctcctc  agaggtccca  gtcacctctg  721
cggggcatgc  cagaaaccac  tcagccagat  aaacagtgtg  gacaggtggc  agcggcggcg  781
gcagcccagc  cccagcctc  ccacggacct  gagcgggtcc  agtctccagc  tgcctctgac  841
tgctcatcct  catcctcctc  ggccagcctg  ccttccctcc  gcaggagcag  cctgggcagt  901
caccagctcc  cgcgggggta  catctccatt  ccggtgatac  acgagcagaa  cgttaccggg  961
ccagcagccc  agccctcctt  ccacaaagcc  cagaagacgc  actaccagc  gcagaggggt  1021
gagtagccaga  cccaccagcc  tgtgtaccac  aagatccagg  gggatgactg  ggagccccgg  1081
cccttgccgg  cggcatcccc  gttcaggtea  tctgtccagg  gtgcatcgag  ccgggagggc  1141
tcaccagcca  ggagcagcac  gccactccac  tccccctcgc  ccattccgtg  gcacaccgtg  1201
gtcgacaggc  ctacgacgcc  catgacctat  cgagaaactg  cacctgtttc  ccagcctgaa  1261
aacaaccag  aaagtaagcc  aggcccagtt  ggaccagaac  tccctcctgg  acacatccca  1321
attcaagtga  tccgcaaaga  ggtggattct  aaacctgttt  cccagaagcc  cccacctccc  1381
tctgagaagg  tagagtgaa  agttccccct  gctccagttc  cttgtcctcc  tcccagccct  1441
ggcccttctg  ctgtccctc  tcccccaag  agtgtggcta  cagaagagag  ggcagcccc  1501
agcactgccc  ctgcagaagc  tacacctcca  aaaccaggag  aagccgaggc  tcccccaaaa  1561
catccaggag  tgctgaaagt  ggaagccatc  ctggagaagg  tgcaggggct  ggagcaggct  1621
gtagacaact  ttgaaggcaa  gaagactgac  aaaaagtacc  tgatgatcga  agagtatttg  1681
accaaagagc  tgctggccct  ggattcagtg  gaccccgagg  gacgagccga  tgtgcgtcag  1741
gccaggagag  accgtgtcag  gaaggttcag  accatcttgg  aaaaacttga  acagaaagcc  1801
attgatgtcc  cagggtcaagt  ccaggtctat  gaactccagc  ccagcaacct  tgaagcagat  1861
cagccactgc  aggcaatcat  ggagatgggt  gccgtggcag  cagacaaggg  caagaaaaat  1921
gctggaaatg  cagaagatcc  ccacacagaa  acccagcagc  cagaagccac  agcagcagcg  1981
acttcaaacc  ccagcagcat  gacagacacc  cctggtaacc  cagcagcacc  gtagcctctg  2041
ccctgtaaaa  atcagactcg  gaaccgatgt  gtgctttagg  gaattttaag  ttgcatgcat  2101
ttcagagact  ttaagtcagt  tggtttttat  tagctgcttg  gtatgcagta  acttgggtgg  2161
aggcaaaaaca  ctaataaaaag  ggctaaaaaag  gaaaatgatg  cttttcttct  atattcttac  2221
tctgtacaaa  taaagaagtt  gcttggtgtt  tgagaagttt  aaccccgttg  cttgttctgc  2281
agccctgtct  acttgggcac  ccccaccacc  tgttagctgt  gggtgtgcac  tgtcttttgt  2341
agctctggac  tggaggggta  gatggggagt  caattaccca  tcacataaat  atgaaacatt  2401
tatcagaaat  gttgccatth  taatgagatg  attttcttca  tctcataatt  aaaatacctg  2461
actttagaga  gagtaaaatg  tgccaggagc  cataggaata  tctgtatgtt  ggatgacttt  2521
aatgctacat tttc

```

## 2. BAG4 nucleotide and predicted amino acid sequence

LOCUS AF095194 1944 bp mRNA PRI 10-SEP-1999  
 DEFINITION Homo sapiens BAG-family molecular chaperone regulator-4 mRNA, complete cds.  
 ACCESSION AF095194  
 NID g4322823  
 KEYWORDS .  
 SOURCE human.  
 ORGANISM Homo sapiens  
 Eukaryota; Metazoa; Chordata; Craniata; Vertebrata; Mammalia; Eutheria; Primates; Catarrhini; Hominidae; Homo. REFERENCE 1 (bases 1 to 1944)  
 AUTHORS Takayama,S., Xie,Z. and Reed,J.C. TITLE An evolutionarily conserved family of Hsp70/Hsc70 molecular chaperone regulators  
 JOURNAL J. Biol. Chem. 274 (2), 781-786 (1999) MEDLINE 99091615  
 REFERENCE 2 (bases 1 to 1944)  
 AUTHORS Takayama,S. and Reed,J.C.  
 TITLE BAG-family regulators of Hsp70/Hsc70  
 JOURNAL Unpublished  
 REFERENCE 3 (bases 440 to 1392)  
 AUTHORS Takayama,S. and Reed,J.C.  
 TITLE Direct Submission  
 JOURNAL Submitted (28-SEP-1998) The Burnham, 10901 N. Torrey Pines Rd., La Jolla, CA 92037, USA

REFERENCE 4 (bases 1 to 1944)  
 AUTHORS Takayama, S. and Reed, J.C.  
 TITLE Direct Submission  
 JOURNAL Submitted (10-SEP-1999) The Burnham, 10901 N. Torrey Pines Rd., La Jolla, CA 92037, USA  
 REMARK Sequence update by submitter  
 FEATURES Location/Qualifiers  
 source 1..1944  
 /organism="Homo sapiens"  
 /db\_xref="taxon:9606"  
 CDS 43..1416  
 /note="member of the molecular chaperone regulator BAG family proteins; BAG-4"  
 /codon\_start=1  
 /product="BAG-family molecular chaperone regulator-4"  
 /db\_xref="PID:g4322824"  
 /translation="MSALRRSGYGPSDGPSTYGRYYGPGGGDVPVHPPPPLYPLRPEPP  
 QPPISWVRVGGGPAETTWLGEGGGGDGYYPSSGGAWPEPGRAGGSHQEQPPYPSYNSNY  
 WNSTARSRAPYPSTYPVRPELQQQSLNSYTNGAYGPTYPPGPGANTASYSGAYYAPGY  
 TQTSYSTVEPSTYRSSGNSPTPVSRIYPQQDCQTEAPPLRGQVPGYPPSQNPGMTLP  
 HYPYGDGNRSVPQSGPTVRPQEDAWASPGAYGMGGRYWPSSAPSAPPGNLYMTESTS  
 PWPSSGSPQSPSPVPVQPKDSSYPYSQSDQSMNRHNFPCSVHQYESSGTVNNDSDSL  
 LDSQVQYSAEPQLYGNATSDHPNNQDQSSSLPEECVPSDESTPPSIKKIIHVLEKVQY  
 LEQVEVEEFVGKTKDAYWLLEMLTKELLELDVETGGQDSVRQARKEAVCKIQAIL  
 KLEKKGL"  
 BASE COUNT 535 a 480 c 443 g 486 t  
 ORIGIN

```

1  cgggtgggagc  gggggcgggaa  gcgcttcagg  gcagcgggac  ccatgtcggc  cctgaggcgc  61
tcgggctacg  gccccagtg  cggtccgctc  tacggccgct  actacgggac  tgggggtgga  121
gatgtgccgg  tacacccacc  tccaccctta  taccctcttc  gccctgaacc  tccccagcct  181
cccatttcct  ggcgggtgcg  cgggggcggc  ccggcggaga  ccacctggct  gggagaaggc  241
ggaggaggcg  atggctacta  tccctcggga  ggcgcctggc  cagagcctgg  tcgagccgga  301
ggaagccacc  aggagcagcc  accatatact  agctacaatt  ctaactattg  gaattctact  361
gcgagatcta  gggctcctta  cccaagtaca  tatcctgtaa  gaccagaatt  gcaaggccag  421
agtttgaatt  cttatacaaa  tggagcgtat  ggtccaacat  acccccagg  ccctggggca  481
aatactgcct  catactcagg  ggcttattat  gcacctgggt  atactcagac  cagttactcc  541
acagaagttc  caagtactta  ccgttcctct  ggcaacagcc  caactccagt  ctctcgttgg  601
atctatcccc  agcaggactg  tcagactgaa  gcaccccttc  ttagggggca  gggtccagga  661
tatccgcctt  cacagaaccc  tggaatgacc  ctgccccatt  atccttatgg  agatggtaat  721
cgtagtgctt  cacaatcagg  accgactgta  cgaccacaag  aagatgcgtg  ggcttctcct  781
ggtgcttatg  gaatgggtgg  ccgttatccc  tggccttcac  cagcgccctc  agcaccaccc  841
ggcaatctct  acatgactga  aagtacttca  ccatggccta  gcagtggctc  tccccagtca  901
cccccttcac  cccagtgca  gcagcccaag  gattcttcac  acccctatag  ccaatcagat  961
caaagcatga  accggcacaa  ctttccttgc  agtgtccatc  agtacgaatc  ctcggggaca  1021
tggaacaatg  atgattcaga  tcttttggat  tcccaagtcc  agtatagtgc  tgagcctcag  1081
ctgtattgta  atgccaccag  tgaccatccc  acaaaagtag  atcaaagtag  cagtcttcct  1141
gaagaatgtg  taccttcaga  tgaaagtact  cctccgagta  ttaaaaaaat  catacatgtg  1201
ctggagaagg  tccagtatct  tgaacaagaa  gtagaagaat  ttgtaggaaa  aaagacagac  1261
aaagcatact  ggcttctgga  agaaatgcta  accaaggaa  ttttggaact  ggattcagtt  1321
gaaactgggg  gccaggactc  tgtacggcag  gccagaaaag  aggctgtttg  taagattcag  1381
gccatactgg  aaaaattaga  aaaaaaagga  ttatgaaagg  atttagaaca  aagtgggaagc  1441
ctgttactaa  cttgaccaa  gaacacttga  ttaggttaat  taccctcttt  ttgaaatgcc  1501
tggtgatgac  aagaagcaat  acattccagc  ttttcctttg  attttatact  tgaaaaactg  1561
gcaaaggaat  ggaagaatat  tttagtcatt  aagttgtttt  cagttttcag  acgaatgaat  1621
gtaataggaa  actatggagt  taccatatt  gccaaagtag  ctcaactcct  aaaaaattta  1681
tggaatatcta  caagctgctt  attaccagca  ggagggaaac  acacttcaca  caacaggctt  1741
atcagaaacc  taccagatga  aactggatat  aatttgagac  aaacaggatg  tgttttttta  1801
aacatctgga  tatcttgta  cattttgtga  cttgtgact  gctttcaaca  tatacttcac  1861
gtgtaattat  agcttagact  ttagccttct  tggacttctg  ttttgttttg  ttatttgcag  1921
tttacaata  tagtattatt  ctct

```

BAG5 nucleotide and predicted aminoacid sequence

LOCUS AF095195 4285 bp mRNA PRI 10-SEP-1999  
 DEFINITION Homo sapiens BAG-family molecular chaperone regulator-5 mRNA,

complete cds.  
ACCESSION AF095195  
NID g4322825  
KEYWORDS .  
SOURCE human.  
ORGANISM Homo sapiens  
Eukaryota; Metazoa; Chordata; Craniata; Vertebrata; Mammalia; Eutheria;  
Primates; Catarrhini; Hominidae; Homo. REFERENCE 1 (bases 1 to 4285)  
AUTHORS Takayama, S., Xie, Z. and Reed, J.C. TITLE An evolutionarily  
conserved family of Hsp70/Hsc70 molecular  
chaperone regulators  
JOURNAL J. Biol. Chem. 274 (2), 781-786 (1999) MEDLINE 99091615  
REFERENCE 2 (bases 1 to 4285)  
AUTHORS Takayama, S. and Reed, J.C.  
TITLE BAG-family regulators of Hsp70/Hsc70  
JOURNAL Unpublished  
REFERENCE 3 (bases 1245 to 1957)  
AUTHORS Takayama, S. and Reed, J.C.  
TITLE Direct Submission  
JOURNAL Submitted (28-SEP-1998) The Burnham Institute, 10901 N. Torrey  
Pines Rd., La Jolla, CA 92037, USA  
REFERENCE 4 (bases 1 to 4285)  
AUTHORS Takayama, S. and Reed, J.C.  
TITLE Direct Submission  
JOURNAL Submitted (10-SEP-1999) The Burnham Institute, 10901 N. Torrey  
Pines Rd., La Jolla, CA 92037, USA  
REMARK Sequence update by submitter  
FEATURES Location/Qualifiers  
source 1..4285  
/organism="Homo sapiens"  
/db\_xref="taxon:9606"  
CDS 224..1567  
/note="member of the molecular chaperone regulator BAG  
family proteins; BAG-5"  
/codon\_start=1  
/product="BAG-family molecular chaperone regulator-5"  
/db\_xref="PID:g4322826"  
/translation="MDMGNQHPSISRLQEIQKEVKSVEQQVIGFSGLSDDKNYKKLER  
ILTKQLFEIDSVDTEGKGDIQQARKRAAQETERLLKELEQNANHPHRIEQNIFEEAQ  
SLVREKIVPFYNGGNCVTDDEFEEGIQDIILRLTHVKTGGKISLRKARYHTLTKICAVQ  
EIIEDCMKKQPSLPLSEDAHPVAKINFVMCEVNKARGVLIALLMGVNNNETCRHLS  
VLSGLIADLDALDVCGRTEIRNYRREVVEDINKLLKYLDLEEEADTTKAFDLRQNH  
SI LKIEKVLKRMREIKNELQAQNPSELYLSSKTELQGLIGQLDEVSLKNPCIREARRR  
AVIEVQTLITYIDLKEALEKRKLFACEEHPHSHKAVVNVNLSEIQGEVLSFDGNRTD  
KNYIRLEELLTKQLLALDAVDPOGEEKCKAARKQAVRLAQNILSYLDLKSDEWEY"  
BASE COUNT 1201 a 875 c 987 g 1222 t  
ORIGIN  
1 gaagacgccc ggagcggctg ctgcagccag tagcggcccc ttcaccggt gccccgtca 61  
gacctagtgc ggaggggtgc gaggcattgca gctggggggcc cagctccggt gccgcacccc 121  
gtaaagggct gatcttcac ctgccacct cagccacggg acgccaagac cgcattccaat 181  
tcagacttct tttggtgctt gtgaaactga acacaacaaa agtatggata tgggaaacca 241  
acatccttct attagtaggc ttcaggaaat ccaaaaggaa gtaaaaagtg tagaacagca 301  
agttatcggc ttcagtgggc tgtcagatga caagaattac aagaaactgg agaggattct 361  
aacaaaacag ctttttgaaa tagactctgt agatactgaa ggaaaaggag atattcagca 421  
agctaggaag cgggcagcac aggagacaga acgtcttctc aaagagtgg agcagaatgc 481  
aaaccacca caccgattg aaatacagaa catttttgag gaagccagt ccctcgtgag 541  
agagaaaatt gtgccatttt ataattggagg caactgcgta actgatgagt ttgaagaagg 601  
atccaagat atcattctga ggctgacaca tggtaaaact ggaggaaaaa tctccttgcg 661  
gaaagcaagg tatcacactt taacaaaaat ctgtgcgggtg caagagataa tcgaagactg 721  
catgaaaaag cagccttccc tgccgctttc cgaggatgca catccttccg ttgccaaaat 781  
caacttcgtg atgtgtgagg tgaacaaggc ccgaggggtc ctgattgcac ttctgatggg 841  
tgtgaacaac aatgagacct gcaggcactt atcctgtgtg ctctcggggc tgatcgctga 901  
cctgatgtgt ctgatgtgt gcggccggac agaaatcaga aattatcgga gggaggtagt 961  
agaagatatc aacaaattat tgaaatatct ggatttggaa gaggaagcag acacaactaa 1021  
agcatttgac ctgagacaga atcattccat tttaaaaata gaaaagggtc tcaagagaat 1081

gagagaaata	aaaaatgaac	ttctccaagc	acaaaaccct	tctgaattgt	acctgagctc	1141
caaaacagaa	ttgcaggggt	taattggaca	gttggatgag	gtaagtcttg	aaaaaaaccc	1201
ctgcatccgg	gaagccagga	gaagagcagt	gatcgagggtg	caaactctga	tcacatatat	1261
tgacttgaag	gagggcccttg	agaaaagaaa	gctgtttgtct	tgtgaggagc	acccatccca	1321
taaagccgtc	tggaaacgtcc	ttggaaactt	gtctgagatc	cagggagaag	ttctttcatt	1381
tgatggaaat	cgaaccgata	agaactacat	cgggctggaa	gagctgctca	ccaagcagct	1441
gctagccctg	ttgctgtttg	atccgcaggg	agaagagaag	tgtaaggctg	ccaggaaaca	1501
agctgtgagg	cttgccgcaga	atattctcag	ctatctcgac	ctgaaatctg	atgaatggga	1561
gtactgaaat	accagagatc	tcacttttga	tactgttttg	cacttcatat	gtgcttctat	1621
gtatagagag	ctttcagttc	attgattttat	acgtgcatac	ttcagctctca	gtattttatga	1681
ttgaagcaaa	ttctatttcag	tatctgtctgc	ttttgatgtt	gcaagacaaa	tatcattaca	1741
gcacgttaac	ttttccattc	ggatcattat	ctgtatgatg	tggtgtgtgt	tgtttgggtt	1801
gtcctttttt	ttgcgtttttt	aatcagaaaa	caaaaatagag	gcagcttttg	tagatttttaa	1861
atgggttgtg	caagcattaa	aatgcaggtc	tttcagaatc	tagaactagg	cataacctta	1921
cataatacta	ggaaaattat	gagaaagggg	aaattttttg	ttaaataaga	gtaagggttca	1981
aacacaagca	gtacatgttc	tgtttcatta	tgctcgatag	aaggcctttt	tttcacttat	2041
aaggcctgat	tggtccctacc	cagcttaacg	gggtgggggt	tttttgtttg	ttcagacagt	2101
ctgttctctt	gtaaacatttt	ttagttggaa	aaacagcatc	tgcatcttcc	ccatcctcta	2161
cgttttagag	aggaatccttg	tttttgtgtg	caacataaga	aaattatgaa	aactaatagc	2221
caaaaaacct	ttgagattgc	attaaagaga	agggataaag	gaccagcaat	aataccttgt	2281
aagttgcttt	tgtttgtaaa	atctgagctt	atagttttcc	ttagttagta	aattcataag	2341
gatgggaaca	tttaaatata	gttaatgggc	ctttaaaaaa	aaaaaaggaa	acactcatac	2401
ctgtagtgtg	aggatgaata	ctggagacgg	gttaccaatg	tcagggtata	ctaaaaactaa	2461
atcagaaaag	ctgaatgtag	cacataatgg	ttctcttctg	ttgtccaagg	agttaaaatg	2521
gacagccttg	tcacacctcc	cgggtgctgt	tttacaacgt	gagggtagac	gctgtcagta	2581
accagagggg	accaggcctt	cctagggtttt	ctaggcagtc	agctgttaac	cactcactta	2641
gtaaatgtca	taactacacc	tgctccagga	ccaatcagtg	aaacctgctc	ggaattaaag	2701
gcttcctctg	ggtgcctgct	gaacaactga	gctcatgtca	tgggcatgtg	gtgggtttctc	2761
tgttgcctga	aagagccatt	aaagtcatgc	gtgctgtgaag	catctctctt	ctaaaggatg	2821
tgtatttcca	taaatgcttt	ctgaggatcc	ggtacaaaaat	gatttcccaa	gtgagcttcc	2881
tgcccttgaga	acatgtgggt	ccgagtgtta	taacagactc	ctccccggg	tcaccttttg	2941
cctgggtcatc	ctggttagagt	acatcttttg	aaatccaggg	taatattctc	tttcagagat	3001
gctcattgtg	taactctgtg	tagggagata	gtcactttta	acagctcaaa	gtagctagct	3061
aaaggagtag	ccttaaatac	ctaaaagatg	acagaagcat	agcccttaac	aaatcttcag	3121
cttgtctctc	agtatttccc	aatcatgaaa	atcccttgct	atgtctttcc	tactagaaat	3181
gttctagaat	cgttggaacg	tggggtcaga	gggcagtcgg	tatttaggcc	gtgagcttcc	3241
catactactg	caggtccaac	tcctggcaac	cgcgggctca	aggcagggtca	ttggaatcca	3301
cgttttggcc	acagtagttg	taggattgct	tttctgtatc	ataatttttag	aatgctctta	3361
aaatcttgag	gaagagtttt	tattttttat	ttatttttga	gatggagtct	ctgttgccca	3421
ggctgcagtg	cagtggtgct	atctcagctc	actgcaacct	ccacctccca	ggttcaagcg	3481
attctcctgc	ctcagccacc	tgagttagctg	ggagtacagg	catgtggcac	catgctggcg	3541
taatttttgt	attttttaata	gagttgagat	ttcaccatga	tggtcaggct	ggtctogaac	3601
tcctgacctc	gtgatccgcc	cgcctcggcc	ccccaaagtg	ctgggattaa	cgggtgtgag	3661
ccacggcgcc	cagcccagga	agagttttta	aattagagct	ctgttttaatt	ataccactgg	3721
gaaatcatgg	ttacgcttca	ggcatattct	tccccagagt	actacttaca	ttttaaattt	3781
cattttgtaa	agttaaatgt	cagcattccc	tttaaaagtg	tccattgttc	tttgaaagta	3841
gacgttttcag	tcattctttt	caaacaagtg	tttgtgtacc	ttttgccaag	ctgtgggcat	3901
cgtgtgtgag	tacagggtgc	tcagctcttc	caccgtcatt	ttgaattgtt	cacatgggta	3961
attgggtcatg	gaaatgatca	gattgacctt	gattgactgt	caggcatggc	tttgtttcta	4021
gtttcaatct	gttctcgttc	cttgtaccgg	attattctac	tcctgcaatg	aacctgtttg	4081
acacccgatt	tagctcttgt	cggccttcgt	ggggagctgt	ttgtgttaat	atgagctact	4141
gcatgtaatt	cttaaaactgg	gcttgtcaca	ttgtattgta	tttttgtgat	ctgtaatgaa	4201
aagaatctgt	actgcaagta	aaacctactc	cccaaaaatg	tgtggccttg	ggtctgcatt	4261
aaacgctgta	gtccatgttc	atgcc				